CHARACTERIZATION OF THE ROLES OF TWO REGULATORS OF VIRUS INFECTION: GP78 AND BPIFB3

by

Jana Lynn Jacobs

B.S., Eastern Michigan University, 2004

Submitted to the Graduate Faculty of

the Graduate School of Public Health in partial fulfillment

of the requirements for the degree of

Doctor of Philosophy

University of Pittsburgh

2014

UNIVERSITY OF PITTSBURGH

GRADUATE SCHOOL OF PUBLIC HEALTH

This dissertation was presented

by

Jana Lynn Jacobs

It was defended on

April 9, 2014

and approved by

Velpandi Ayyavoo, PhD, Professor, Department of Infectious Diseases and Microbiology, Graduate School of Public Health, University of Pittsburgh

Todd A. Reinhart, ScD, Professor, Department of Infectious Diseases and Microbiology, Graduate School of Public Health, University of Pittsburgh

Saumendra N. Sarkar, PhD, Assistant Professor, Department of Microbiology and Molecular Genetics
School of Medicine, University of Pittsburgh

Dissertation Advisor: Carolyn B. Coyne, PhD, Associate Professor, Department of Microbiology and Molecular Genetics
School of Medicine, University of Pittsburgh

Carolyn B. Coyne, PhD

CHARACTERIZATION OF THE ROLES OF TWO REGULATORS OF VIRUS INFECTION: GP78 AND BPIFB3

Jana Lynn Jacobs, PhD

University of Pittsburgh, 2014

ABSTRACT

Over the course of the viral life cycle many host cell factors act to either restrict or facilitate viral infection. Identification of these factors gives insight into the cell biology and virology of viral infection, perhaps even leading to identification of therapeutic targets. A highly efficient and un-biased method for identifying these factors is high-throughput RNAi screening. Our lab previously conducted such a screen in search of host cell factors that regulate enterovirus infection, and this dissertation describes characterization of two screen 'hits': Gp78, whose depletion restricted enterovirus infection, and BPIFB3, whose depletion enhanced enterovirus infection. In aim 1 we show that the E3 ubiquitin ligase Gp78 is a regulator of the retinoic acid-inducible gene 1 (RIG-I)-like receptor (RLR) antiviral signaling pathway. We show that depletion of Gp78 results in enhancement of type I interferon (IFN) signaling, restricting RNA virus infection. Mechanistically, we show that Gp78 modulates type I IFN induction by altering both the expression and signaling of the mitochondria-localized RLR adaptor mitochondrial antiviral signaling (MAVS). Our data implicate two parallel pathways by which Gp78 regulates MAVS signaling—one pathway requires its E3 ubiquitin ligase activity to directly degrade MAVS, whereas the other pathway occurs independently of these activities, but requires association between the Gp78 RING domain and MAVS. In aim 2, we characterize the role of bactericidal

permeability-increasing protein (BPI) fold-containing family B member 3 (BPIFB3), a member of the lipid-binding antimicrobial BPI/lipopolysaccharide (LPS) binding protein (LBP) family of proteins, in viral infection. We show that BPIFB3 is ER-localized, and examination of ER morphology upon BPIFB3 depletion shows that it is involved in maintenance of ER architecture. We further show that ER-regulated calcium homeostasis is also disrupted in the absence of BPIFB3. Examination of the role of BPIFB3 in viral infection led to the finding that depletion of BPIFB3 enhances VSV-induced syncytia formation. The increase in syncytia could be correlated with an observed increase in endosome/lysosome number and size, although concrete evidence to support this connection is lacking at this time. Lastly, we show that BPIFB3 plays a role in infection of a diverse panel of viruses, all of which require host-derived membranes for their life cycles. Taken together, our data show that BPIFB3 is a novel component of the ER that is responsible for maintenance of ER morphology, and that depletion of BPIFB3 affects replication of viruses that utilize host-derived ER membranes or trafficking for their life cycles. This project is significant to public health because it furthers understanding of virus-host cell interaction, which is crucial for development of efficient and targeted anti-viral therapeutics.

TABLE OF CONTENTS

LIST OF TABLES

LIST OF FIGURES

PREFACE

I would first like to thank my advisor Dr. Carolyn Coyne. I have been fortunate to have the chance to learn from such a smart and accomplished scientist. I am grateful that she agreed to take me into her lab with the commitment to graduate me in an accelerated time frame, and have learned an immense amount from her over the last year and a half, not only about science but also the valuable skills of presenting, writing, and the overall process of science. She gave me so many opportunities that most people wouldn't have bothered with given my short stay in her lab, such as the opportunity to write a review article, attend a conference, and review papers with her. I will always feel lucky to have landed in the lab of such a capable and supportive advisor.

I would like to thank my committee, Dr. Saumendra Sarkar, Dr. Velpandi Ayyavoo and Dr. Todd Reinhart for their support and advisement over the course of my project. I would like to acknowledge Dr. Ayyavoo for her involvement with the students as the director of the PhD program. You do so much for us (a good example was the career day on March 22, which was extraordinarily helpful), and it is greatly appreciated. I would also like to acknowledge Dr. Reinhart for being a highly supportive member of the IDM faculty. Throughout my time at IDM he has always been highly approachable and willing to help, and I have always felt that he truly has the students' best interest at heart.

I would like to acknowledge the members of the Coyne lab, Katie Harris, Coyne Drummond, Avi Bayer, Elizabeth Delorme-Axford and Stef Morosky for camaraderie and support. This is such a great group of people and I have enjoyed our many lunches together as well as our trip to ASV!

I would like to thank the administrative staff at GSPH and within IDM for everything they

do on a daily basis for the students, and the IDM students (past and present). The IDM students represent such a great, collaborative, and supportive group of colleagues. I have really enjoyed working with all of them. In particular, I would like to acknowledge Kevin McCormick and Amanda Smith. They have both become close friends, whose support of me has been invaluable throughout this process. Believe or not, those half-drunk conversations about science were extremely helpful!

Lastly, I would like to thank my family. My mother's support of me has been unwavering, and I really couldn't have made it this far without her. The support from my step-father, brother, and grandfather has also been very important to me. Of course, I would like to thank my husband Chuck for being understanding of the late nights and weekends, high amount of stress and sometimes even tears. If it wasn't for you, I'm not sure I could have made it to the end. I would like to acknowledge our dog William for keeping me company all of the months of writing at home, and our little girl Clara or Tessa Mae Rohrer, due June 24, 2014, for providing me the motivation to hurry up and finish!

Chapter 4 is published in:

Jacobs JL, Zhu J, Sarkar SN, Coyne CB. Regulation of mitochondrial antiviral signaling (MAVS) expression and signaling by the mitochondria-associated endoplasmic reticulum membrane (MAM) protein Gp78. J Biol Chem. 2014 Jan 17;289(3):1604-16.

Chapter 1.2, including Figure 3 and Table1 are published in:

Jacobs, JL, Coyne, CB. Mechanisms of MAVS Regulation at the Mitochondrial Membrane. J Mol Biol. 2013 Dec. 13;425(24):5009-19.

1.0 INTRODUCTION

There are many critical interactions between a virus and host cell during the course of viral infection. These interactions include those that restrict and those that facilitate completion of the viral life cycle, and identification of host cell factors involved provides valuable information on the cell biology and virology of viral infection. To identify novel host cell factors involved in enterovirus infection our lab previously performed a high-throughput RNAi screen for novel regulators of enterovirus infection, identifying Gp78 and BPIFB3 as potential regulators of infection. In this dissertation introduction, various aspects of virus-host cell interaction, as well as host cell components known to be hijacked for the viral life cycle, are discussed with a particular focus on host cell components involved in the life cycle of positive-sense RNA viruses. The screen "hits" chosen for follow-up in this dissertation (Gp78 and BPIFB3) are also discussed.

1.1 HOST-VIRUS INTERACTION

1.1.1 Positive-sense RNA virus life cycle

The nucleic acid contained within a virus can take one of seven different forms, including RNA or DNA, single (ss) or double-stranded (ds), and a positive or negative polarity in the case of ssRNA

viruses. The ssRNA virus group contains the most members, and among the ssRNA viruses, the positive sense RNA viruses are the most numerous (1). The following section outlines the general life cycle of positive sense RNA viruses, and includes the steps of viral entry, genome release, genome translation and replication, virus assembly, maturation, and egress.

Positive sense RNA viruses have small genomes encoding a limited number of proteins, thus they rely on many host cell factors throughout their life cycle. A schematic of the general life cycle of positive-sense RNA viruses is shown in Figure 1 (2). Viral attachment and entry involves the engagement of host cell surface molecules with viral surface proteins, resulting in direct fusion and uncoating at the membrane of some enveloped viruses, or receptor-mediated endocytosis of non-enveloped and some enveloped viruses (1).

Following entry, the positive sense RNA contained within the viral capsid is released into the cytoplasm of the host cell. Like viral entry, genome release requires a set of host cell endocytic trafficking proteins. Genome release is commonly accomplished through fusion of the incoming virus-containing endocytic vesicle with lower pH-containing early/late endosomes, thus triggering pH-dependent conformational changes in viral proteins to allow genome escape by either membrane fusion (enveloped viruses) or disruption of the endosomal membrane (non-enveloped viruses) (3). From early endosomes to late endosomes/lysosomes the pH of the compartment lowers progressively to a pH of 5.0 (4). Therefore, the stage of post-entry endocytic trafficking from which a particular viral genome escapes its vesicle depends on its individual pH requirement.

Once the RNA has reached the cytoplasm direct translation of the positive sense genome occurs. This step relies almost exclusively on the host cell translation machinery since the polarity of viral positive-sense RNA mimics the mRNA of the host cell. RNA viruses whose genome lacks the usual 5’ terminal cap and 3’ poly-A tail of host cell mRNA utilize a variety of different

strategies to hijack the host cell translation machinery, including utilization of an internal ribosome entry site (IRES) in the 5' untranslated region of the RNA for recruitment of the ribosome (5-8). Whereas host cell mRNA molecules are monocistronic (meaning they encode for only one functional protein each) most viral RNA molecules are polycistronic. This allows for more efficient protein production from a limited genome. An example of this is illustrated by the picornaviruses. Translation of the picornaviral RNA is initiated by ribosome binding at the IRES, resulting in the translation of a polyprotein containing all viral proteins. The polyprotein is then cleaved into individual functional proteins by two viral proteases (7, 9, 10).

Once the production of viral proteins has begun, replication of the viral RNA can commence. This is because the host cell does not normally produce RNA from an RNA template, and therefore the host cell does not contain the correct polymerase to achieve this (an RNA-dependent RNA polymerase, or RDRP). Thus, viral RNA replication cannot begin until the RDRP has been translated. There are host cell proteins involved in the active replication of positive-sense RNA viruses. For example poliovirus (PV) requires the host protein poly (rC) binding protein for initiation of replication (11, 12). However, many of the host cell factors required for positive-sense RNA virus replication are the membranes and lipids that provide the scaffolding and protection for the viral replication complex (13), and this will be addressed in further detail in section 1.1.2.

The last steps in the viral life cycle include assembly of the progeny virions followed by their maturation and release. During assembly of the progeny virions the viral structural proteins are assembled into a viral capsid structure and the newly replicated viral RNA packaged inside it to produce new virions, which often takes place at or near host cell-derived membranes. In some cases, the newly assembled virion must undergo a maturation process prior to becoming a fully

infectious viral particle. An example of this is illustrated by PV. Cleavage of structural protein VP0 into VP2 and VP4 is required for a fully mature and infectious PV particle to be released (14). In other cases the acquisition of a viral envelope from the host cell membranes constitutes part of the maturation process. Viral egress is a diverse process among positive-sense RNA viruses, and includes the cytopathic event of host cell lysis to allow release of viral particles (as for most non-enveloped viruses such as poliovirus), viral hijacking of the host exocytic pathway, or budding from the membrane in the case of viruses that assemble at the plasma membrane. During all of these different exit strategies the virus relies heavily on host cell factors to achieve release of the mature infectious virus particle (1).

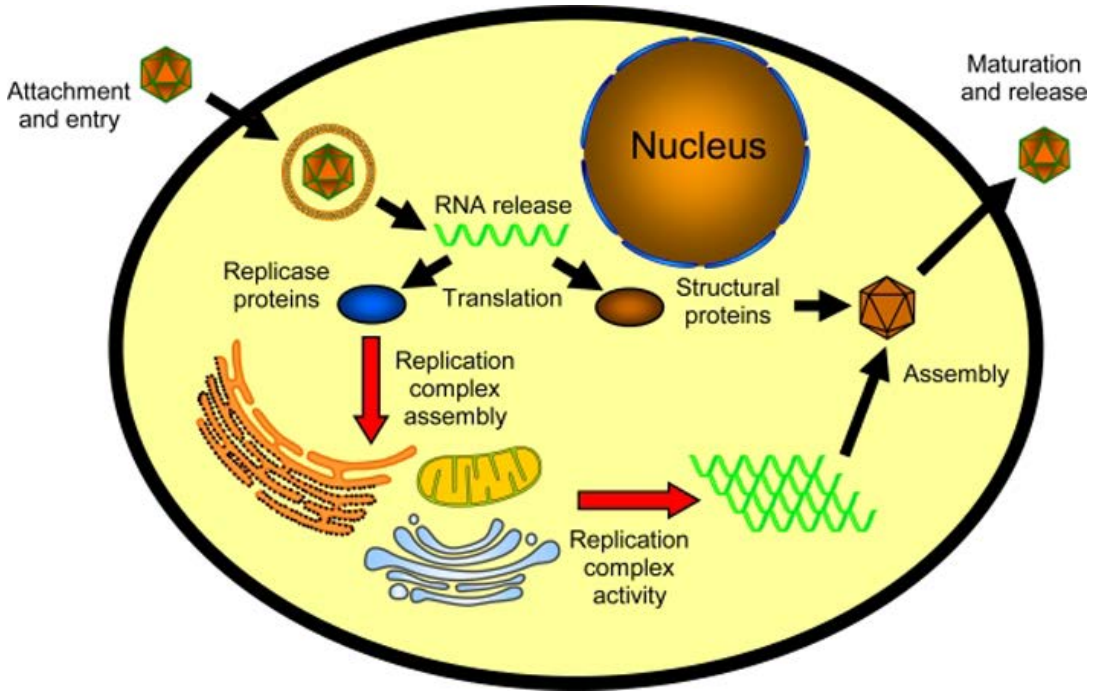

Figure 1. Positive-Sense RNA virus life cycle.

A general schematic of the positive-sense RNA virus life cycle, including attachment and entry, RNA release into the host cell cytoplasm, translation of viral RNA to produce structural proteins and those required for replication complex assembly, viral assembly, and finally maturation and release. From Stapleford *et al*., 2010 (full reference in text).

1.1.2 Positive-sense RNA virus replication and host membranes

Host cell membranes and lipids are recognized as vital to the replication of many RNA viruses, including picornaviruses and flaviviruses. Viruses have diverse mechanisms and intracellular sources for construction of viral replication centers from the host membranes. Picornavirus replication, including PV and coxsackievirus B (CVB), was shown to induce an extensive reorganization of ER, Golgi and lysosome membranes into membrane-bound vesicles, providing a scaffold on which to organize replication machinery and for protection from innate immune recognition (15-18). CVB begins replication on the Golgi and trans-Golgi membranes where it remains until newly synthesized viral proteins assemble on viral replication complexes formed near ER exit sites (19). The viral proteins 3A and 3CD are involved in inhibition of secretory system trafficking and reorganization of the membranes into viral replication centers (19, 20), which are enriched in many factors of the host secretory system, including the GTPase ADP-ribosylation factor 1 (ARF1) and its guanine exchange factor (GEF) GBF1 (19). ARF1 seems to be involved in recruiting factors to ensure the appropriate membrane curvature and lipid content for viral replication (20, 21). Viral replication centers are also enriched in the Golgi protein PI4Kβ, which participates in synthesis of phosphoinositide membrane lipids. Higher levels of these

membrane lipids, in turn, recruit the PV RDRP to viral replication centers and provide the appropriate lipid microenvironment for PV replication (19).

The flavivirus hepatitis C virus (HCV) was shown to form a similar ER membrane-derived viral replication center referred to as the membranous web (22). It contains ER-derived membranes organized into a web of vesicles in close proximity to lipid droplets. Interestingly, HCV seems to have the same requirement of enriched phosphoinositide membrane lipids as PV for replication and therefore recruits a similar yet distinct ER-localized PI4K (PI4Kα) via the viral protein NS5A for this purpose (22-25).

Viral exploitation of host-derived membranes to facilitate replication has now been shown to be a requirement of all positive sense RNA viruses (26-28). These sites of replication exist in close proximity to sites of viral translation and assembly, allowing coordination of these closely linked processes (29). In fact, PV assembly requires actively replicating RNA, raising the notion that the membranous replication centers are important for steps in the viral life cycle beyond replication (30).

Regulation of the lipid content of host-derived membranes for viral replication seems to be a common theme among positive-sense RNA viruses. The viral requirement of membranes for replication explains the early observation that PV, like many other RNA viruses, modulates lipid biosynthesis (31). The flavivirus Dengue virus was also shown to affect lipids by modulating expression and distribution of the essential lipid synthesis molecule fatty acid synthase (FASN) to promote formation of its replication complexes (32). This is achieved by the viral protein NS3, which recruits FASN to the ER membrane where DENV replication centers are located and increases its activity in order to increase local availability of fatty acids. This in turn results in further formation of viral replication centers.

1.1.3 Innate Immunity

RNA viruses produce RNA species during their replication cycle that are recognized by the host cell as “foreign”, which is crucial for containment of RNA virus infection by the host innate immune response. As such, recognition of pathogen-derived nucleic acids is among the most important of the host cell’s defense against invading pathogens and represents another example of how host-pathogen interaction affects the outcome of disease. Endosome-localized toll like receptors (TLRs) and the cytosolic sensors of the RLR pathway are the major sensors of viral RNA (Fig 2).

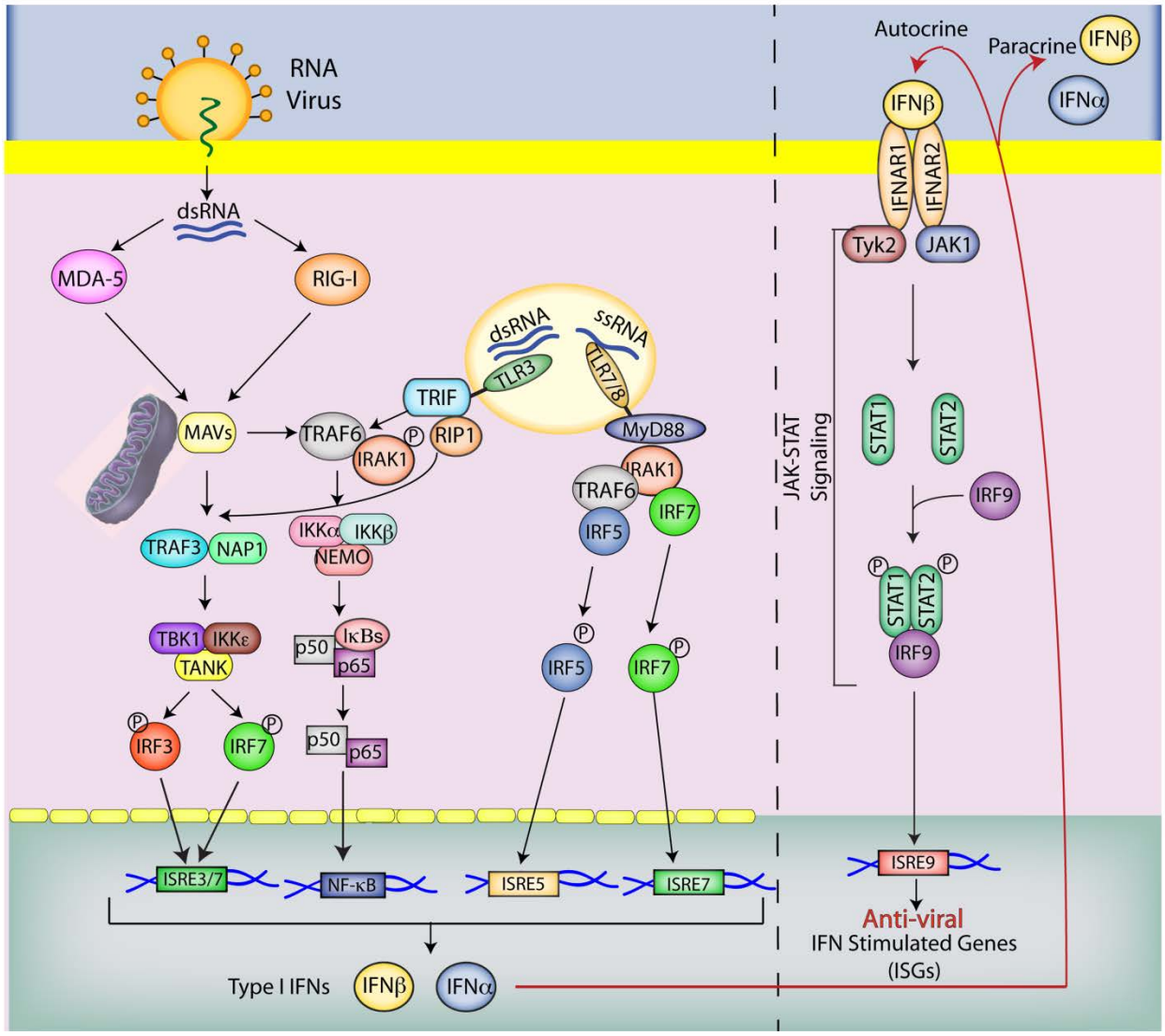

Figure 2. Innate Immune Signaling.

Incoming viral RNA is recognized by either the endosomal TLRs or the cytosolic RLRs. Type I interferon signaling then ensues to create an antiviral state. Schematic courtesy of Dr. Carolyn Coyne.

The endosome-localized TLRs known to recognize viral RNA are TLR3, TLR7, and TLR8. Although it remains unclear where exactly viral RNA sensing takes place, some evidence suggests

that in some cell types they may sense viral RNA directly following receptor-mediated endocytosis of viruses that utilize this entry pathway or through the fusing of infection-induced autophagasomes with the TLR-containing endosomes (33-40). TLR7 and TLR8 recognize ssRNA (37-39) and TLR3 recognizes dsRNA, including replication intermediates and by-products from a range of viruses with different nucleic acid compositions (35, 36, 40-42). Upon recognition of their respective ligands, the aforementioned TLRs initiate a signaling cascade resulting in the production of type I interferon and/or pro-inflammatory cytokines. TLR3 signals through TRIF and TRAF3, ultimately resulting in phosphorylation and nuclear translocation of IRF3 to activate transcription of IFN-β (43-46). TLR7 and TLR8 signal through MyD88 and TRAF6 ultimately resulting in the degradation of IκB and nuclear translocation of NF-κB to activate transcription of pro-inflammatory cytokines and/or the phosphorylation and nuclear translocation of IRF7 to activate transcription of IFN-α (47, 48).

Although there exists a certain degree of redundancy in terms of pathogen recognition and type I interferon/pro-inflammatory cytokine induction between endosomal TLRs and the RLR pathway, there are also important differences. Whereas the endosome-localized TLRs sense viral nucleic acids from within an endosome, the RLR pathway consists of cytosolic RNA sensors for recognition of actively replicating RNA viruses, which takes place only in the cytosol. Since some RNA viruses avoid exposure to the endosome, either due to the nature of their life cycle or strategies to evade innate immunity, this redundancy ensures recognition. It is important to note however, that like the endosomal TLRs, the exact location of RNA recognition by cytosolic RLRs remains unclear, and could include locations that are not strictly cytosolic. The cytosolic sensors of the RLR pathway also exist in a broader range of cell types than the endosomal TLRs, enabling many cell types to protect themselves and neighboring cells from viral infection.

The RLR pathway begins with recognition of distinct species of viral-derived RNA by one of the two cytosolic sensors retinoic acid inducible gene-I (RIG-I) and melanoma differentiation-associated gene 5 (MDA5). The first identified sensor of the RLR pathway was RIG-I, consisting of two N-terminal caspase recruitment domains (CARDs) that were sufficient to induce downstream signaling, a central DEAD box helicase/ATPase domain and a C-terminal regulatory domain necessary to prevent constitutive activation (49). The model holds that once RNA is bound an ATP-dependent conformational change takes place allowing the N-terminal CARD domains to interact with the downstream adaptors, an interaction that is facilitated by ubiquitination of RIG-I by the E3 ubiquitin ligase TRIM25 (50, 51). It recognizes RNA with uncapped 5'-ppp generated by viral polymerases and RNA containing short dsRNA structure motifs and/or poly-uridine motifs that mark RNA as non-self (49, 52-56). These ligands represent genetic material produced during replication of a variety of different positive and negative strand RNA viruses including some flaviviruses and orthomyxoviruses (57-59). The less characterized cytosolic sensor is MDA5, which structurally resembles RIG-I in that it contains two N-terminal CARD domains and a central DEAD box helicase/ATPase domain but lacks the C-terminal regulatory domain (60). MDA5 does not recognize uncapped 5'ppp RNA, and is thought to bind to activated long stable dsRNA structures such as RNA replication intermediates that might be hybridized to genome RNA during infection (61). Importantly, it is thought to be the main sensor responsible for recognition and response to picornavirus infection (62). There are also some groups of viruses that are recognized by both RIG-I and MDA5, including some flaviviruses, paramyxoviruses and reoviruses (57-59). The discrepancies and similarities between virus groups recognized by each sensor have been key in discovering their respective ligands, since each viral life cycle gives clues to the RNA species produced.

Although RIG-I and MDA5 differ in the cytoplasmic ligands they sense, they signal through a common mitochondria-localized adaptor (mitochondrial antiviral signaling, MAVS, also known as IPS-I, CARDIF, VISA) through interactions with their CARD domains. MAVS also contains an N-terminal CARD domain that mediates the interaction and the downstream signaling event, as well as a C-terminal transmembrane domain localizing it to the mitochondrial membrane. This localization is required for downstream signaling events as well (63-66). Beyond MAVS, many of the downstream signaling molecules overlap with those of the endosomal TLRs. MAVS-mediated antiviral signaling is propagated through assembly of a MAVS 'signalosome' including TRAF3, TRAF6, TRAF family member-associated NF-κB activator (TANK) and TANK binding kinase 1 (TBK1). The formation of a MAVS signaling complex results in the phosphorylation and nuclear translocation of interferon regulatory factor (IRF)-3 by TANK binding kinase 1 (TBK1) and/or IKKε, as well as activation of nuclear factor kappa beta (NF-κB) to induce type I interferons (IFNs) and pro-inflammatory cytokines (43, 45, 67, 68).

1.2 MAVS REGULOME

Because enhanced levels of inflammation can elicit cell damage and/or insufficient levels of inflammation can inhibit the ability of cells to remove the invading threat, mechanisms must be in place to tightly regulate antiviral signaling. Regulation at the mitochondrial level is quite strategic given that signals propagated by independent cytosolic sensors converge on MAVS at the mitochondrial membrane. Therefore, regulators of MAVS exert a higher level of control than they might if they targeted upstream components of RLR signaling such as RIG-I or MDA5

individually. In the following sections are detailed the variety of mechanisms by which regulators specifically modulate MAVS expression and/or signaling, with a focus on those that regulate by *(1)* protein-protein interactions, *(2)* alterations in mitochondrial dynamics, and/or *(3)* post-translational modifications (Figure 3 and Table 1, note: not all regulators presented in Figure 3 and Table 1 are discussed in the text).

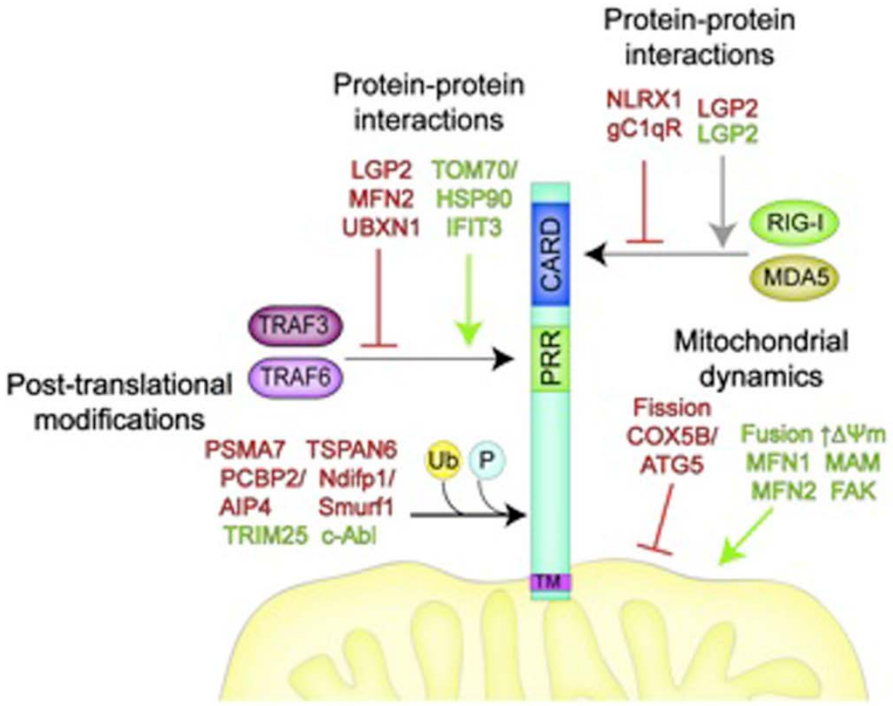

Figure 3. Mechanisms of MAVS regulation.

There are multiple mechanisms by which MAVS is regulated to exert cellular control over innate immune signaling. MAVS can be regulated by host cell factors that inhibit MAVS signaling by direct protein-protein interactions, by altering mitochondrial properties or dynamics, or by post-translational modifications. PRR, Proline-rich region; Ub, Ubiquitination; P, Phosphorylation. Positive regulators of MAVS signaling are shown in green text and negative regulators of MAVS signaling are shown in red text. Note that LGP2 is shown in both red and green given conflicting results on its role in the regulation of RLR signaling.

Table 1. The MAVS Regulome categorized by mechanism of regulation.

Ub, Ubiquitination; P, Phosphorylation; (+), positive regulation; (-), negative regulation

Protein-Protein Interactions	Mitochondrial Dynamics	Post-translational Modifications (Ub or P)
LGP2 (+/-) **(60, 69-74)**	Fusion (+)/Fission(-) **(75, 76)**	PSMA7 (-) (Ub) **(77)**
NLRX1 (-) **(78-82)**	MFN1 (+) **(75, 83)**	PCBP2/AIP4 (-) (Ub) **(84)**
MFN1 (+) **(75, 83)**	MFN2 (+) **(75, 76, 85)**	TRIM25 (+) (Ub) **(86)**
MFN2 (-) **(87)**	$\uparrow\Delta\Psi_m$ (+) **(76)**	Ndifp1/Smurf1 (-) (Ub) **(88)**
TOM70/HSP90 (+) **(89)**	MAM (+) **(75, 85)**	TSPAN6 (-) (Ub) **(90)**
IFIT3 (+) **(91)**	FAK (+) **(92)**	PLK1 (-) (P)* **(93)**
gC1qR (-) **(94)**	COX5B/ATG5 (-) **(95)**	C-Abl (+) (P) **(96)**
UBXN1 (-) **(97)**		

*PLK1 does not directly phosphorylate MAVS, but rather may require phosphorylation of MAVS for docking of PLK1 at an upstream site prior to PLK1 binding near the C terminus of MAVS where it exerts regulatory activity.

1.2.1 Regulation of MAVS by protein-protein interactions

In addition to RIG-I and MDA5, a third RNA helicase harboring a DExD/H box RNA helicase domain exists and is termed LGP2 (laboratory of genetics and physiology gene 2). LGP2 exhibits 30-40% amino acid sequence identity to RIG-I and MDA5 and is capable of dsRNA binding (60, 69). However, and quite importantly, LGP2 lacks a CARD with which to signal to downstream mediators of IFN induction, which has suggested a different function for LGP2 than for either RIG-I or MDA5. Consistent with a possible role in innate immune function, the expression of LGP2 is induced by type I IFNs, dsRNA, and virus infection (60, 69). However, unlike RIG-I and MDA5, overexpression of LGP2 results in a downregulation of IFN-β promoter activity (60, 69). Indeed, LGP2 has been suggested to serve as a negative regulator of the RLR pathway via its interaction with MAVS at the mitochondrial membrane, thus preventing its vital association with the downstream signaling molecule TRAF3 (70). A later study reported that MAVS homooligomerization of its N-terminal CARD domain, dependent on the C-terminal mitochondrial localization domain, resulted in more efficient signaling (73). This suggests that while LGP2 association with MAVS might prevent its association with TRAF3, it could also interfere with MAVS dimerization.

In addition to the negative regulation of MAVS, LPG2 has also been suggested to directly regulate RLRs themselves. $LGP2^{-/-}$ MEFS are more susceptible to synthetic RNA (poly (I:C)) stimulation of IFN production and $LGP2^{-/-}$ mice are less sensitive to lethal vesicular stomatitis virus (VSV) infection, a rhabdovirus known to signal through RIG-I (presumably due to enhanced IFN production and subsequent infection control). However, these results were not observed with encephalomyocarditis virus (EMCV), a picornavirus known to signal through MDA5 (74). These seemingly disparate results suggest that RIG-I may actually serve as the target of LGP2-mediated

downregulation of IFN production (71). A later study showed that LGP2 was actually a positive regulator of RLR signaling, facilitating RNA sensing by RIGI-I and MDA5, and was essential for the response of MDA5 to picornaviruses (72). Thus, the role of LGP2 in innate immunity remains somewhat unclear and more work is needed to determine at which step(s) of the RLR pathway LGP2 exerts its effect.

Mitochondrially-localized proteins represent logical candidates for the regulation of MAVS. The first mitochondrial protein that was identified as a negative regulator of MAVS was the nucleotide-binding domain (NBD)- and leucine-rich-repeat (LRR)-containing family member, NLRX1 (98). NLRXs are members of the NOD-like receptor family of cytosolic pattern recognition receptors (PRRs) that are involved in innate immunity independent of RLR signaling. This study successfully confirmed the putative localization of NLRX1 to the outer mitochondrial membrane, and went on to show that it interacted with MAVS via its CARD, disrupting vital MAVS interactions with upstream signaling partners (98). These data were corroborated in NLRX1$^{-/-}$ MEFs. IFN-β production was increased in NLRX1$^{-/-}$ MEFs infected with a variety of viruses known to engage RIG-I. However, there was no change in response to EMCV, a virus known to engage MDA5 (78). Interestingly, cells deficient in NLRX1 exhibited RIG-I/MAVS association even in the absence of infection whereas the MDA5/MAVS association was only present after viral infection (78). The constitutive association between RIG-I and MAVS in the absence of NLRX1 could account for the increase in IFN-β in response to infection with RIG-I-engaging viruses but not MDA5 engaging viruses. Conflicting results do exist, however, as subsequent studies in two independently-derived NLRX1$^{-/-}$ MEFs found no potentiation of IFN induction or IRF3 phosphorylation in response to poly (I:C) stimulation or Sendai virus (SeV) infection compared to WT MEFs, and no change in the serum level of IFN-β in NLRX1$^{-/-}$ mice

compared to WT mice upon injection with poly (I:C) (81, 82). Another study reported NLRX1-mediated inhibition of RLR signaling to be an artifact of inhibition of luciferase activity, which is quite relevant since many of the previous studies used luciferase-based assays to measure RLR signaling (79). Like LGP2 inhibition of MAVS activity, NLRX1 inhibition of MAVS activity has yielded conflicting results. It is certainly possible that NLRX1 has multiple regulatory roles, depending on whether positive or negative regulation is advantageous for the cell but more studies are needed to reconcile disparate findings and elucidate the role of NLRX1 in MAVS signaling.

The mitofusins (MFN1 and MFN2) are residential outer mitochondrial membrane proteins that play roles in regulating mitochondrial dynamics by controlling fusion, and MFN2 has been reported to act as a mitochondria-ER tethering protein (99, 100). While screening the MAVS mitochondrial supramolecular complex by mass spectrometry for MAVS interacting partners, MFN2 was identified as an interacting partner of MAVS (87). Upon further investigation, overexpression of MFN2, but not MFN1, was found to inhibit RIG-I-, MDA5-, and MAVS-mediated type I IFN induction. Conversely, RNAi–mediated silencing of MFN2 as well as studies in MFN2$^{-/-}$ MEFs showed that RLR signaling was enhanced in knockdown cells, a phenotype that was reversed upon addition of exogenous MFN2 into these cells. These results were corroborated in a later study (76). Immunoprecipitation studies confirmed that MAVS and MFN2 interact and that this interaction was dependent upon the mitochondrial localization of MAVS and occurred between a central hydrophobic heptad repeat (HR1) region of MFN2 and a C terminal region of MAVS (87).

1.2.2 Regulation of MAVS by mitochondrial dynamics

Utilizing protein-protein interactions as a means of regulating of MAVS-mediated innate immune signaling is clearly important. However, the physical properties of the mitochondria and the resulting changes in MAVS distribution and/or aggregation can also play an important role in its regulation. Initial evidence for the role of mitochondrial dynamics in MAVS signaling came from studies demonstrating that infection of cells with Sendai virus or transfection of poly (I:C) resulted in elongation and/or fusion of mitochondria, leading the authors to conclude that activation of RLR signaling results in physical alterations in the mitochondria themselves (75). Indeed, this study also showed that phosphorylation of IRF3 was delayed in cells with fragmented mitochondria and that RLR signaling was attenuated by mitochondrial fragmentation, but enhanced upon mitochondrial fusion. Immunoprecipitation experiments showed that MAVS forms an interaction with mitofusin 1 (MFN1), a protein that regulates mitochondrial fusion events, suggesting a possible role for this interaction in the regulation of the mitochondrial dynamics that accompany antiviral signaling. Interestingly, a later study also reported on the interaction of MFN1 with MAVS and further showed that MFN1 acts as a positive regulator of MAVS-mediated antiviral signaling by redistributing MAVS to speckle-like aggregates observed upon activation of RLR signaling (83). This could explain why MFN1 and mitochondrial fusion seem to be important for RLR signaling given that fusion of the mitochondria could facilitate MAVS aggregation. Others further investigated the role of MFNs in MAVS signaling using MEFs deficient in both MFN1 and MFN2 (MFNs-dm) (76). These cells were unable to undergo mitochondrial fusion, and were impaired in their ability to produce IFN-β and IL-6 in response to viral infection. In light of the results of these studies, it is likely that the role of MFNs in innate immune signaling is multifold. Not only do both MFN1 and MFN2 interact directly with MAVS to exert a regulatory role, but

their activities in mitochondrial dynamics also appear to be important for MAVS functioning. This is in accordance with earlier reports that MAVS activation requires self-association into higher order oligomers (73) as well as formation of large prion-like aggregates for potent propagation of antiviral signaling (101). Other studies have also pointed to a direct role for another mitochondrial process in RLR signaling as carbonyl cyanide *m*-chlorophenylhydrazone (CCCP), a compound known to dissipate mitochondrial membrane potential ($\Delta\Psi_m$), resulted in suppressed innate immune signaling (76), thus suggesting that $\Delta\Psi_m$ is another example of a mitochondrial process that is important for regulation of MAVS-mediated signaling. Taken together, these reports suggest that mitochondrial elongation and fusion may facilitate the aggregation of MAVS into active complexes primed for maximum signaling capacity.

In addition to regulating mitochondrial fusion, MFN2 is also important in the tethering of the mitochondria to the ER at the mitochondria-associated membrane (MAM). The MAM is emerging as an important subcellular domain in MAVS signaling. For example, virally-infected cells exhibit increased numbers of ER contacts with elongated mitochondria compared to uninfected control cells, suggesting that ER-mitochondria contacts increase upon infection-induced mitochondrial fusion and elongation (75). This of particular significance given that the population of MAVS residing at the MAM is important for antiviral signaling (85).

Regulation of reactive oxygen species (ROS) production has also been reported to play a role in the regulation of RLR signaling from the mitochondria (102-105). While examining the mechanism for this phenomenon, Zhao et al. described cytochrome C oxidase (COX) 5B as a MAVS interacting partner responsible for repression of ROS- and RLR-signaling (95). COX5B is a mitochondrial protein and is a member of the cytochrome c oxidase complex (CcO), the complex that catalyzes the last step in the electron transport chain (106). Overexpression of

COX5B decreased MAVS-mediated antiviral signaling without having any effect on TLR-mediated or TNF-α-induced signals, suggesting the effect was specific to the RLR pathway (95). Cells depleted of COX5B also exhibited enhanced antiviral signaling. Interestingly, in addition to its role in ATP production, COX5B has been shown to be involved in the negative regulation of ROS production (107). To investigate the possible role of this pathway in COX5B-mediated regulation of MAVS, the authors utilized two compounds reported to alter ROS levels and found that an increase in ROS resulted in an increase in MAVS-mediated signaling and decreasing ROS levels resulted in a decrease of MAVS-mediated signaling. In addition, cells expressing exogenous MAVS produced higher levels of ROS, which was abrogated by exogenous COX5B (95). Interestingly, COX5B expression was not induced by addition of purified IFN-β, but was induced in the presence of overexpressed MAVS, suggesting that it is not an interferon-inducible gene but its expression is coordinated with MAVS expression for its specific negative regulation.

MAVS overexpression induces autophagy (or perhaps, more specifically, mitophagy) (95) and ROS production has also been associated with the induction of autophagy (108). Because autophagy is involved in the removal of aggregated proteins (109, 110) and the aggregation of MAVS during RLR activation is known to potentiate signaling (73, 83, 101), COX5B and regulators of autophagy such as ATG5 might regulate MAVS-mediated signaling by affecting MAVS aggregation upon its activation. Indeed, MAVS aggregation is affected by the expression of ATG5 and COX5B, with overexpression leading to decreased aggregation and depletion leading to increased aggregation (95). These results suggest that COX5B works coordinately with ATG5 to negatively regulate MAVS-mediated antiviral signaling through an increased clearance of MAVS aggregates in addition to its role in repression of ROS production.

1.2.3 Regulation of MAVS by post-translational modification

The post-translational control of proteins is a common means by which cells regulate diverse pathways and processes. It is thus not surprising that post-translational modifications of MAVS and/or its interacting partners are a key aspect of host cell regulation of antiviral signaling. A yeast two-hybrid screen for MAVS interacting partners identified the proteasomal component PSMA7 as a MAVS interacting partner (77). PSMA7 is a subunit comprising the outer ring of the 20S catalytic core complex of the 26S proteasome and is involved in proteasomal activity regulation (111, 112). MAVS interaction with PSMA7 requires both the C-terminal transmembrane domain and the CARD region of MAVS (77). Overexpression of PSMA7 reduced IFN-β induction and suppressed VSV infection whereas its silencing yielded the opposite results. Consistent with these findings, overexpression or depletion of PSMA7 decreased or increased endogenous MAVS protein levels, respectively (77). Importantly, MAVS mRNA levels remained unchanged in response to these manipulations, suggesting that PSMA7 modulated MAVS levels post-transcriptionally. Indeed, PSMA7 overexpression induced the ubiquitination of MAVS, implicating the PSMA7-mediated proteasomal degradation of MAVS. However, given that PSMA7 protein has not been shown to be involved in the process of protein ubiquitination itself, it is clearly not the only player in this process. Thus, it remains to be seen if PSMA7 recruits enzymes of the ubiquitination pathway for MAVS ubiquitination prior to recruiting ubiquitinated MAVS to the proteasome for degradation.

The multi-protein requirement for ubiquitin-mediated degradation and negative regulation of MAVS is emerging as a common theme in the regulation of RLR signaling. After performing a yeast two-hybrid screen in search of interacting partners of MAVS, poly(rC) binding protein 2 (PCBP2) was identified as a negative regulator of MAVS (84). PCBP2 is involved in RNA and

DNA binding with many different purposes in the cell, including mRNA stability and translation regulation (113). Overexpression of PCBP2 resulted in suppression of MAVS-mediated IFN-β induction, but had no effect on TBK1- or IRF3-induced signaling. PCBP2 expression was highly inducible by interferon treatment and virus infection, and the interaction between endogenous PCBP2 and endogenous MAVS was inducible by Sendai virus infection. Subcellular localization studies showed that endogenous PCBP2 localized primarily to the nucleus, but relocalized to the cytoplasm where it colocalized with MAVS upon viral infection or MAVS overexpression. Despite lacking any ubiquitin ligase activity itself, PCBP2 overexpression induced a dramatic proteasome-dependent degradation of MAVS. Using mutational analysis of MAVS, the authors showed that ubiquitination of two specific lysine residues led to its degradation, and that the levels of MAVS polyubiquitination were higher in the presence of overexpressed PCBP2. Given that PCBP2 is not an enzyme of the ubiquitination pathway, the authors hypothesized that PCBP2 could be acting as physical scaffold linking MAVS to an E3 ubiquitin ligase. Screening known E3 ubiquitin ligases for a candidate that both mediates degradation of MAVS and binds to PCBP2, the authors found the Nedd4-like E3 ubiquitin ligase AIP4. Overexpression of AIP4 partially abrogated IFN-β signaling and induced MAVS degradation in a manner dependent on its E3 ubiquitin ligase activity. Although AIP4 and MAVS were shown to interact, this interaction required PCBP2, suggesting that PCBP2 acts as a scaffold to facilitate AIP4-mediated degradation of MAVS. This was confirmed using *in vitro* ubiquitination assays which showed that PCBP2 expression greatly increased the AIP4-mediated ubiquitination and degradation of MAVS. Finally, type I IFN signaling was enhanced in Itch (the mouse homologue of AIP4)$^{-/-}$ MEFs further linking this E3 ligase to MAVS signaling. Collectively, this study nicely showed that PCBP2 acts as an adaptor for AIP4-mediated ubiquitination and subsequent proteasomal degradation of MAVS for

negative regulation of RLR signaling, elucidating a quite novel and interesting mechanism of RLR regulation. A later report by the same group showed that PCBP1, a protein highly similar to PCPB2 (114, 115), is also involved in negative regulation of MAVS-mediated signaling using a similar mechanism (116). However, unlike PCBP2, PCBP1 is not induced by type I IFNs, leading the authors to conclude that it is a "housekeeper" of MAVS levels rather than a negative feedback inhibitor.

Ndfip1 has also been classified as a negative regulator of MAVS at the mitochondria through enhancement of ubiquitination and proteasomal degradation (88). In light of mounting evidence linking E3 ubiquitin ligase activity to MAVS regulation, Ndifp1 is a logical candidate given its reported role in enhancement of protein ubiquitination through interaction with a family of E3 ubiquitin ligases known as Nedd4 ubiquitin ligases, particularly in signaling pathways (117, 118). MAVS-mediated signaling was inhibited by Ndfip1 in a proteasome dependent manner. As these results pointed to ubiquitination-mediated proteasomal degradation as the mechanism of negative regulation of MAVS by Ndifp1, the authors next screened the four known members of the Nedd4 E3 ubiquitin ligase family for their ability to induce MAVS degradation in the presence of Ndifp1. The Nedd4 E3 ubiquitin ligase Smurf1 was shown to lead to degradation of MAVS, but not of RIG-I or TBK1, in the presence of Ndifp1. The interaction between Smurf1 and MAVS was increased in the presence of Ndifp1, as was the Smurf1-mediated ubiquitination of MAVS, indicating that Ndifp1 likely serves as an adaptor for recruitment of Smurf1 to MAVS. This study described a mechanism of MAVS negative regulation that is quite similar to that of PCBP2 and AIP4 as discussed above, and provides yet another example of the complexity of ubiquitination in the regulation of MAVS signaling.

Adding a different twist to the recently emerging and growing role of ubiquitination in RLR signaling, tetraspanin protein 6 (TSPAN6) was recently described to play a role in MAVS-mediated RLR signaling (90). TSPAN6 is a member of the membrane-embedded tetraspanin protein family that has been shown to have many different functions in the cell, including various roles in host immunity (119). Interestingly, TSPAN6 does not promote the ubiquitination of MAVS either directly or indirectly, but is itself ubiquitinated in order to promote its association with MAVS and disrupt the mitochondrial-localized signalosome. Overexpression of TSPAN6 resulted in a reduction of exogenous MAVS-induced signaling and was shown to interact with MAVS. TSPAN6 is ubiquitinated in response to RLR activation, which is involved in its association with MAVS. The authors propose that ubiquitination of TSPAN6 in the presence of viral infection promotes its recruitment to the mitochondria where it interacts with MAVS, abrogating the assembly of the signalosome and thus inhibiting antiviral signaling. The enzyme(s) responsible for ubiquitination of TSPAN6 in the context of RLR activation remains to be discovered.

Like ubiquitination, phosphorylation represents a post-translational mechanism of protein regulation in many cellular processes. Yeast two-hybrid screening identified the Polo-like kinase 1 (PLK1) as an interacting partner for MAVS (93). PLK1 is a serine/threonine Polo-like kinase (120-122). Contrary to other known regulators of MAVS, induction of antiviral signaling did not enhance the association between MAVS and PLK1. PLK1 interacts with MAVS at two unique regions, downstream of the CARD region and just upstream of the C terminus (the interaction downstream of the CARD region is dependent upon phosphorylation of MAVS at position Thr^{234}) (93). The phosphorylation-independent C-terminal interaction was shown to be responsible for the attenuation of IFN signaling due to a disruption of MAVS-TRAF3 interaction. This finding has

been corroborated by more recent work that has uncovered a second TRAF3 binding site in MAVS corresponding to this same region (123). Work is ongoing to determine the specific kinase(s) responsible for the primary phosphorylation of MAVS that facilitates PLK1 binding.

More recently, the tyrosine kinase c-Abl was identified as a MAVS-interacting partner that acts as a positive regulator of MAVS by direct interaction and phosphorylation (96). c-Abl is a nuclear and cytoplasmic Src-like non-receptor protein tyrosine kinase that is known to serve many cellular functions (124). The interaction between MAVS and c-Abl was shown to require both the transmembrane domain and CARD of MAVS, likely suggesting that mitochondrial localization of MAVS is required for this interaction. Depletion of c-Abl resulted in abrogation of MAVS signaling and pharmacological inhibition of c-Abl abrogated IFN-β production in response to VSV infection. The tyrosine phosphorylation of MAVS was enhanced by c-Abl expression, but not by a c-Abl mutant defective in kinase activity. In a later report, tyrosine-scanning mutational analysis revealed that inducible phosphorylation at Tyr^9 of MAVS was involved in the recruitment of TRAF3/TRAF6 to propagate MAVS-mediated RLR signaling (125). Whether c-Abl is involved in phosphorylation of Tyr^9 of MAVS remains to be determined, and would represent an interesting follow-up to these two studies.

In conclusion, antiviral signaling is an extremely powerful cellular response that necessitates tight regulation in order to adequately neutralize invading threats while avoiding damage to the cell from excessive inflammation. A large portion of antiviral signaling regulation has evolved at the mitochondria due to its pivotal position in the antiviral signaling pathway. Strategically, this is a logical step for regulation because of the convergence of independent upstream sensors on the common mitochondrial signaling adaptor protein MAVS. As discussed above, the cell employs many diverse mechanisms to regulate MAVS, including protein-protein

interactions for physical blockage of MAVS association with upstream or downstream signaling partners, alterations of mitochondrial physical dynamics as well as the physical distribution/aggregation of MAVS, and post-translational modifications such as phosphorylation and ubiquitination. Although remarkable progress has been made, there is still much to be learned regarding the myriad of mechanisms by which host cells regulate MAVS-mediated signaling. Ongoing work in the field will continue to identify MAVS regulators, hopefully providing a complete picture of the MAVS regulome.

1.3 GP78/AMFR

Autocrine motility factor receptor (AMFR, gp78) was discovered as a cell surface receptor for the cytokine autocrine motility factor (AMF), the activity of which has been linked with increased cancer metastasis presumably due to its role in cell differentiation, survival and growth. The presence of AMF and AMFR has been correlated with poor cancer prognosis and tumor cell motility (126-131). Sequence analysis later pointed to a putative role as an E3 ubiquitin ligase due to the presence of a RING domain and a Cue domain (132), and it has now been extensively characterized as a five transmembrane ER-localized E3 ubiquitin ligase of the ER-associated degradation (ERAD) pathway. The ERAD pathway recognizes misfolded proteins in the ER, marking them for proteasomal degradation by the process of ubiquitination (133). The process of ubiquitination relies on three classes of enzymes: E1, E2 and E3. E1s are the ubiquitin activating enzymes, which bond to the ubiquitin molecule via a thiol ester bond, passing the activated ubiquitin to the E2s. The E2s are the ubiquitin conjugating enzymes, and the E3s are the ligases responsible for transfer and ligation of the ubiquitin from the E2s to the

substrate. Addition of ubiquitin molecules to the substrate is repeated until a polyubiquitin chain is formed and the substrate is degraded (134). The E3 ubiquitin ligase activity of Gp78 requires a C-terminal RING domain (responsible for ubiquitin ligase activity), Cue domain (responsible for ubiquitin binding), and E2 binding site (135-137). The C-terminus also contains a site of interaction with the AAA ATPase p97 (VCP), which provides the driving force for translocation of the polyubiquitinated substrates to the cytosol for subsequent degradation by the proteasome (Figure 4) (138-141). Known substrates of Gp78 include the mutant cystic fibrosis transmembrane regulator (CFTRΔ508) (142), HMGCoA reductase (a key enzyme in the cholesterol synthesis pathway), which is degraded in a regulatory manner in response to high cholesterol levels (143), apolipoprotein B (the protein component of low and very low density lipoprotein), which is also degraded in a regulatory manner (144), and KAI1 (CD82), which is a tetraspanin metastasis suppressor (145). In localization studies it was found both in the plasma membrane in caveolae, consistent with its role as a cell surface receptor, and, importantly, at the peripheral smooth ER in close association with mitochondria (146-150). The Gp78-specific antibody 3F3A was shown early on to label smooth ER tubules distinct from the rough ER, representing a distinct subpopulation of Gp78 (147, 149). These 3F3A-labeled tubules were shown to exhibit direct calcium-dependent interactions with mitochondria, thus Gp78 can be described as MAM-localized (148, 150). Interestingly, this interaction may have consequences for the mitochondria since exogenous Gp78 was recently shown to induce proteasomal degradation of the mitofusin proteins MFN1 and MFN2 resulting in mitochondrial fragmentation. Gp78 was further shown to induce mitophagy upon depolarization of the mitochondrial membrane (151).

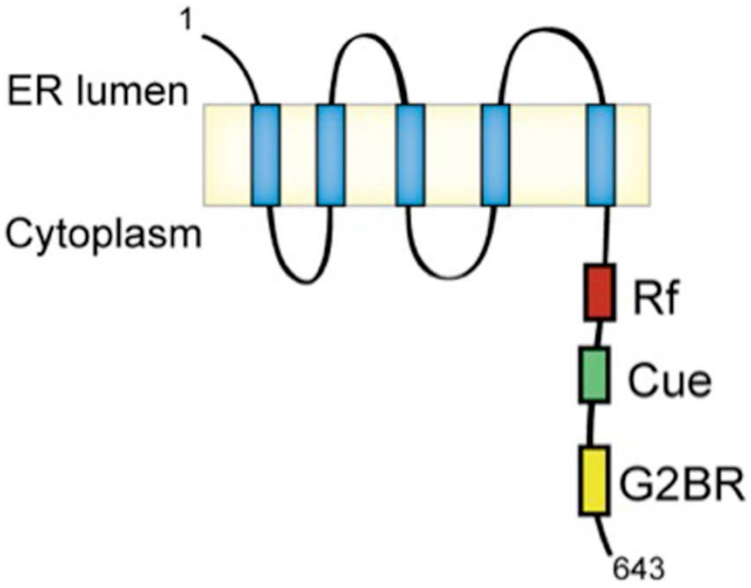

Figure 4. Topology of Gp78.

Gp78 is an ER-localized membrane-bound E3 ubiquitin ligase of the ERAD pathway, requiring its ring finger (RF), Cue, and E2 binding region (G2BR) for its ligase activity**.** Schematic courtesy of Dr. Carolyn Coyne.

1.4 ER MORPHOLOGY

The endoplasmic reticulum (ER) is a large cellular organelle that is involved in production of membrane-bound and secreted proteins, lipids, maintaining calcium homeostasis, and protein quality control. It consists of an extensive and dynamic continuous membrane-bound system throughout the interior of the cell that is contiguous with the nuclear membrane and stretches into the periphery of the cell. The ER membrane system can be divided into two distinct morphological categories. The nuclear envelope and perinuclear region of the ER is formed from sheet-like

cisternal structures, in which flat membranes are arranged closely spaced to one another. The peripheral ER is comprised of tubules of ~50 nm diameter (152-155). These distinct domains appear to have distinct functions as well. The ER sheets that make up the perinuclear ER consist mostly of "rough" ER, meaning the sheets are studded with ribosomes. Therefore, this region of the ER is involved in production of secreted and membrane proteins. The tubular peripheral ER is comprised of mostly smooth ER (lacking ribosomes) and is involved in functions other than protein production, such as lipid synthesis, calcium homeostasis, contact with other cellular organelles (such as endosomes and mitochondria) and lipid droplet formation (156-160). The proportion of rough perinuclear ER sheets to tubular, smooth peripheral ER is often dependent on the function of the cell type, as well as the cellular growth stage and external conditions. For example, professional secretory cells contain a higher amount of rough ER sheets than smooth ER tubules due to the necessity for high levels of protein production, whereas a hepatic cell contains a higher amount of smooth ER tubules because of an increased need for carbohydrate metabolism (154).

An important feature of ER membranes that accounts for morphologic differences between regions is the degree of membrane curvature. The diameter of ER tubules as well as the luminal thickness of ER sheets are ~50 nm, but the difference in their shapes lies in the degree of membrane curvature. ER tubules have a much higher degree of membrane curvature than sheets, which are curved only at the ends of longer leafs (161). Interestingly, the sites of ER-to-Golgi secretory pathway initiation, termed ER exit sites (where COP-II-coated vesicles bud bearing newly synthesized proteins headed for the Golgi apparatus), have been shown in highly curved tubular regions of the ER such as the tubular regions and the ends of ER sheets, possibly due to the ease of vesicle budding from a highly curved membrane surface (162).

Generating and maintaining ER curvature is accomplished by a number of proteins. The high curvature in ER tubules is achieved by the reticulon and DP1/Yop1p families of proteins, and this is reflected by their enrichment in tubular regions of the ER as well as the curved edges of ER sheets (163, 164). Both families of proteins are proposed to work by inserting into the ER membrane outer leaflet using two transmembrane domains, therefore causing a wedge in the membrane and forcing membrane curvature (163, 165).

Although the previously mentioned proteins are required for the membrane curvature required at the ends of ER sheets, an independent set of proteins is responsible for the formation of the flat apposed membranes characteristic of the interior of ER sheets. These proteins were implicated in formation of ER sheets when identified via a screen for proteins enriched in the sheet-containing domain of the ER, and they include Climp63, p180, and kinectin (164). All three of these proteins contain coiled-coil domains that function in the formation and stabilization of ER sheets in different ways. Whereas the coiled-coil domain of Climp63 inserts into the lumen of the ER and aids in attachment of the two apposed membranes holding them at a fixed distance from each other, the coiled-coil domains of both p180 and kinectin are extra-lumenal and are proposed to maintain the flatness of the ER sheets (166). There is also evidence that the presence of ribosomes on ER sheets is important in formation and/or stabilization of sheet morphology (164, 167).

1.5 ENDOSOME MATURATION

Endosomes are the intracellular membrane-bound vesicles resulting from cellular endocytosis. They function to recycle cellular components to and from the plasma membrane and/or to shuttle

cellular components to lysosomes for degradation. Endosome maturation begins with fusion of incoming endocytic vesicles to form early endosomes (EE). The membrane of the EE contains Rab5 and a phosphatidylinositol 3- kinase (PI3K) complex responsible for converting the lipid phosphatidylinositol (PI) to phosphatidylinositol 3- phosphate (PI3P). Both Rab5 and the PI3K complex are important markers of immature EE, and serve to recruit factors necessary for cargo sorting as well as fusion and maturation of the EE (168-170). As PI3P accumulates in the membrane of the EE, EEA1 is recruited, which marks the EE as mature (171). Most EEs are small compared to late endosomes (LE) and lysosomes, and exist in the periphery of the cell close to the plasma membrane (172, 173). Interestingly, as endosomes mature they become larger due to fusion events, migrate towards the perinuclear region of the cell, become more closely associated with the ER, and become progressively more acidic (159, 174).

Maturation of EE to LE involves what is known as a 'Rab switch', in which Rab5 recruits Rab7 resulting in loss of Rab5 from the LE (175, 176). This switch begins maturation to LE and therefore commitment of the endosome to later fusion with a lysosome for cargo degradation rather than recycling of cargo back to the plasma membrane. Maturation of LE also involves further conversion of the endosomal membrane phosphoinositides to phosphatidylinositol (3,5)-phopshate-2 (PI(3,5)P2), with accumulation of PI(3,5)P2 in the membrane indicative of progression to LE (177, 178). This is important for further endosomal maturation because PI(3,5)P2 recruits a different profile of effector proteins to the membrane of the LE than PI3P recruits to the membrane of EE, directing the differential functions of EE vs. LE. Notably, inhibition of PI conversion leads to a highly vacuolated phenotype and enlarged endosomes (179-181). The final step in the degradative endocytic pathway is fusion of the LE with a lysosome, which contains low pH and degradative enzymes.

1.6 BPI/LBP PROTEIN FAMILY

1.6.1 BPI

Bactericidal permeability increasing protein (BPI) is an inducible cationic antimicrobial peptide expressed in several types of leukocytes, fibroblasts and epithelial cells (182-185). It exerts its antimicrobial function by binding to the Lipid A motif of the lipopolysaccharide (LPS) present on the exterior of all gram-negative bacteria, effectively neutralizing the endotoxicity of LPS and opsonizing the bacterium for phagocytosis by immune cells (186). It also exerts direct antimicrobial activity by damaging bacterial membrane integrity thus leading to bacterial cytotoxicity (187). The crystal structure of BPI has been solved, and reveals a 55 kDa boomerang-shaped structure (Figure 5, (188)), the N-terminus of which contains the lysine-rich cationic region responsible for LPS-neutralizing and direct anti-bacterial activity (189). The C-terminus contains the opsonizing activity (190).

1.6.2 LBP

LPS-binding protein (LBP) is a member of the BPI/LBP family of proteins and shares significant primary structural homology to BPI. LBP also plays a significant role in lipid recognition and host defense, however its role is seemingly antagonistic to that of BPI. It is an anionic protein residing in the plasma that enhances immune responses to monomeric LPS by binding and delivering it to

the TLR4/CD14/MD2 receptor complex (191, 192). Although they are structurally similar, it is differences in the C-termini of BPI and LBP that determine their differential functions (193). The higher affinity of BPI for LPS as well as its concentrated presence at sites of high inflammation favor the binding of the antimicrobial and endotoxin neutralizing BPI to LPS, and therefore precludes the ability of LBP to cause an excessive amount of inflammation in response to LPS (194, 195). This is also achieved simply by the binding of aggregated LPS by BPI preventing its disassociation into monomers, and therefore preventing the binding of LBP to monomeric LPS (196).

1.6.3 BPIFB3/LPLUNC3

BPIFB3 (RYA3, LPLUNC3) was originally described in rats as a lipid-binding protein exclusively found in olfactory mucosa. Due to its lipid-binding properties and its expression pattern in rats it was proposed to be an oderant-binding protein (197). This initial characterization was later expanded when it was genetically mapped to a region about 5 Mb upstream of the bactericidal permeability increasing (BPI)/LPS-binding protein (LBP) family of lipid binding and antimicrobial genes. The RY gene cluster and other genes of the BPI/LBP family share significant sequence homology, including cholesterylester transfer protein (CETP) and phospholipid transfer protein (PLTP), both of which are involved in lipid transport in plasma (198). Around the same time the RY gene cluster was described, the PLUNC subfamily of BPI/LBP proteins (palate, lung and nasal epithelium clone) was discovered, consisting of at least 10 different proteins with predicted expression in humans (199-201). They are described as BPI homologs expressed at mucosal surfaces, although little is known about their function. They appear to have the ability to bind to bacteria and LPS, but do not directly neutralize or kill

bacteria (202). The PLUNC proteins are divided into two groups, the long (LPLUNC) and short (SPLUNC). LPLUNCS have sequence and structure homology to both the LPS-binding N-terminus and the C-terminus of BPI (Figure 5, (188)), which is responsible for its opsonization activity, and SPLUNCS have homology to only the N-terminal half of BPI (200). The RY genes were reported to be members of the PLUNC family (LPLUNC2-4), RYA3 (BPIFB3) as LPLUNC3 (203). BPIFB3 has not been functionally characterized, and any assigned putative function is largely due to its homology with lipid-binding antimicrobial proteins of the LBP/BPI superfamily and its previously reported expression profile in olfactory mucosa.

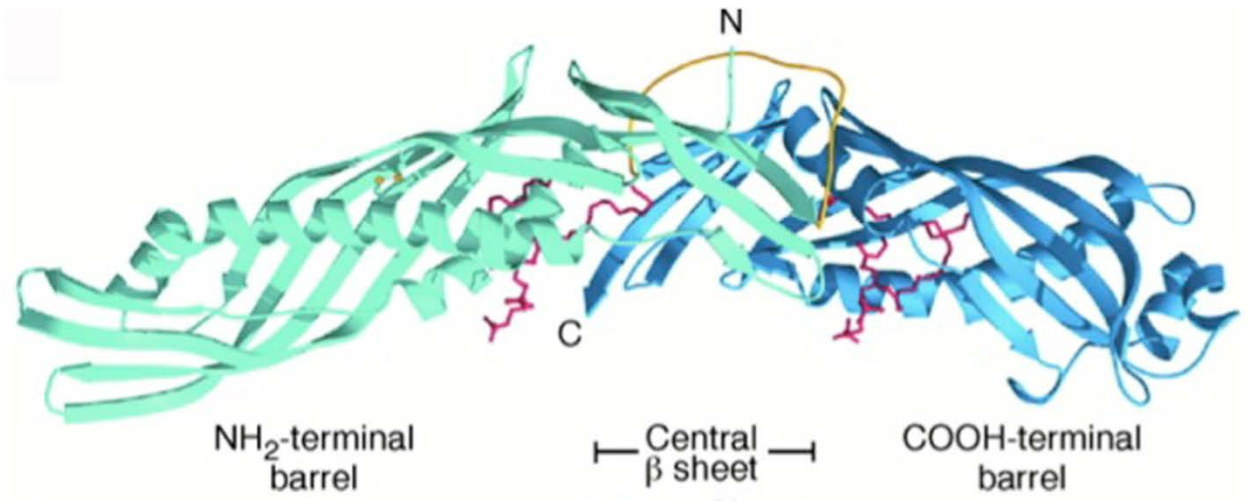

Figure 5. Structure of bactericidal permeability increasing protein (BPI).

The structure of BPI is described as a boomerang shape, with lipid-binding regions at both the C- and N-termini. BPIFB3 is reported to contain a similar structure. From Beamer, L. J., S. F. Carroll, and D. Eisenberg. 1997. Crystal structure of human BPI and two bound phospholipids at 2.4 angstrom resolution. Science 276:1861-1864. Reprinted with permission from AAAS.

2.0 STATEMENT OF THE PROBLEM

To develop therapeutics for viral infections, it is crucial to understand the relationships between viruses and host cells, because this complex interplay often dictates the outcome of infection at both the cellular and organismal levels. There are many different steps in a virus' lifecycle that lead to interactions with components of the host cell it is invading. Some of these interactions are beneficial to the virus or crucial for completion of its life cycle, and others are detrimental to the virus and serve to aid the host cell in recognition and eradication of virus infection. For example, the RLRs are host proteins that reside in the host cell cytoplasm and recognize foreign nucleic acid derived from viral infection, resulting in initiation of an anti-viral state that is detrimental to the virus. Conversely, all positive-sense RNA viruses are known to utilize host cell-derived membranes to facilitate their replication and thus successful completion of the viral life cycle. To identify novel regulators of enterovirus replication, we previously performed a high-throughput RNAi screen (HTS) using human brain microvascular endothelial cells (hBMECs), an *in vitro* model of the blood brain barrier (204). **We chose two screen 'hits' for follow-up (Gp78 and BPIFB3), and hypothesized that they were novel regulators of enterovirus infection that may function more broadly in the life cycles of other unrelated viruses as well.**

Aim 1: Define the role of Gp78 in regulating enterovirus replication. Gp78 exists both at the cell membrane where it regulates motility in response to autocrine motility factor binding and at the mitochondria-ER interface where it acts in the ERAD pathway as an E3 ubiquitin ligase. In this aim we showed that Gp78 depletion restricts infection of two unrelated RNA viruses, CVB and VSV. We went on to show that Gp78 negatively regulates type I IFN signaling. We showed that Gp78 regulates MAVS-mediated type I IFN signaling by two independent mechanisms: (1)

by specific and post-translational Gp78-mediated degradation of MAVS, a critical adaptor for RLR-mediated antiviral signaling; and (2) by protein-protein interaction between Gp78 and MAVS. Gp78-mediated degradation of MAVS was proteasome-dependent and required the E3 ubiquitin ligase activity of Gp78, and the Gp78-MAVS interaction required the RING domain of Gp78. We therefore showed that Gp78 regulates enterovirus infection by modulating MAVS-mediated type I IFN signaling, also providing a mechanistic explanation for this modulation.

Aim 2: Characterize the role of BPIFB3 in enterovirus infection. BPIFB3 (RYA3, LPLUNC3) is a largely uncharacterized protein of the BPI/LBP family of proteins. This family of lipid-binding antimicrobial proteins includes the PLUNC group of proteins, which has been described as a family of candidate host defense proteins in the upper airways. In this aim we showed that depletion of BPIFB3 in hBMECs significantly enhances enterovirus infection. We went on to investigate its localization and showed that BPIFB3 localizes to the ER, and that this localization has consequences for ER morphology and calcium homeostasis since depletion of BPIFB3 resulted in disruption of ER morphology and ER-regulated calcium homeostasis. In order to further unravel its role in virus infection, we examined the effect of BPIFB3 depletion on infection of a diverse group of viruses and show that whereas infection by the other enteroviruses PV and enterovirus 71 (EV71) is enhanced, infection by VSV and VV is restricted in the absence of BPIFB3. Additionally, VSV-mediated syncytia formation was enhanced in the absence of BPIFB3, a phenomenon that may correlate with an observed increase in size and number of cellular vesicles and endosomes/lysosomes. Overall, these results led us to the conclusion that the disruptions of ER morphology and endo/lysosome trafficking likely account for the alterations in virus infection seen in the absence of BPIFB3.

In this study, we defined the specific functions of two of the potential novel regulators of enterovirus infection identified by HTS: Gp78 (AMFR), whose depletion significantly restricted infection, and BPIFB3 (RYA3, LPLUNC3), whose depletion significantly enhanced infection. We showed that these two proteins are crucial components of the virus-host cell interaction, playing previously uncharacterized roles in modulating viral infection.

3.0 MATERIALS AND METHODS

3.1 CELLS AND VIRUSES

HEK293T cells, human fibrosarcoma HT1080 cells, human osteosarcoma U2OS cells, HeLa cells, and Vero cells were cultured in DMEM-H supplemented with 10% FBS and 1× penicillin/streptomycin. Human brain microvascular endothelial cells (HBMEC) were obtained from Dr. Kwang Sik Kim, and were cultured in RPMI 1640 supplemented with 10% FBS, 10% Nuserum, 1mM sodium pyruvate, non-essential amino acids, vitamins, and penicillin/streptomycin (1x), as previously described (204, 205). Stable U2OS cells expressing BPIFB3-Flag were constructed by selection in G418 (500µg/mL) followed by isolation by limiting dilution. Experiments were performed with CVB3-RD at 3 plaque forming units (pfu)/cell (expanded as previously described (92)), PV Sabin 2 at 1 pfu/cell (previously described in (206)), recombinant GFP-expressing vesicular stomatitis virus Indiana at 2 pfu/cell (VSV, as described in (92)), and Sendai virus at 25 hemagglutination units (HAU)/mL (SeV, Cantell strain purchased from Charles River Laboratories). Experiments measuring productive virus infection were performed with 0.5-1 plaque forming units (pfu)/cell for ~16 hours. Plaque assays were performed as described previously (207). VV-YFP Western Reserve was obtained from Dr. Sara Cherry and has been described previously (208). CellLight ER-RFP BacMam 2.0 baculovirus was purchased from Invitrogen.

3.2 VIRUS PREPARATIONS

3.2.1 CVB3-RD

HeLa cells (clone 7B) were plated in T-150 flasks and grown to confluence. CVB3-RD was bound to the cells at room temperature for 1 hour in serum-free MEM containing 20 mM HEPES. Binding medium was then replaced with complete medium and the cells incubated until severe cytopathic effect was observed (16-24 hours). Cells were lysed using three rounds of subsequent freezing and thawing followed by addition of 10% Triton-X-100, a debris spin, and addition of 10% SDS. Cleared virus-containing cell lysate was then spun in an ultracentrifuge on a 30% sucrose cushion using the SW28 rotor at ~30,000 rpm for 2.5 hours at 4ºC. Virus was then resuspended in 1mL PBS and titered by plaque assay.

3.2.2 VSV-GFP Indiana

Vero cells were plated in T-150 flasks and grown to confluence. VSV-GFP Indiana (0.01 pfu/mL) was bound to the cells at 37ºC for 1 hour in complete media containing 2% FBS. Binding medium was then replaced with complete medium (2% FBS) and cells were incubated until severe cytopathic effect was observed (36-48 hours). Virus-containing supernatant was subjected to a debris spin, and the cleared virus-containing supernatant was recovered and titered by plaque assay.

3.3 PLAQUE ASSAYS

3.3.1 CVB

At a time period of 24 hours prior to performing the plaque assay, HeLa 7b cells were plated in 12-well plates at $1x10^6$ cells/well. Serial dilutions of CVB were bound to cells at room temperature for 1 hour in complete media. The virus-containing binding media was removed and 0.8% agarose overlay containing 2X phenol-free MEM, FBS and Pen/Strep was added and allowed to solidify. After a 36-48 hour incubation at 37ºC, agarose plugs were removed, cells rinsed, and plaques visualized using crystal violet.

3.3.2 VSV-GFP

At a time period of 24 hours prior to performing the plaque assay, Vero cells were plated in 12-well plates at $5x10^5$ cells/well. Serial dilutions of VSV-GFP were bound to cells at 37ºC for 1 hour in complete media. The virus-containing binding media was removed, cells washed with PBS, and 1.6% agarose overlay containing 2X phenol-free MEM, FBS, NEAA, and Pen/Strep was added and allowed to solidify. After a 24 hour incubation at 37ºC, agarose plugs were removed, cells rinsed, and plaques visualized using crystal violet.

3.4 ANTIBODIES

Mouse anti-enterovirus VP1 (Ncl-Entero) was obtained from Novocastra Laboratories. Mouse anti-GFP (B-2), mouse anti-V5 (H-9), rabbit and mouse anti-Flag (OctA, D-8 or H-5), rabbit anti-GAPDH (FL-335), and goat anti-Gp78 (N-18) were obtained from Santa Cruz Biotechnology. Rabbit anti-MAVS was obtained from Bethyl Laboratories. Mouse monoclonal antibody to mitochondria (MTCO2) was obtained from Abcam. Alexa fluor-conjugated secondary antibodies were from Invitrogen. Rat anti-Gp78 IgM (3F3A) was a generous gift from Dr. Ivan Nabi (University of British Columbia, Vancouver, Canada) and was previously described (129).

3.5 PLASMIDS, SIRNAS AND TRANSFECTIONS

Unless otherwise specified, all Gp78 constructs were of human origin. pCI-Neo-gp78/JM20 was purchased from Addgene and was previously described (136). For subsequent cloning, the ORF of Gp78 was amplified by PCR from pCI-Neo-Gp78/JM20 using primers also encoding an N-terminal Flag tag, and was then subcloned into pcDNA3.1 using BamHI and XbaI sites. C-terminal Gp78 mutants were generated by standard PCR cloning. Primer sequences are available upon request. Flag-tagged mouse Gp78 and the mouse Gp78 RING mutant were provided by Dr. Ivan Nabi and have been previously described (151). EGFP-MAVS, EGFP-MAVS-CT and NT, EGFP-RIG-I, V5-IRF3-5D and EGFP-STING have been described previously (92) (209). Flag-tagged BPIFB3 was generated by amplification of BPIFB3 cDNA with primers encoding a C-terminal Flag tag and cloned into pcDNA3.1/V5-His TOPO TA as per the manufacturer's instructions (Invitrogen).

The siRNA targeting Gp78 was purchased from Sigma Aldrich (GGACGAACUCCUCCAGCAAtt). The siRNA used to target BPIFB3 (GCUUAACGUGGCCCUGGAUtt) was also purchased from Sigma. Control (scrambled) siRNAs were purchased from Ambion or Sigma.

Plasmid transfections were performed using X-tremeGENE 9 or HP (Roche) essentially per the manufacturer's protocol. For siRNA transfections, HBMEC or HT1080 were transfected with siRNAs (final concentration 25-75 nM) using DharmaFECT-1 transfection reagent (Thermo-Fisher Scientific) according to the manufacturer's protocol.

3.6 IMMUNOBLOTS

Cells were grown to confluence in 24-well plates, and lysates prepared with RIPA buffer (50 mM Tris-HCl [pH 7.4], 1% NP-40, 0.25% sodium deoxycholate, 150 mM NaCl, 1 mM EDTA, 1 mM phenylmethanesulfonyl fluoride, 1 mg/ml aprotinin, leupeptin, and pepstatin). Lysates (~30µg) were run on 4%–20% Tris-HCl gels (Bio-Rad, Hercules, CA) and transferred to nitrocellulose membranes. Membranes were blocked using 5% nonfat dry milk, probed with the indicated antibodies, and developed using horseradish peroxidase-conjugated secondary antibodies (Santa Cruz Biotechnology) and SuperSignal West Pico or Dura chemiluminescent substrates (Pierce Biotechnology). Densitometry was performed using Image J (NIH).

3.7 IMMUNOPRECIPITATIONS

Confluent HEK293T cells transiently transfected in 6-well plates with the indicated plasmids were lysed with 0.5mL RIPA buffer (450 mM NaCl, 1 mM EDTA, 50 mM Tris-HCl [pH 7.8], 1% Nonidet P-40, 1 mM phenylmethylsulfonyl fluoride, 0.5 μg/ml leupeptin, and 0.5 μg/ml pepstatin), and insoluble material was cleared by centrifugation. 350μL lysate was incubated with the indicated antibodies for 1-2 hr at 4°C followed by the addition of Sepharose G beads for an additional 1-2 hr at 4°C. After centrifugation, the beads were washed with RIPA buffer a minimum of five times and heated at 95 °C for 10 min in Laemmli sample buffer. Following a brief centrifugation, the entire supernatant was immunoblotted with the indicated antibodies.

3.8 REPORTER-GENE ASSAYS

Activation of IFN-β and NF-κB promoters was quantified using dual luciferase reporter-gene assays. Cells were transfected in 96-well plates with p-125 luc (which contains the entire IFN-β promoter upstream of firefly luciferase) or NF-κB reporter (which contains NF-κB responsive promoter elements upstream of firefly luciferase) plasmids together with a control renilla luciferase plasmid (pRL-null, Promega) and the indicated plasmids. Cells were lysed and prepared for luciferase measurement using the Dual-Luciferase assay kit (Promega) according to manufacturer's instructions, and luciferase activity was measured using a Synergy 2 luminescence plate reader (Bio-Tek). Data are presented as fold induction over uninfected or vector-transfected

controls, and are normalized to renilla luciferase activity. All experiments were performed in triplicate and conducted a minimum of three times.

3.9 RT-QPCR

Total cellular RNA was extracted using TRI reagent (MRC) according to manufacturer's protocol. RNA samples were treated with RNAse-free DNAse (Qiagen) prior to cDNA synthesis. Total RNA (1µg) was reverse transcribed using iScript cDNA synthesis kit (Bio-Rad). RT-qPCR was performed using iQ SYBR Green Supermix (Bio-Rad) in an Applied Biosystems StepOnePlus real-time PCR machine. Gene expression was calculated using the 2-ΔΔCT method and was normalized to actin (210). QuantiTect primers against Gp78 and BPIFB3 were purchased from Qiagen. Primer sequences are reported in Table 2 below.

Table 2. RT-qPCR primers.

Gene	Forward (5'-3')	Reverse (5'-3')
MAVS	GTCACTTCCTGCTGAGA	TGCTCTGAATTCTCTCCT
Actin	ACTGGCACGACATGGAGAAAA	GCCACACGCAGCTC
CVB	ACGAATCCCAGTGTGTTTTGG	TGCTCAAAAACGGTATGGACAT
GFP	CACATGAAGCAGCACGACTTCT	AACTCCAGCAGGACCATGTGAT
ISG56	CAACCAAGCAAATGTGAGGA	AGGGGAAGCAAAGAAAATGG

3.10 IMMUNOFLUORESCENCE AND ELECTRON MICROSCOPY

Cells cultured in 8-well chamber slides (LabTek, Nunc) were washed and fixed with either 4% paraformaldehyde or with ice-cold methanol. Cells were then permeablized with 0.1% Triton X-100 in phosphate buffered saline (PBS) and incubated with the indicated primary antibodies for 1 hr at room temperature (RT). Following washing, cells were incubated with secondary antibodies for 30 min at room temperature, washed, and mounted with Vectashield (Vector Laboratories) containing 4′,6-diamidino-2-phenylindole (DAPI). Images were captured using a FV1000 confocal laser scanning microscope (Olympus), analyzed using Image J (NIH) or FV10-ASW (Olympus) (Bitplane), and contrasted and merged using Photoshop (Adobe). Electron microscopy was performed essentially as described (208). Briefly, cells in 12-well plates were fixed with 2.5% glutaraldehyde for 1 hour at room temperature, and the remaining preparation steps performed by the University of Pittsburgh Center for Biological Imaging. Samples were washed for 10 minutes, 3 times in PBS. The monolayers were post-fixed in 1% OsO4 with 1% potassium ferricyanide for 1 hour at 4ºC, then washed again 3 times for 10 minutes each in PBS. The monolayers were dehydrated in a graded series of alcohol (30%, 50%, 70%, 90%) for 10 minutes each, then three times in 100% ethanol for 15 minutes each. Samples were then incubated three times in epon (1:1 propylene oxide:Polybed 812 epoxy resin) for 1 hour each. The samples were then embedded in molds, and subsequently cured at 37ºC overnight and 65 ºC for 48 hours. Samples were then sectioned on mesh copper grids and microscopy performed on a JEOL JEM 1011 transmission electron microscope.

3.11 SUBCELLULAR FRACTIONATION

Stable U2OS cells expressing BPIFB3-Flag were grown in a T-25 flask to confluence and fractionation performed using the Subcellular Protein Fractionation Kit for Cultured Cells from Pierce essentially per the manufacturer's instructions.

3.12 FLUO-4 AND FURA-2 IMAGING

Ca^{2+} measurements were conducted essentially as described using either the ratiometric dye Fura-2 AM or Fluo-4 AM (211). For Fura-2 experiments, cells were plated 24 hours prior to the experiment in 35mm Mattek dishes. The following day the cells were loaded with 1µM Fura-2 AM for 30 minutes at 37ºC. Cells were then rinsed 3 times in PBS (no calcium or magnesium). Cells were imaged live in 1 mL PBS (no calcium or magnesium) using an Olympus IX81 motorized inverted microscope. Images were acquired at excitations 340nm and 380nm every 5 seconds for about 15 minutes using Slidebook 5.0 advanced imaging software. Intensity ratios (340nm/380nm) for 30 selected regions of interest (ROIs)/dish were calculated using Slidebook and replicates averaged and plotted over time. Thapsigargin (1µM) was added to stimulate ER calcium flux at 5 minutes after image capturing was begun.

For Fluo-4 experiments, cells were plated 24 hours prior to the experiment in 8 well chamber slides. The following day the cells were loaded with 1µM Fluo-4 AM for 30 minutes at 37ºC. Cells were then rinsed 3 times in PBS (no calcium or magnesium). Cells were imaged live in 1 mL PBS (no calcium or magnesium) using an Olympus IX81 motorized inverted microscope. Images were acquired every 5 seconds for about 10 minutes using Slidebook 5.0 advanced imaging

software. Fluorescence intensity values for 30 selected regions of interest (ROIs)/well were plotted over time using Slidebook. Thapsigargin (1μM) was added to stimulate ER calcium flux at ~1.5 minutes after image capturing was begun.

3.13 STATISTICAL ANALYSIS

Data are presented as mean ± standard deviation or standard error of the mean. Paired, or unpaired, two-tailed t-test or one-way analysis of variance (ANOVA) and Bonferroni's correction for multiple comparisons were used to determine statistical significance (*$p<0.01$).

4.0 SPECIFIC AIM ONE: DEFINE THE ROLE OF GP78 IN REGULATING ENTEROVIRUS INFECTION

4.1 BACKGROUND

Recognition of pathogen-derived nucleic acids is amongst the most important mechanisms by which a host cell defends against pathogen infection. Upon recognition of these nucleic acids, the transcription of myriad antiviral genes ensues, culminating in a cellular antimicrobial state that equips the cell to resist and/or suppress infection. The cytosolic pattern recognition receptors RIG-I and MDA5 are largely responsible for initiating the innate immune response to cytosolic dsRNA derived from the replication of viral pathogens (212). The signaling initiated by one or both of these cytosolic sentinels converges on a common mitochondria-localized adaptor molecule, MAVS, which in turn leads to nuclear translocation of NF-κB and IRF-3 for induction of type I IFN production (65). MAVS contains an N-terminal CARD, which is required for both upstream and downstream interactions, as well as a C-terminal mitochondrial localization sequence, which is required for downstream signaling events (63-66).

Because enhanced inflammation can lead to cell damage, mechanisms must exist to tightly regulate antiviral signaling. There are a variety of mechanisms by which regulators specifically modulate MAVS expression and/or signaling. This can be achieved by protein-protein interactions that physically disrupt or enhance upstream or downstream interactions required for propagating MAVS-mediated signaling (87, 89, 91, 94, 97, 98, 213). MAVS regulation can also be achieved by post-translational modifications such as ubiquitination that lead to inactivation or proteasomal degradation (77, 84, 88, 213). Variations in mitochondrial dynamics have also

been reported to play a role in MAVS regulation, such as alterations in mitochondrial fusion/fission (75, 76), membrane potential (76), reactive oxygen species generation (95), and mitochondrial-endoplasmic reticulum contacts (MAMs) (75, 85).

MAMs are defined as sites of close physical contact (~10-30nm (214, 215)) between the ER and mitochondria. It is estimated that between 5-20% of mitochondria are in direct contact with the ER (216). The MAM is an important cellular domain that regulates a variety of functions involved in cellular homeostasis such as lipid biosynthesis (217, 218), Ca^{2+} signaling, and cell survival pathways (219-221). Quite interestingly, activated MAVS-containing innate immune synapses form at MAMs, and the population of MAVS at the MAM is targeted by the hepatitis C virus (HCV) NS3/4A protease, underscoring the importance of this compartment in innate antiviral signaling (85). In addition, the mitochondria and MAM have been associated with the induction of inflammasome signaling (222).

The MAM proteome includes Gp78 (147-150), an E3 ubiquitin ligase active in the ER-associated degradation (ERAD) pathway. Gp78 is also a cell surface receptor for the cytokine autocrine motility factor (AMF), the activity of which has been linked with increased cancer metastasis presumably due to its role in cell differentiation, survival and growth (126). Gp78 is responsible for conjugation of ubiquitin to misfolded proteins, which are then directed to the cytosolic proteasome for subsequent degradation (132, 135, 136). Gp78-mediated ERAD participation requires its C-terminal RING domain (responsible for ligase activity), Cue domain (responsible for binding of ubiquitin), and E2 (the enzyme responsible for bringing in the ubiquitin) binding site (132, 135, 136). The C-terminus of gp78 also contains a site of interaction with the AAA ATPase p97 (VCP), which provides the driving force for translocation of the polyubiquitinated substrates to the cytosol for subse-

quent degradation by the proteasome (138-141). It has also been recently reported that Gp78 induces mitochondrial fragmentation in a ligase-dependent manner, leading to mitophagy upon mitochondrial membrane depolarization (151).

Previously, we conducted RNAi high-throughput screening and identified Gp78 as a gene whose depletion led to a significant reduction in infection of the enteroviruses CVB and PV (205). In the current study, we provide a molecular mechanism for these previous findings and show that Gp78 is a novel regulator of RLR signaling. We show that in addition to CVB and PV, depletion of Gp78 results in a robust decrease of VSV infection. Mechanistically, we show that expression of Gp78 dramatically represses type I IFN signaling upstream of IRF3, and that this decrease in signaling corresponds to decreases in MAVS protein levels. Expression of Gp78 mutants defective in E3 ubiquitin ligase activity or ERAD participation lost their ability to decrease MAVS levels, but surprisingly maintained their ability to repress RLR-mediated IFN-β signaling. In contrast, Gp78 lacking its entire C-terminus lost both its ability to induce reductions in MAVS expression and repress RLR signaling. These studies point to an unexpected role for the MAM-localized Gp78 E3 ubiquitin ligase in the negative regulation of MAVS signaling. Our data implicate two parallel pathways by which Gp78 regulates MAVS expression and signaling—one pathway requires its E3 ubiquitin ligase and ERAD activity, while the other pathway occurs independently of E3 ubiquitin ligase and ERAD activity, but requires the Gp78 C-terminus and occurs via an association between this region and the N- and C-terminal domains of MAVS.

4.2 RESULTS

4.2.1 Gp78 is a regulator of RNA virus infection

We previously conducted high throughput RNAi screens for novel regulators of enterovirus infection in human brain microvascular endothelial cells (HBMEC) (205), and identified Gp78 as a regulator of CVB and PV infection whose depletion led to a robust (~3-fold) decrease of infection (205) (Figure 6A). To expand on these findings, we also determined the effects of Gp78 depletion on CVB infection in the fibrosarcoma cell line HT1080 (a cell type reported to express high levels of Gp78 (223)). Similar to our results in HBMEC, we found that RNAi-mediated Gp78 silencing decreased CVB infection about 3-fold (Figure 6C). In addition, we found that Gp78 silencing also reduced the infection of the unrelated RNA virus VSV, a member of the rhabdovirus family, about 10-fold (Figures 6B and 6C). Efficient reduction of Gp78 expression in the presence of RNAi (~50%) was achieved in these experiments (Figure 6D). Taken together, these data show that depletion of Gp78 in both HBMEC and HT1080 cells results in a decrease of CVB, PV and VSV infection, suggesting a mechanism that is common to two independent families of RNA viruses in disparate cell types.

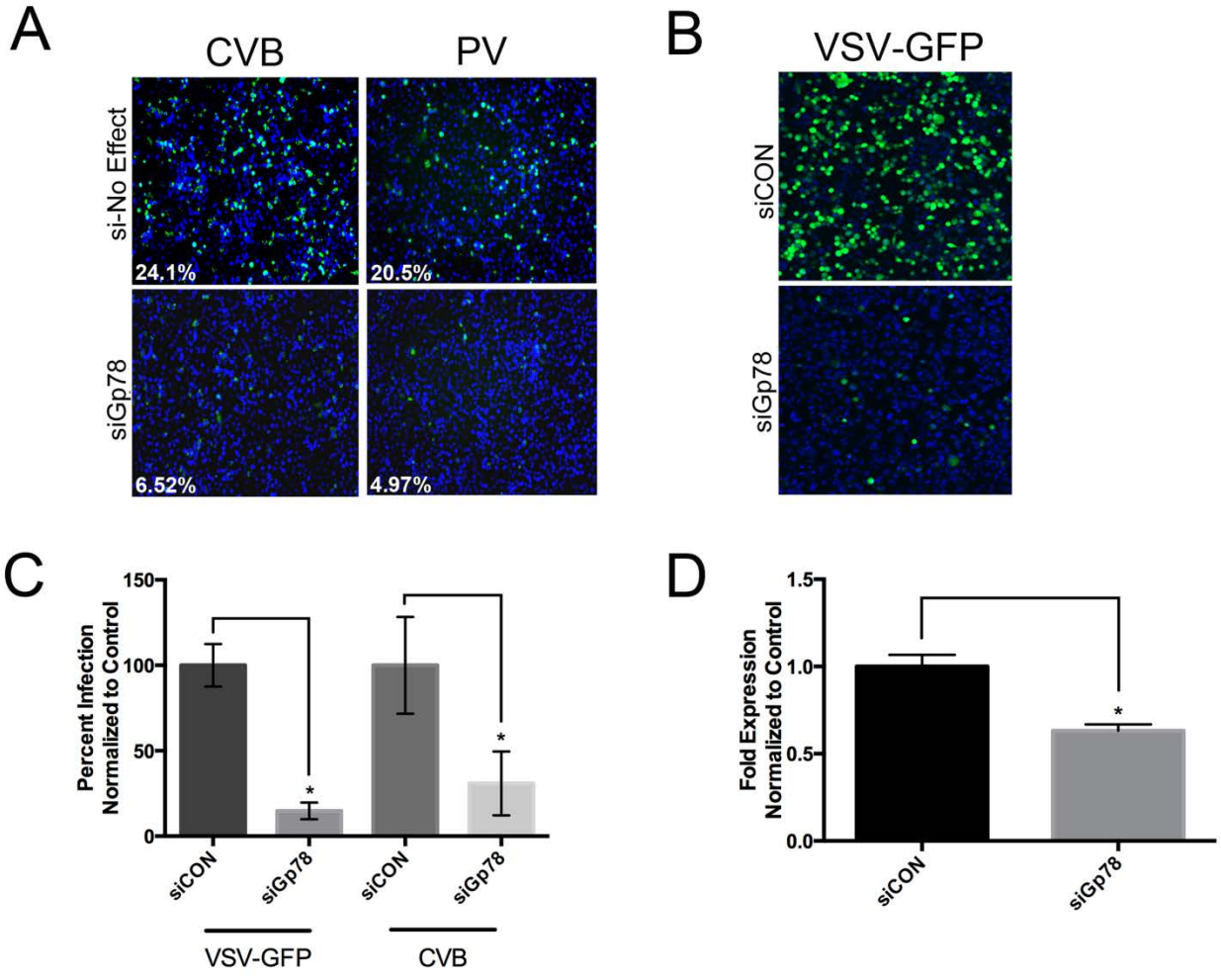

Figure 6. Gp78 depletion restricts RNA virus replication.

(A), Decreased CVB and PV replication by high-throughput RNAi screening in HBMEC transfected with Gp78 siRNAs (siGp78) compared to an siRNA targeting a gene within the library that had no effect on viral replication (si-No Effect). VP1 staining is shown in green and DAPI-stained nuclei are shown in blue. White text at bottom left denotes the level of infection (%). **(B),** Decreased VSV-GFP replication in HT1080 cells transfected with siGp78 compared to control siRNA (siCON), as assessed by immunofluorescence microscopy at 8 hrs post-infection. VSV-GFP is shown in green and DAPI-stained nuclei are shown in blue. **(C),** Decreased VSV-GFP and CVB replication in HT1080 cells transfected with siGP78 compared to control siRNA (siCON), as assessed by immunofluorescence microscopy at 8 hrs (VSV-GFP) or 16 hrs (CVB) post-infection. **(D),** Level of Gp78 expression in HT1080 cells

transfected with siGp78 compared to a control siRNA, as assessed by RT-qPCR 48 hr post-transfection. Data in (A) and (B) are representative of at least 3 independent experiments, and data in (C) and (D) are from at least 3 independent experiments and are presented as mean ± standard deviation (*$p<0.01$).

4.2.2 Gp78 negatively regulates type I IFN signaling

Because depletion of Gp78 resulted in a decrease of infection by two unrelated families of RNA viruses, we next determined whether Gp78 regulated some aspect of type I IFN signaling. We found that expression of exogenous Gp78 led to a significant decrease in Sendai virus (SeV)-induced signaling to both the IFN-β (~3-fold) and NF-κB (~2-fold) promoters (Figure 7A and 7B). SeV is specifically recognized by RIG-I (139). In addition, we found that overexpression of Gp78 greatly attenuated the induction of the interferon stimulated gene (ISG)-56 by both cytosolic poly (I:C) (~10-fold) or SeV infection (Figure 7C, 7E). In contrast, RNAi-mediated silencing of Gp78 greatly enhanced this induction (~2-fold) (Figure 7D, 7E). Of note, the expression levels of ISG56 slightly increased in the absence of Gp78 (by ~16 fold) even without stimulation by SeV (Figure 7D), which could point to a steady state regulatory role for Gp78 in type I IFN signaling. Taken together, these data suggest a negative regulatory role for Gp78 in type I IFN signaling.

A common characteristic of many type I IFN mediators is their inducible expression upon treatment with virus infection, purified interferon and/or PRR agonists (65, 222, 224-226). Given the possible role of Gp78 in the regulation of type I IFN signaling, we determined if its expression was inducible under these conditions. We found that expression of Gp78 was not induced by treatment with purified IFN-β or cytosolic poly (I:C) or by infection with SeV (Figure 7F), a result underscoring the possible steady state regulatory role for Gp78 in type I IFN signaling.

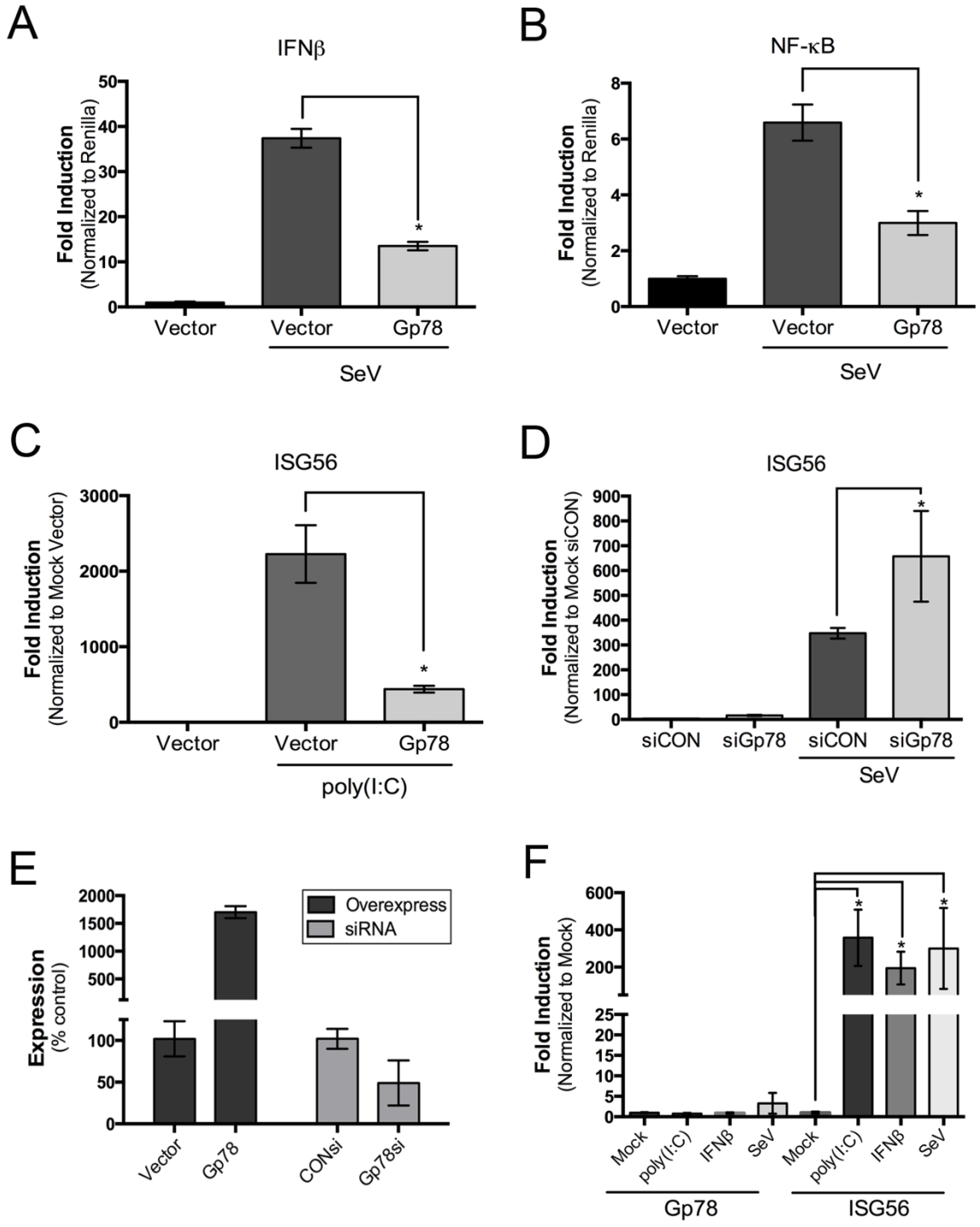

Figure 7. Gp78 regulates type I interferon signaling.

(A and B), Dual luciferase assays from 293T cells transfected with IFN-β (A) or NF-κB (B) promoted luciferase constructs and the indicated plasmids. Cells were infected with SeV 24 hr post-transfection and luciferase activity was measured 16 hr post-infection. **(C and D),** Levels of ISG56 in untreated 293T (C) or HT1080 (D) cells transfected with the indicated plasmids (C) or siRNAs (D), transfected with 500ng poly (I:C) (C), or infected with SeV (D) at 48 hr post-transfection for 16 hr, as assessed by RT-qPCR. **(E),** Gp78 expression from 293T (overexpression) or HT1080 (siRNA) cells transfected with the indicated plasmids (left) or siRNAs (right), as assessed by RT-qPCR. Data are presented as mean ± standard deviation and correspond to data shown in Figure (2C), (2D). **(F),** Level of Gp78 (left) or ISG56 (right) expression in untreated HT1080 cells, or cells transfected with 500ng poly (I:C), treated with 500 U/mL IFN-β overnight, or infected with SeV for 24hrs, as assessed by RT-qPCR. All data besides (E) are representative of at least 3 independent experiments, data in (E) are from at least 3 independent experiments, and all data are presented as mean ± standard deviation (*$p<0.01$).

4.2.3 Gp78 negatively regulates RLR signaling

RLR signaling is one of the most important components of the type I IFN response to RNA viruses. Given that depletion of Gp78 restricted the replication of both CVB and VSV, and enhanced type I IFN signaling, we next investigated the role of Gp78 in RLR signaling. We found that expression of exogenous Gp78 greatly decreased signaling to the IFN-β promoter induced by overexpression of RIG-I, MDA5, and MAVS (~10-fold) (Figure 8A). However, exogenously expressed Gp78 had no effect on signaling to the IFN-β promoter induced by overexpression of a constitutively active mutant of IRF-3 (IRF3-5D) (227) (Figure 8B). These results suggest that Gp78 exerts its regulatory role within the RLR pathway upstream of IRF3 activation.

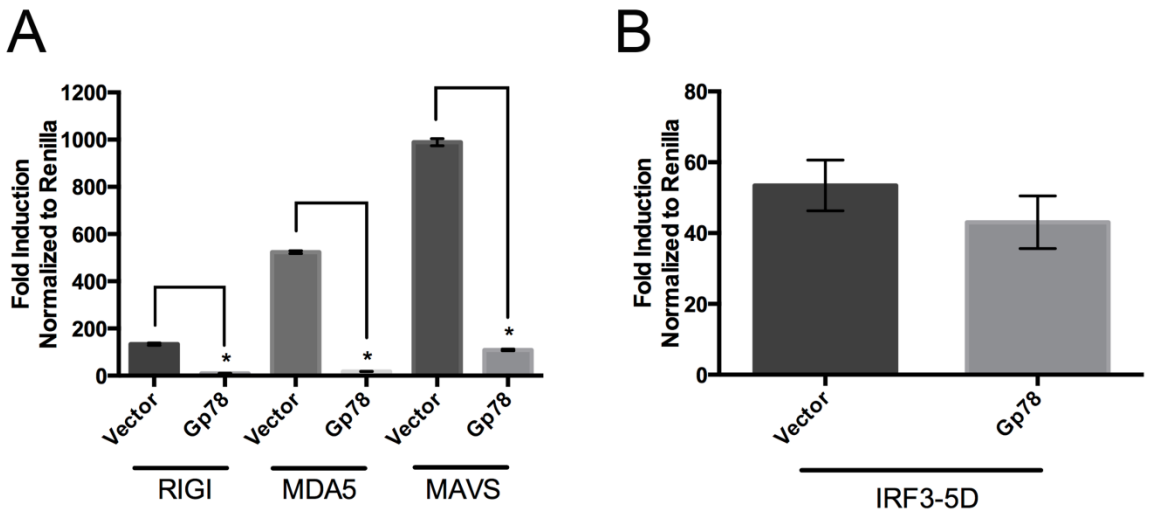

Figure 8. Gp78 regulates RLR signaling.

(A and B), Dual luciferase assays from 293T cells transfected with IFN-β promoted luciferase constructs, RIG-I, MDA5, MAVS (A), or IRF3-5D (B) and the indicated plasmids (vector or Gp78). Luciferase activity was measured 48 hr post-transfection. All data are representative of at least 3 independent experiments and presented as mean ± standard deviation (*$p<0.01$).

4.2.4 Gp78 expression results in the post-translational downregulation of MAVS

Because silencing of Gp78 restricted the replication of CVB and VSV, which are detected by different RLRs (97, 228, 229), and because Gp78 expression abrogated RLR signaling upstream of IRF3, we next investigated the effect of Gp78 on the expression of various innate immune-

associated components. Strikingly, we found that overexpression of Gp78 resulted in a marked decrease in EGFP-MAVS protein levels by immunoblotting (Figure 9A). In contrast, expression of Gp78 had no effect on the expression of EGFP-RIG-I, V5-IRF3-5D, or the unrelated ER-localized IFN signaling molecule EGFP-STING (Figure 9A). Importantly, overexpression of Gp78 had no effect on MAVS mRNA levels, suggesting that the Gp78-mediated decrease in MAVS protein levels occurs post-translationally (Figure 9B).

Because our previous results relied on the overexpression of MAVS, we also determined whether expression of Gp78 reduced levels of endogenous MAVS. Similar to our findings with exogenously expressed MAVS, we found that Gp78 also decreased the levels of endogenous MAVS in a dose-dependent manner (Figure 9C). In addition, we observed a pronounced loss of endogenous MAVS immunofluorescence in cells transfected with Gp78 (Figure 9D).

Given that Gp78 has been associated with mitochondrial fragmentation and mitophagy (151), we also determined whether overexpression of Gp78 would lead to the possible degradation of other mitochondria-localized components. We found that expression of Gp78 had no effect on the levels of the constitutive mitochondrial marker MTC02 (Figure 9E). Taken together, these data show that MAVS protein levels are post-translationally decreased in the presence of Gp78 in a specific manner that does not rely on mitophagy or mitochondrial fragmentation.

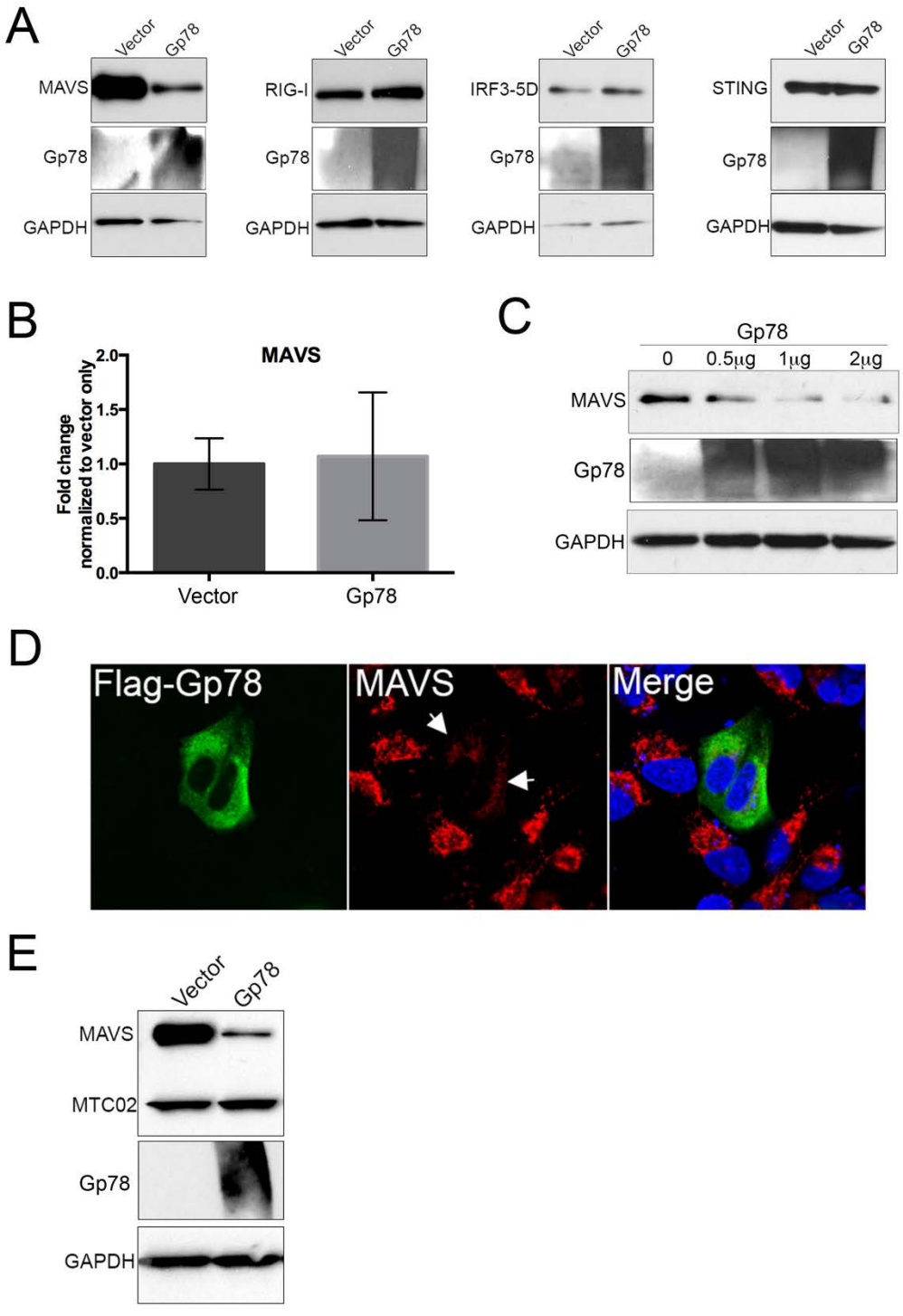

Figure 9. Gp78 specifically alters MAVS levels.

(A), Immunoblot analysis from 293T cells 48 hrs post-transfection with EGFP-MAVS, EGFP-RIG-I, V5-IRF3-5D, or EGFP-STING constructs and either vector or Gp78 constructs. Antibodies directed against GFP or V5 were used. Immunoblotting for Gp78 (middle panel) is included to demonstrate transfection and GAPDH (bottom panels) is included as a loading control. **(B),** Levels of MAVS in 293T cells transfected with vector or Gp78 as assessed by RT-qPCR at 48 hrs post-transfection. **(C),** Immunoblot analysis for endogenous MAVS 48 hrs post-transfection with increasing amounts of Gp78 construct (from 0μg to 2μg). Immunoblotting for Gp78 (middle panel) is included to demonstrate transfection and GAPDH (bottom panels) is included as a loading control. **(D),** Immunofluorescence microscopy for endogenous MAVS in U2OS cells 48 hr post-transfection with Flag-Gp78 construct. MAVS is shown in red and Flag-Gp78 is shown in green. DAPI-stained nuclei are shown in blue. White arrows denote areas of decreased MAVS staining in the presence of Gp78. **(E),** Immunoblot analysis from 293T cells 48 hrs post-transfection with EGFP-MAVS construct and either vector or Gp78 constructs. Antibodies directed against GFP and MTCO2 (an unrelated mitochondrial protein) are included as a measure of specificity, and immunoblotting for Gp78 (middle panel) is included to demonstrate transfection and GAPDH (bottom panels). All data besides (B) are representative of at least 3 independent experiments and data in (B) are from at least 3 independent experiments and are presented as mean ± standard deviation (*$p<0.01$).

4.2.5 Gp78 colocalizes with MAVS and specifically targets the MAVS CARD

Consistent with the work of others (148, 150), we found that exogenously expressed Gp78 partially localized with a marker of mitochondria (Figure 10A). In addition, we found that endogenous Gp78 colocalized with endogenous MAVS, likely at the ER-mitochondria interface in uninfected cells and in cells infected with SeV (Figure 10B). MAVS contains a C-terminal domain that mediates its mitochondrial localization and is required for its activity, and an N-terminal CARD-containing region that is required for upstream and downstream interactions (65). In order to investigate which region of MAVS is required for Gp78-mediated degradation, we cotransfected

the Flag-Gp78 construct with either the full length MAVS construct (MAVS-WT), or with deletion mutant constructs of MAVS containing 148 N-terminal amino acids including the CARD (MAVS-NT) or 391 C-terminal amino acids including the transmembrane domain, but lacking the CARD (MAVS-CT). We found that expression of Gp78 induced a reduction in the expression of both MAVS-WT (~3-fold) and MAVS-NT (~2.5-fold), but had no significant effect on the expression of MAVS-CT (Figure 10C). These data suggest that the CARD-containing N terminus of MAVS is required for Gp78-mediated decreases in MAVS expression.

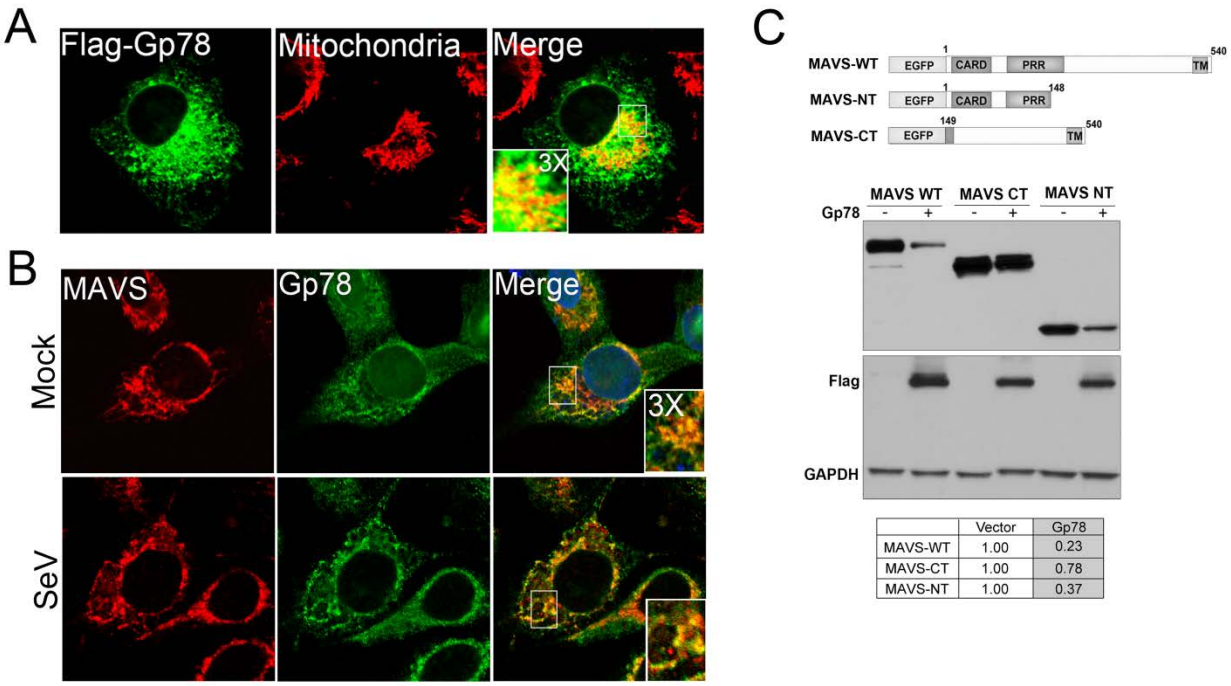

	Vector	Gp78
MAVS-WT	1.00	0.23
MAVS-CT	1.00	0.78
MAVS-NT	1.00	0.37

Figure 10. Gp78 is localized at the mitochondria in close proximity to MAVS, and targets the CARD of MAVS. **(A),** Immunofluorescence microscopy of U2OS cells 48 hr post-transfection with the Flag-Gp78 construct. Mitochondria are shown in red and were stained with MTCO2 antibody and Gp78 is shown in green and was stained with a Flag-specific antibody. **(B),** Immunofluorescence microscopy of endogenous MAVS and endogenous Gp78 in

U2OS cells in uninfected (Mock) or SeV infected HT1080 cells. MAVS is shown in red, and Gp78 is shown in green and was stained using the 3F3A antibody specific for Gp78. **(C),** Top**,** schematic of MAVS constructs used. Bottom, immunoblot analysis from 293T cells 48 hrs post-transfection with EGFP-MAVS, EGFP-MAVS-CT, or EGFP-MAVS-NT constructs with either vector or Gp78 constructs. Antibody directed against GFP was used. Immunoblotting for Flag and GAPDH (bottom panel) are included to show expression of Gp78 and as a loading control, respectively. Table at bottom, densitometry (MAVS/GAPDH normalized to vector control) in cells transfected with vector of Gp78. All data are representative of at least 3 independent experiments.

4.2.6 Gp78-mediated degradation of MAVS requires its E3 ubiquitin ligase and ERAD activity

Several domains within the C-terminus of Gp78 are critical for its E3 ubiquitin ligase and ERAD activities (schematic, Figure 11A, left). These include a RING finger domain, a CUE domain, an E2-binding region (G2BR) (132, 135, 136), and a VCP-interacting motif (VIM) for translocation of the polyubiquitinated substrates to the cytosol for subsequent degradation by the proteasome) (138-141). We next sought to determine the role of the E3 ubiquitin ligase and ERAD functions of Gp78 in its degradation of MAVS using a panel of point and truncation mutants (schematic, Figure 11A, right). When MAVS was cotransfected with human or mouse Gp78 constructs (hGp78 or mGp78, respectively), a robust decrease in MAVS protein levels (~3-fold each) was evident by immunoblotting (Figure 11B, compare lane 1 to lanes 2 and 3). However, MAVS protein levels were unaffected by a point mutant of mGp78 described previously (151) that abolishes its E3 ligase activity (mGp78 RING mut) (Figure 11B, compare lane 1 to lanes 3 and 4). Furthermore, truncation mutants of hGp78 that have been described previously to inhibit its

participation in the ERAD pathway (135, 136) (lacking the VIM (ΔVCP), VIM and G2BR (ΔG2BR), VIM, G2BR and CUE (ΔCUE), or the entire C terminus (ΔC)), lost their ability to decrease MAVS (Figure 11B, compare lane 1 to lanes 4-8). Importantly, when treated with MG132 (a proteasome inhibitor), MAVS protein levels were partially restored (~2.5 fold restoration) in the presence of Gp78 (Figure 11C). Interestingly, consistent with the work of others (225), we found that MAVS protein levels (Figure 11D), but not RNA levels (not shown), were significantly decreased in response to SeV infection. Together, these data point to a role for the E3 ubiquitin ligase and ERAD activity of Gp78 in MAVS degradation.

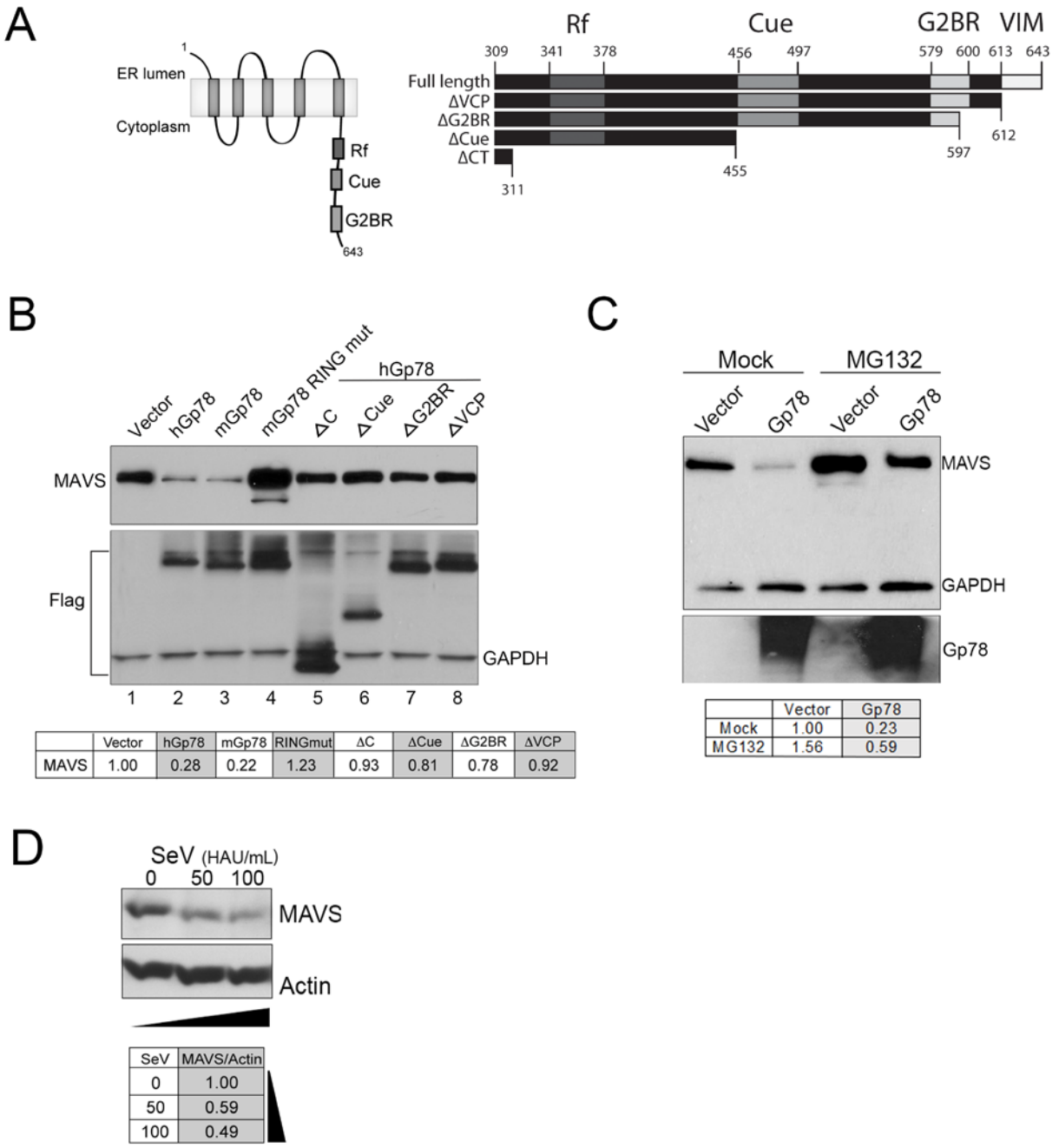

	Vector	hGp78	mGp78	RINGmut	ΔC	ΔCue	ΔG2BR	ΔVCP
MAVS	1.00	0.28	0.22	1.23	0.93	0.81	0.78	0.92

	Vector	Gp78
Mock	1.00	0.23
MG132	1.56	0.59

SeV	MAVS/Actin
0	1.00
50	0.59
100	0.49

Figure 11. The E3 ubiquitin ligase activity of Gp78 and its association with the ERAD pathway is required for Gp78-mediated MAVS degradation.

(A), Left panel**,** schematic of Gp78 showing important regions for E3 ubiquitin ligase activity. Right panel**,** schematic of the C-terminus of Gp78 illustrating deletion mutants used in this panel. **(B),** Immunoblot analysis from 293T cells

48 hrs post-transfection with EGFP-MAVS and the indicated plasmids. Antibody directed against GFP was used. Immunoblotting for Flag and GAPDH (bottom panel) are included to show expression of wild-type and mutant Gp78 and as a loading control, respectively. Table at bottom, densitometry (MAVS/GAPDH normalized to vector control) for cells transfected with the indicated plasmids. Densitometry was performed and data are presented as fold-change from vector untreated cells (bottom panel). **(C),** Immunoblot analysis from 293T cells 48 hrs post-transfection with EGFP-MAVS and either vector control or Gp78. MG132 (20 μM) was added 16 hours post-transfection. Antibodies directed against GFP and GAPDH were used. Table at bottom, densitometry (MAVS/GAPDH normalized to vector control) in cells transfected with the indicated plasmids and either Mock- or MG132-treated. **(D),** Immunoblot analysis of MAVS (top) from 293T cells infected with SeV (50 or 100 HAU/mL) for ~24hrs. Immunoblotting for actin (bottom) is included as a loading control. Table at bottom, densitometry (MAVS/Actin normalized to control (mock infection). Data in 11D were provided by Dr. Saumendra Sarkar.

4.2.7 Gp78-mediated abrogation of MAVS-mediated signaling occurs independently of E3 ubiquitin ligase and ERAD activities

We found that the E3 ubiquitin ligase and ERAD activities of Gp78 were required for its degradation of MAVS. Thus, we next determined whether this activity was also required for Gp78-mediated abrogation of type I IFN signaling. Surprisingly, we found that most of the mutants of Gp78 that ablated its ability to alter MAVS expression (mGp78 RING mut, hGP78-ΔVCP, -ΔG2BR, and -ΔCUE), retained their ability to suppress SeV-induced IFN-β signaling (Figure 12A). In contrast, only the hGp78 mutant lacking almost the entire C-terminus (hGP78-ΔC) lost the ability to attenuate antiviral signaling (Figure 12A). These data suggested that there are divergent mechanisms by which Gp78 induces MAVS degradation and attenuates MAVS-mediated signaling.

4.2.8 The C-terminus of Gp78 interacts with MAVS and binds to both the N- and C-terminal domains of MAVS

There are several pathways by which cellular components attenuate MAVS-mediated signaling. One of these includes the use of specific protein-protein interactions to inhibit the binding of key upstream and/or downstream innate immune signaling components to MAVS (87, 94, 98). Given that Gp78 localizes in close proximity to MAVS (Figure 9B) and can attenuate MAVS-mediated signaling even in the absence of Gp78-mediated degradation (Figure 12A), we next determined whether Gp78 and MAVS form an interaction by performing coimmunoprecipitation studies. For these studies, we utilized the ΔVCP, ΔCUE, and ΔC mutants of Gp78, but not wild-type Gp78, to avoid experimental difficulties related to the decrease in MAVS levels mediated by full length Gp78. We found that MAVS coimmunoprecipitated with both Gp78-ΔVCP and Gp78-ΔCUE (Figure 12B). In contrast, MAVS did not coimmunoprecipitate with Gp78-ΔC, despite this modification not significantly altering its localization (Figure 12B, 12C). These data suggest that Gp78 utilizes a domain between amino acids 311 and 455 of its C-terminus, most likely its RING region, to interact with MAVS.

Both the N- and C-terminal domains of MAVS play critical roles in its activation by upstream components and propagation of downstream signals. For example, whereas both RIG-I and MDA5 bind to the N-terminal CARD of MAVS (65), tumor necrosis factor (TNF) receptor-associated factor (TRAF)-3 binds to a region within the C-terminus of MAVS (230). Because we observed an association between Gp78 and MAVS, and a possible ablation of MAVS-mediated signaling as a result of this interaction, we next determined whether Gp78 interacted with the N- or C-terminal regions of MAVS. We found that Gp78-ΔVCP interacted with both the N- and C-

terminal domains of MAVS, whereas we did not detect any association of either of these domains with Gp78-ΔC, as expected (Figure 12D). These data show that Gp78 utilizes a region within its C-terminus to interact with multiple regions of MAVS.

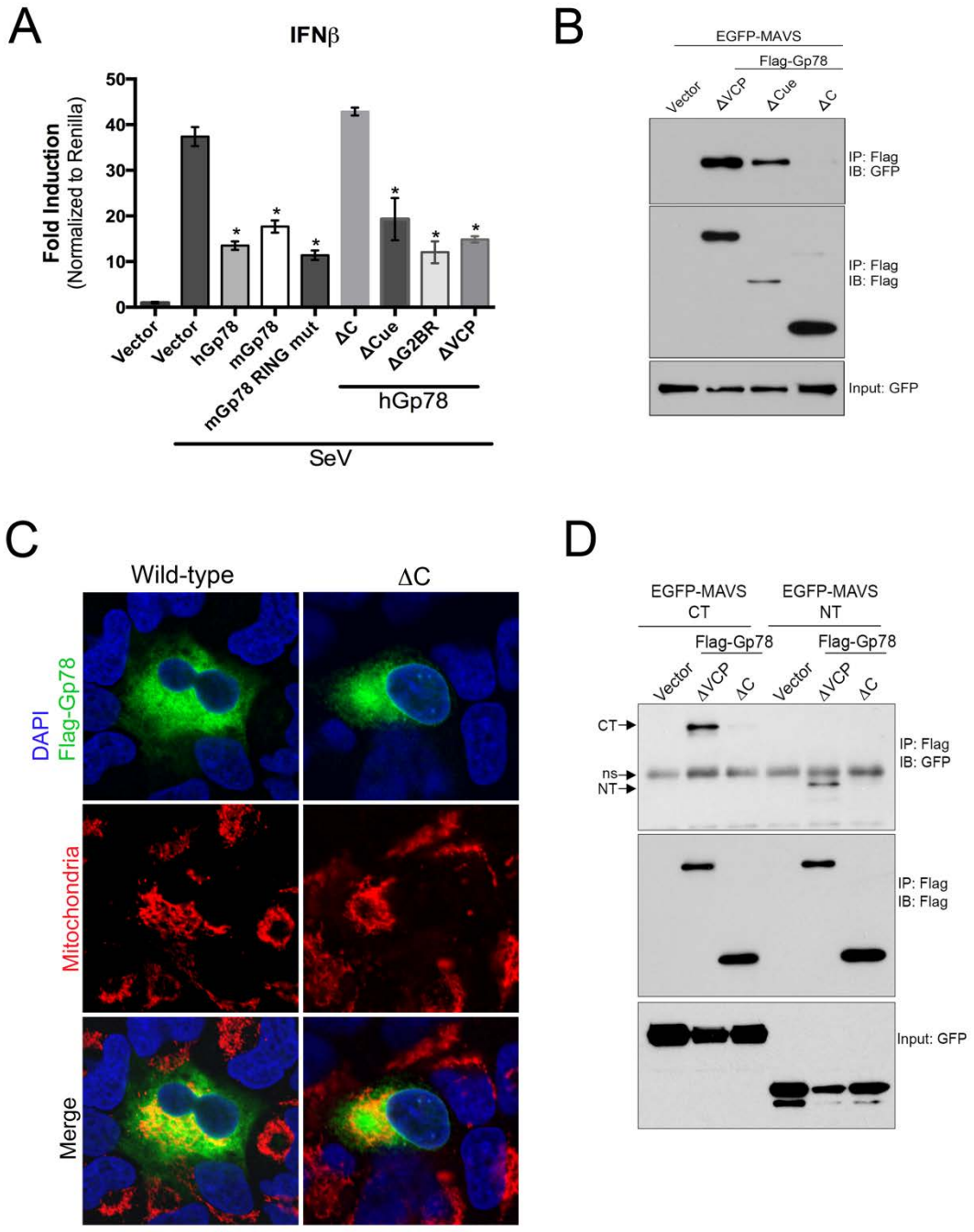

Figure 12. The C-terminus of Gp78 interacts with the N- and C-terminal regions of MAVS and is required to ablate MAVS-mediated signaling**.**

(A), Dual luciferase assays from 293T cells transfected with IFN-β promoted luciferase constructs and the indicated plasmids (a schematic of these constructs is shown in Figure 6A, right). Cells were mock-infected or infected with SeV 24 hr post-transfection and luciferase activity was measured 16 hrs post-infection. **(B),** Immunoblot analysis from 293T cells immunoprecipitates transfected with EGFP-MAVS and the indicated plasmids. Immunoprecipitation was performed with anti-Flag antibody and immunoblotting was performed with anti-GFP antibody. Input (GFP) is shown at bottom. **(C),** Immunofluorescence microscopy for Flag-Gp78 wild-type (left) or ΔC (right) (in green) ~24hrs following transfection in U2OS cells. Mitochondria are shown in red and were detected using anti-MTCO2. DAPI-stained nuclei are shown in blue. **(D),** Immunoblot analysis from 293T cells immunoprecipitates transfected with EGFP-MAVS-NT or -CT and either vector, Flag-Gp78 ΔVCP, or Flag-Gp78-ΔC. Immunoprecipitation was performed with anti-Flag antibody and immunoblotting was performed with anti-GFP antibody. Input (GFP) is shown at bottom. Arrows denote NT and CT fragments and ns denotes a nonspecific band. Data are representative of at least 3 independent experiments and data in (A) are presented as mean ± standard deviation (*$p<0.01$).

4.3 DISCUSSION

Here we report on the regulation of MAVS expression and signaling by the MAM-associated E3 ubiquitin ligase Gp78. We identified Gp78 initially using an unbiased high throughput RNAi screen to identify novel regulators of enterovirus infection (205). In the follow-up studies presented here, we found that RNAi-mediated silencing of Gp78 also restricted VSV infection and correlated with enhancements of type I IFN antiviral signaling. Mechanistically, we found that Gp78 alters RLR signaling by both enhancing the degradation of MAVS via its E3 ubiquitin ligase and ERAD-mediated functions and by specifically interacting with MAVS via a region within its C-terminus. Collectively, these data report on the unexpected role of Gp78 in the regulation of MAVS-mediated antiviral signaling and suggest that it specifically functions to attenuate antiviral

signaling of MAVS at the MAM by two parallel pathways (reviewed in the schematic shown in Figure 13).

Whereas CVB and other enteroviruses are sensed by MDA5, RLR-mediated anti-VSV signaling is specifically mediated by RIG-I (97, 228, 229). Our findings that Gp78 depletion suppressed infection by both viruses supports its specific regulation of an innate-immune associated factor common to both viruses, such as MAVS. Regulation of antiviral signaling at the mitochondrial level is quite strategic given that signals propagated by two independent cytosolic sensors converge on MAVS at the mitochondrial membrane. Therefore, regulators of MAVS such as Gp78 exert a higher level of control than they might if they targeted upstream components of RLR signaling such as RIG-I or MDA5 individually.

The MAM is emerging as a critical platform for MAVS-mediated innate antiviral signaling (85). In light of evidence that the active population of MAVS in virus-infected cells is localized to the MAM (85, 148, 150), negative regulation of MAVS in this compartment is critical to prevent excessive inflammation. Therefore, MAM-localized Gp78 is an ideal candidate to negatively regulate MAVS. Interestingly, we found that type I IFN signaling is enhanced in the absence of Gp78 in uninfected cells. This could indicate that Gp78 plays a 'housekeeping role' in the regulation of MAVS signaling to suppress MAVS-mediated innate immune signaling under basal states, likely as a means of avoiding hyperinflammatory signaling. This notion is supported by our findings that Gp78 expression is not induced by purified IFN-β treatment, transfection of cells with a synthetic ligand of RLR signaling, or SeV infection. Given the lack of a robust induction of Gp78 in response to any RLR ligand, it is possible that other interferon-inducible regulators of MAVS exist within the MAM, and that these would be important for immediate regulation during an acute viral infection. However, in the event of excessive inflammation after a viral infection has been

contained, or in the context of excessive inflammation in the absence of a viral threat (i.e., autoimmunity), negative regulation of MAVS at the MAM by a steady-state protein such as Gp78 would become critical for cellular homeostasis.

Ubiquitin–mediated proteasomal degradation of MAVS is a known mechanism for its negative regulation (75, 77, 84, 88, 231). Moreover, Gp78 is a well-characterized E3 ubiquitin ligase of the ERAD pathway. Given that Gp78-induced degradation of MAVS was E3 ubiquitin ligase- and ERAD-dependent, and that the effect was partially rescued with the proteasome inhibitor MG132, we conclude that Gp78-mediated MAVS degradation is achieved at least in part by its Gp78-mediated ubiquitination and proteasomal degradation. Whereas the RING, Cue, and G2BR regions are important for the E3 ubiquitin ligase activity of Gp78 (135, 136), the VIM region is not required for the enzymatic addition of ubiquitin to the substrate and is instead required for translocation of the ubiquitinated substrate out of the ER membrane and to the cytosol for completion of the ERAD pathway (138-141). Importantly, mutant Gp78 lacking this domain did not degrade MAVS, supporting a specific role for ERAD in MAVS degradation. The ERAD pathway is an ER-specific mechanism of protein quality control, and is mainly responsible for destruction of misfolded proteins exiting the ER by marking them with ubiquitin for proteasomal degradation (133). Although the requirement of the VIM region seems to point to a role for the ERAD pathway in Gp78-mediated MAVS degradation, it is important to note that MAVS is a membrane-localized protein in the mitochondria that, like ERAD substrates in the ER, would require translocation into the cytosol for interaction with the proteasome even in the absence of traditional ERAD. In fact, there are specific substrates recognized and negatively regulated by Gp78-mediated ubiquitination and proteasomal degradation in a manner distinct from ERAD's traditional role of non-specific protein quality control (143, 144), including MAVS.

We show that the CARD-containing N-terminal region of MAVS, but not the C terminal region of MAVS, is targeted for Gp78-mediated degradation. However, RIG-I, which also contains CARDs that are subject to ubiquitination (232), is not sensitive to Gp78-mediated degradation. These data point to the specificity of the Gp78-mediated degradation of MAVS and suggest that it may not target all CARDs. In addition, as we observed degradation of MAVS-NT, this suggests that the mitochondrial localization of MAVS is not required for its degradation mediated by Gp78.

Surprisingly, we observed a repression of MAVS-mediated signaling by Gp78 mutants incapable of participating in the ERAD pathway. We show that Gp78 binds to both the N- and C-terminal regions of MAVS, and that the region of Gp78 required for this binding is within RING-containing residues 311-455, as binding was lost when these residues were removed. Because RING domains are known to mediate protein- protein interactions (233, 234), it is likely that this region of Gp78 mediates its interaction with MAVS. Protein-protein interaction is a well-defined mechanism of regulating MAVS-mediated signaling. This is often achieved by physically blocking key interactions of MAVS with up or downstream signaling partners (87, 89, 91, 94, 98). It is possible that binding of Gp78 to MAVS within its CARD would disrupt the interaction between MAVS and RIG-I/MDA5 that is required for downstream signaling (63-66). However, it is also possible that Gp78 binds to a different region of MAVS, such as the proline rich region or TRAF interaction motifs (TIMs) required for MAVS interaction with the downstream signaling adaptors TRAF2/3/5/6 (66, 230, 235, 236), effectively disrupting and suppressing signaling. In addition, Gp78 may inhibit some aspect of MAVS oligomerization, which has been shown to play an important role in its signaling (101, 237, 238).

Taken together, our study provides evidence for two possible mechanisms for the regulation of MAVS expression and signaling by Gp78. The first mechanism requires the ERAD activity of Gp78 and likely corresponds to enhancements in MAVS ubiquitination and proteasomal degradation while the second occurs independently of ERAD function, but requires Gp78–MAVS interactions (Schematic, Figure 8). Both of these mechanisms likely require physical interaction of Gp78 with MAVS. These results shed light on a novel function of Gp78 in the regulation of MAVS-mediated antiviral signaling. Moreover, our work suggests that other MAM-localized components might also serve to specifically target MAVS as a means to regulate inflammatory signaling within the cell. Defining the specific components of the MAVS 'regulome' specifically within the MAM will undoubtedly provide exciting new insights into the regulation of antiviral signaling.

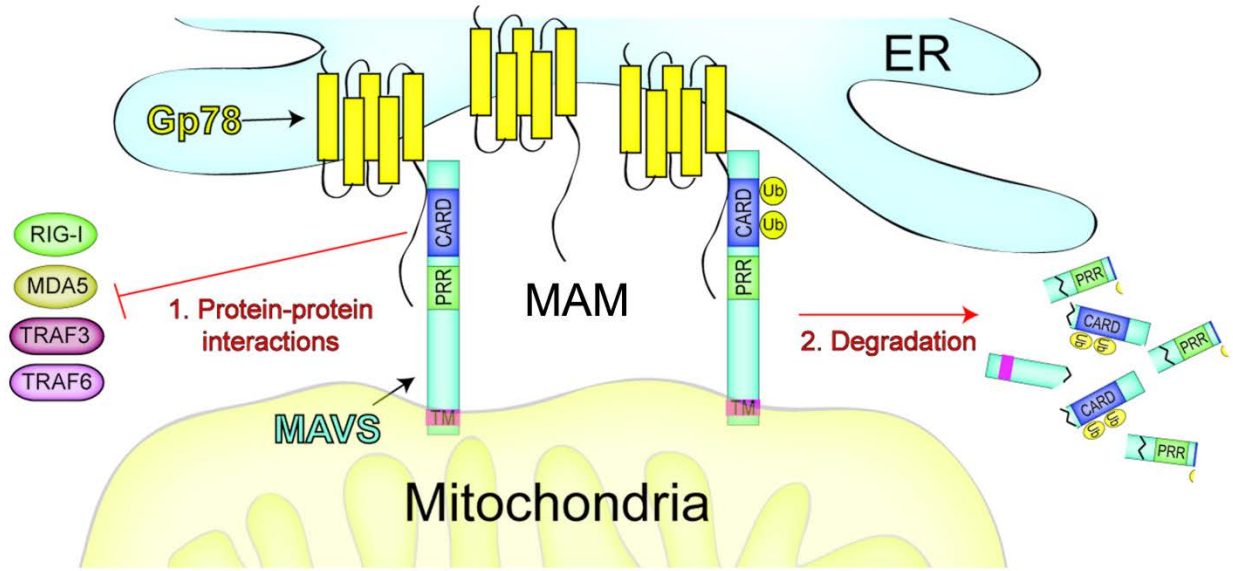

Figure 13. Schematic of the proposed mechanisms of Gp78-mediated regulation of MAVS signaling**.**

Based on the data presented here, we propose a model by which MAM-associated Gp78 regulates MAVS signaling by two mechanisms: (1) protein-protein interactions and (2) ubiquitin-mediated degradation. In (1), Gp78 binding to MAVS might prevent its association with upstream (RIG-I/MDA5) or downstream (TRAF3/TRAF6) components associated with antiviral signaling. In (2), Gp78 utilizes its E3 ubiquitin ligase and ERAD functions to induce the degradation of MAVS. Although not specifically depicted in this schematic, MAVS oligomerization is a critical component of its signaling (101, 237, 238).

5.0 SPECIFIC AIM TWO: CHARACTERIZE THE ROLE OF BPIFB3 IN ENTEROVIRUS INFECTION

5.1 BACKGROUND

A newly emerging theme in ER function includes its role in the replication of viruses. This phenomenon was first observed decades ago by electron microscopy when it was noticed that the intracellular membranes of PV-infected cells were morphologically different than that of uninfected cells, and it was concluded that viruses must induce some sort of membrane rearrangement upon infection (239-241). It has since been shown that many viruses, including all positive-sense RNA viruses, hi-jack host-derived membranes for their replication (26-28), commonly from the ER or secretory system. It is believed that this strategy serves to form scaffolding on which to assemble the replication machinery as well as protect the replicating RNA from cytosolic immune surveillance. Picornaviruses, including PV and CVB, form double membrane-bound vesicular replication complexes derived from the ER, Golgi, and lysosomes (18, 239-243). It has been shown that CVB replication begins on the membranes of the Golgi and trans-Golgi network. With the production of new viral proteins the secretory system is arrested and reorganized to provide a source for more viral replication complexes, and additional replication complexes are formed close to ER exit sites (19, 20).

The rhabdovirus VSV is a single-stranded negative-sense RNA virus that has also been shown to utilize host-derived membranes. During replication the virus was shown to form cytoplasmic inclusion bodies for the purpose of compartmentalization of replication (244-246). Early in the replication cycle these inclusion bodies do not seem to be enclosed by a membrane,

but later on in viral replication these inclusion bodies are enclosed by membranes derived from the ER (244).

The use of host-derived membranes for viral replication is not limited to RNA viruses, as the poxvirus VV was shown to also utilize this phenomenon for its replication. VV is a large DNA virus that, unlike all other DNA viruses, replicates its DNA in the cytoplasm of the host cell, and its replication centers are typically organized into foci (247, 248). Later EM studies showed that these foci of DNA replication are surrounded by rough ER, resembling mini-nuclei in the cytoplasm due to DNA labeling of the interior of the foci (249).

Previously, we conducted RNAi high-throughput screening and identified BPIFB3 (LPLUNC3, RYA3) as a gene whose depletion led to a significant enhancement in infection of the enteroviruses CVB and PV (205). BPIFB3 belongs to the PLUNC group within the BPI/ LBP family of proteins, whose members include host defense proteins in the upper airways (197-203). We found this target particularly interesting since BPIFB3 has not been functionally characterized and sequence and structural analyses point to a role in lipid content and/or localization due to the presence of lipid-binding regions. In these studies, in order to further characterize BPIFB3 and its role in enterovirus infection we first showed that CVB infection was enhanced in the absence of BPIFB3. We went on to analyze the previously unreported subcellular localization of BPIFB3 and found that it is localized to the ER, and that depletion of BPIFB3 resulted in a severe disruption of the architecture and calcium homeostasis function of the ER. In an attempt to further unravel the role of BPIFB3 in enterovirus infection we found that the infection of several other enteroviruses, as well as VSV and vaccinia virus, were greatly affected by the depletion of BPIFB3. Taken together, in this work we have provided characterization of a previously undescribed and novel component of the ER that appears to be

crucial in regulation of infection of diverse viruses, possibly by affecting their ability to co-opt host membranes required for replication or trafficking.

5.2 RESULTS

5.2.1 Depletion of BPIFB3 results in a dramatic increase in CVB infection

We previously conducted high throughput RNAi screens for novel regulators of enterovirus infection in hBMECs and identified BPIFB3 as a regulator of CVB and PV infection whose depletion led to a robust enhancement of infection (205). Figure 14A shows recapitulation of the screen results in hBMECs, confirming that depletion of BPIFB3 in hBMECs leads to a robust enhancement of CVB infection. This result was further confirmed using plaque assay to compare the titer of CVB propagated in hBMECs transfected with a control siRNA to the titer of CVB grown in hBMECs transfected with siBPIFB3. Depletion of BPIFB3 resulted in nearly a $\log_{10}$ increase in resulting CVB titers (Figure 14B). Efficient knockdown of BPIFB3 was achieved (~50%), as measured using qPCR of BPIFB3 expression in cells transfected with siBPIFB3 and siCON (Figure 14C). Together, these results show that BPIFB3 plays a role in CVB infection.

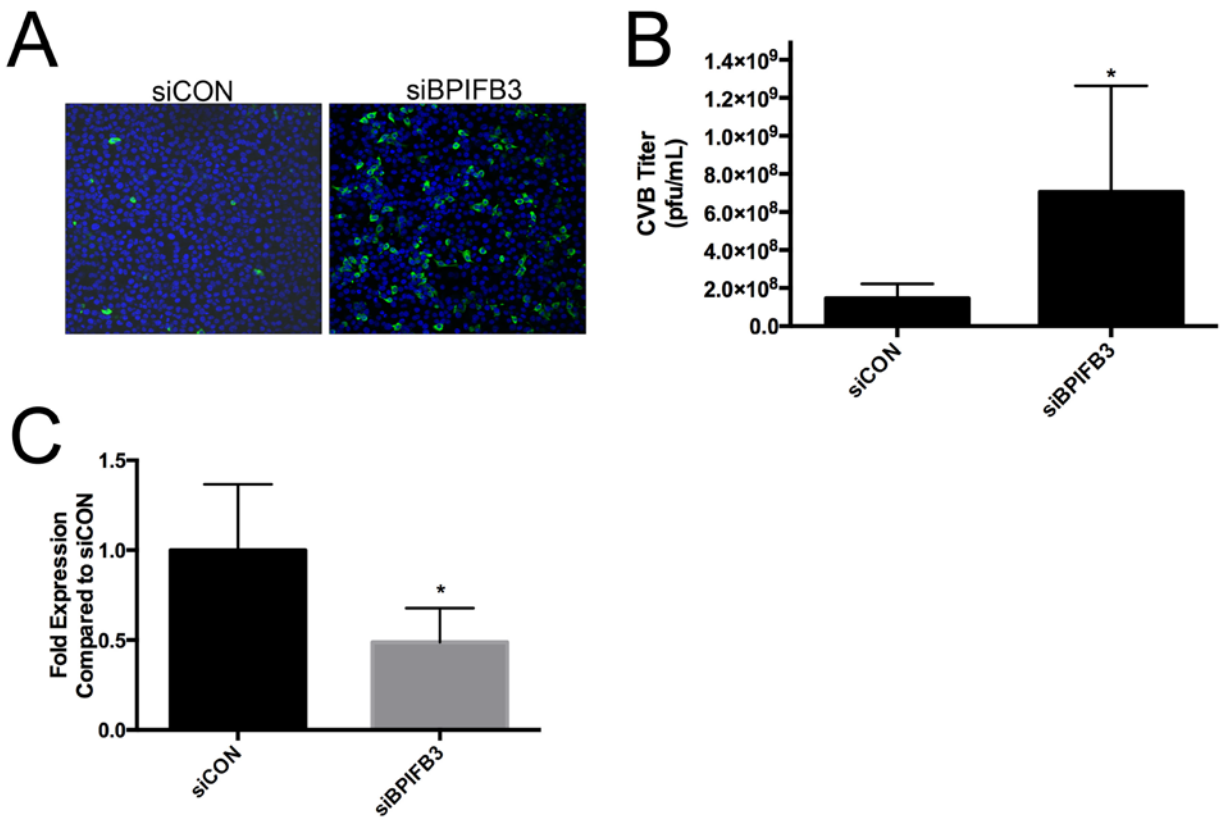

Figure 14. Confirmation of BPIFB3 as a regulator of CVB infection.

(A), Enhanced CVB infection in hBMECs transfected with an siRNA targeting BPIFB3 (siBPIFB3) compared to cells transfected with a control siRNA (siCON). Enteroviral VP1 is shown in green and DAPI-stained nuclei are shown in blue. **(B),** Titers (pfu/mL) of CVB propagated for ~16 hrs on hBMECs transfected with siBPIFB3 or siCON. **(C),** Knockdown efficiency of siBPIFB3 as measured using qPCR. Data in (A) are representative of at least 3 independent experiments, and data in (B) and (C) are from at least 3 independent experiments and are presented as mean ± standard deviation (*$p<0.05$).

5.2.2 BPIFB3 is localized to the endoplasmic reticulum

Many members of the BPI/LBP family, including BPIFB3, are largely uncharacterized and their localization patterns undetermined. In order to provide clues to the role of BPIFB3 in viral

infection we examined the subcellular localization of BPIFB3. U2OS cells stably expressing BPIFB3-Flag were co-stained for early endosomes (EEA1), Golgi, lipid droplets (BODIPY), mitochondria and ER. BPIFB3 highly co-localized only with a marker of the ER shown by immunofluorescence staining (Figure 15A), and its localization to the membrane/organelle fraction (i.e., ER-containing fraction, as shown by calnexin expression) was confirmed using subcellular fractionation of U2OS cells stably expressing BPIFB3-Flag (Figure 15B).

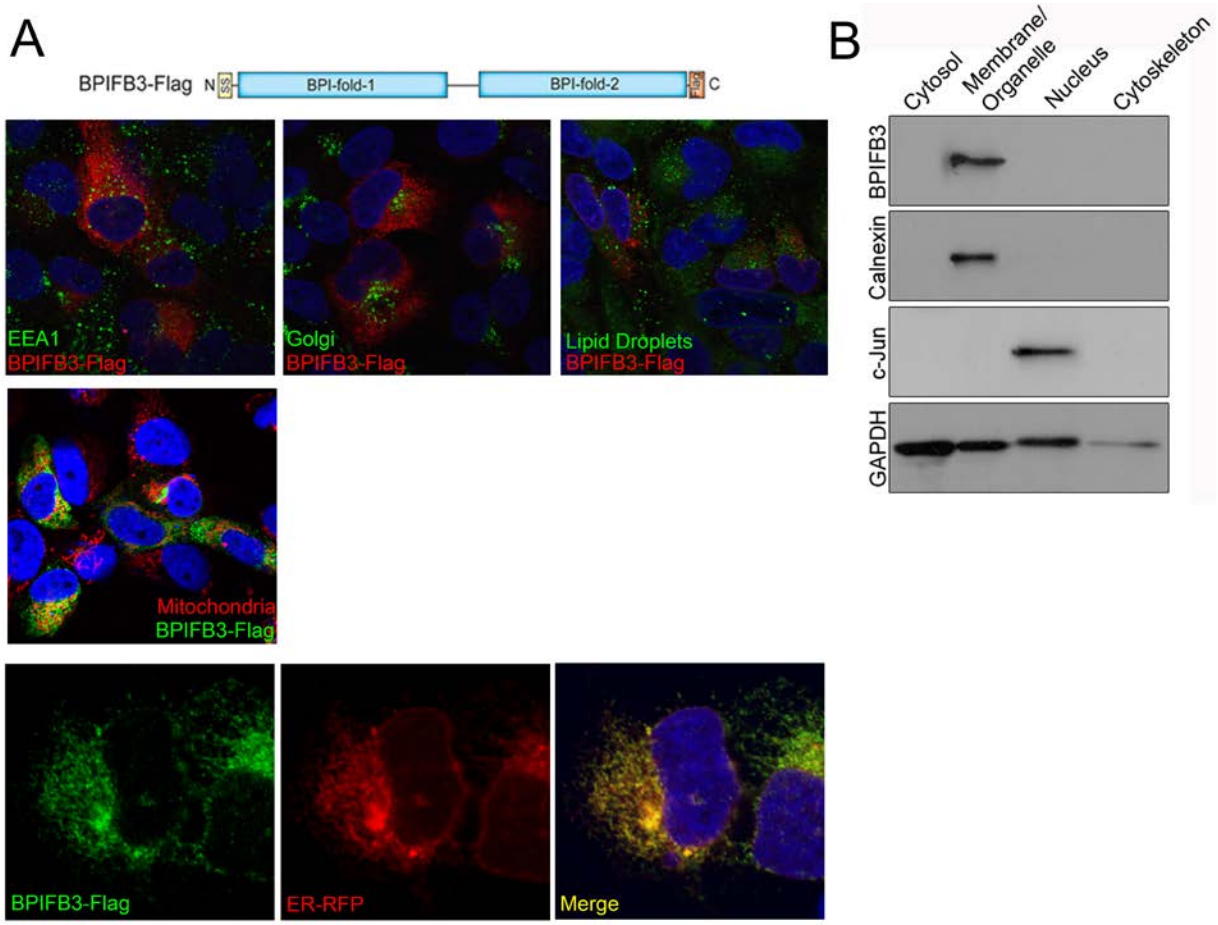

Figure 15. ER localization of BPIFB3.

(A), Top, schematic of BPIFB3-Flag, courtesy of Dr. Carolyn Coyne. Bottom, immunofluorescence microscopy of BPIFB3-Flag-expressing U2OS cells stained for early endosomes (EEA1=green, BPIFB3-Flag=red), Golgi (Golgi=green, BPIFB3-Flag=red), lipid droplets (lipid droplets=green, BPIFB3-Flag=red), mitochondria (mitochondria=red, BPIFB3-Flag=green), or infected with ER-RFP-expressing baculovirus (ER-RFP=red, BPIFB3-Flag=green). DAPI-stained nuclei are shown in blue. **(B),** Immunoblotting of fractions obtained from subcellular fractionation of U2OS cells stably expressing BPIFB3-Flag. Blotting performed using anti-Flag antibody for BPIFB3-Flag, anti-calnexin antibody, anti-c-Jun antibody, and anti-GAPDH antibodies. Data are representative of at least 3 independent experiments.

5.2.3 Depletion of BPIFB3 results in disruption of ER architecture

Since BPIFB3 clearly localized to the ER, we next sought to determine its role in maintenance of ER morphology. To this end we performed electron microscopy on hBMECs transfected with either siBPIFB3 or siCON, and left untreated or treated with the vacuolar type H+-ATPase inhibitor Bafilomycin A (BafA) to induce cell stress and resulting alterations in ER morphology. Normal hBMEC ER morphology is shown in Figure 16A (left) and consists of prominent and regularly interspaced ER sheets. Figure 16A right shows a moderately disrupted ER morphology with interrupted spatial organization of the ER sheets and increased curvature in the absence of BPIFB3, similar to that in cells treated with BafA (compare Figure 16A, right to Figure 16B, left). However, in cells treated with BafA those depleted of BPIFB3 showed an exaggerated phenotype of ER morphology disruption (compare Figure 16B, left to Figure 16B, center and right panels). Cells treated with siBPIFB3 as well as BafA showed dramatically altered spatial organization as compared to those treated with siCON and BafA (compare Figure 16B, left to Figure 16B center), as well as clear bulging of the ER sheets (i.e., a larger inner lumen space. Compare Figure 16B,

left to Figure 16B, right). These data suggest that BPIFB3 plays a role in maintaining ER structure and morphology.

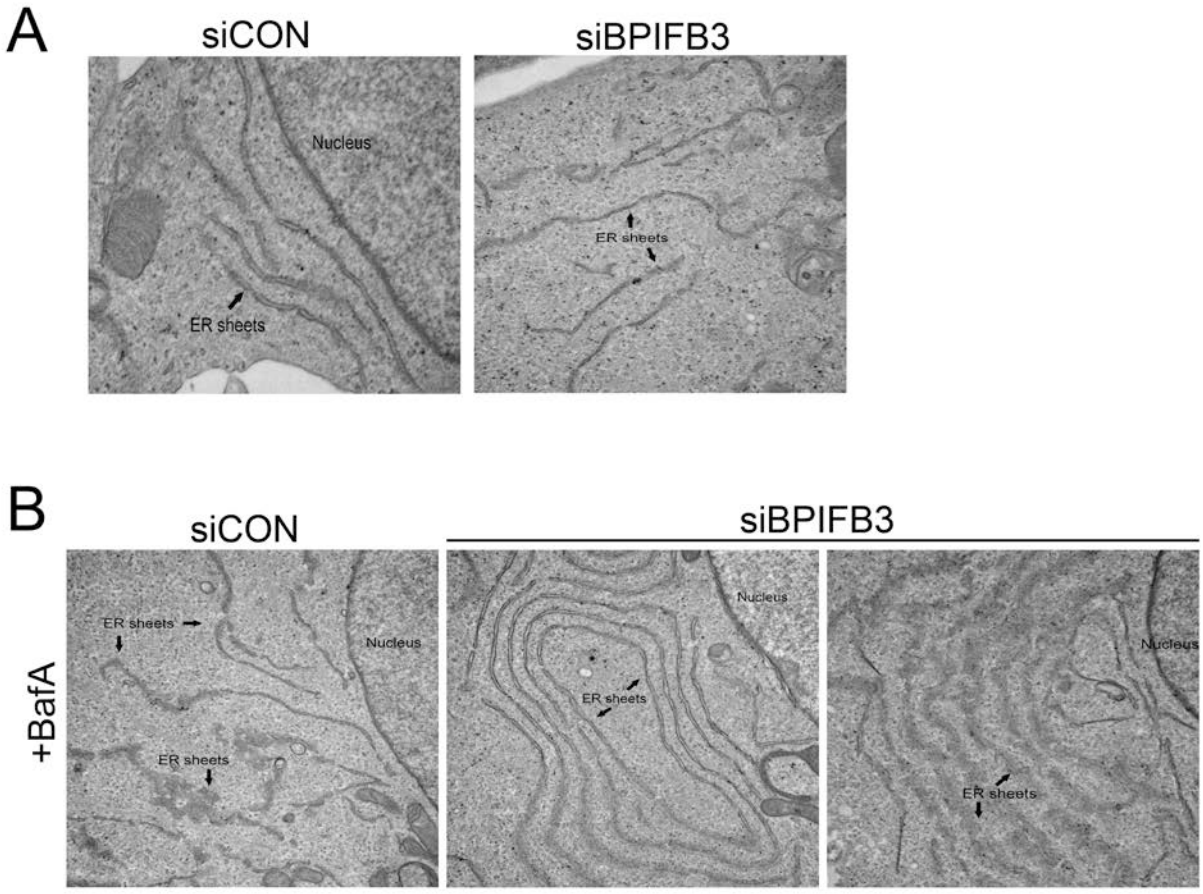

Figure 16. BPIFB3 plays a role in ER morphology.

(A and B), Electron microscopy was performed on hBMECs transfected with siCON or siBPIFB3 and left untreated (A) or treated with 2 nm BafA for 3 hours (B). Cells were treated by Dr. Carolyn Coyne, sections were prepared by the University of Pittsburgh Center for Biological Imaging EM Core, and microscopy was performed by Dr. Elizabeth Delorme-Axford. Data are representative of at least 2 independent experiments.

5.2.4 Depletion of BPIFB3 results in disruption of ER calcium homeostasis activity

The observation that BPIFB3 plays a role in regulation and maintenance of ER morphology led us to investigate the effect of depletion of BPIFB3 on ER function. As a measure of ER function we chose to monitor release of ER-derived calcium stores since regulation of calcium signaling is one of the ER's main functions (154). We achieved this using the cytosolic calcium indicators Fluo-4 and Fura-2 to directly measure cytosolic calcium levels after thapsigargin treatment-triggered release of calcium stores from the ER to the cytosol. Interestingly, cytosolic calcium levels as measured using Fluo-4 in siBPIFB3-transfected cells fluctuated strikingly as compared to siCON-transfected cells, suggesting a disruption of the ER's ability to maintain its calcium levels (Figure 17A, timepoints 0-20). When measured using the ratiometric dye Fura-2, thapsigargin-mediated release of ER-derived calcium in siBPIFB3-treated cells was ~1.5-fold lower than siCON-treated cells, further suggesting an inability to adequately regulate ER calcium stores (Figure 17B). Together, these data suggest that BPIFB3 depletion-mediated loss of ER morphology corresponds to a loss of ER calcium homeostasis function as well.

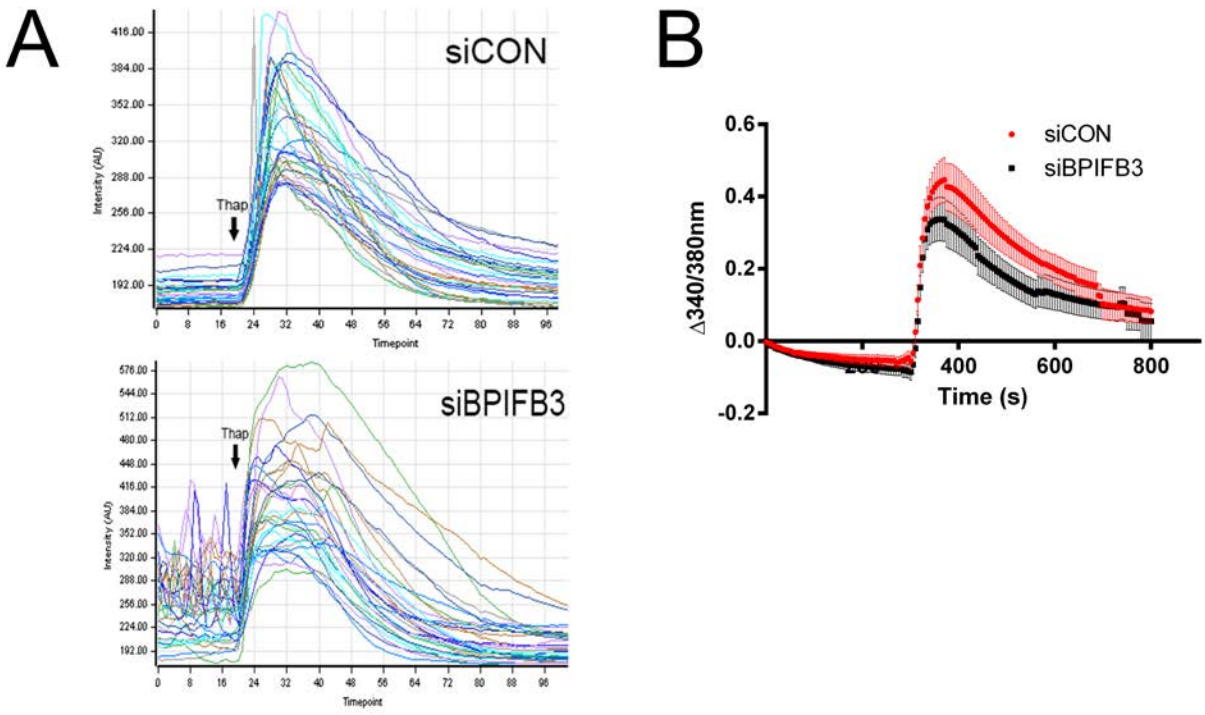

Figure 17. BPIFB3 affects maintenance of ER-derived calcium stores.

(A), Fluctuations in cytosolic calcium levels prior to thapsigargin-mediated release of ER-derived calcium stores. Graphs depict fluorescence intensity of 30 regions of interest (ROIs) over time chosen from images of hBMECs transfected with siBPIFB3 or siCON and loaded with Fluo-4, prior to treatment with 1μM thapsigargin. **(B),** Thapsigargin (1μM)-mediated calcium release in hBMECs transfected with siBPIFB3 or siCON and loaded with the ratiometric dye Fura-2. Data in (A) are representative of at least 3 independent experiments and data in (B) are from at least 3 independent experiments and are shown as mean±SEM for 30 ROIs.

5.2.5 Depletion of BPIFB3 results in a dramatic enhancement of VSV syncytia formation and alterations in vesicular trafficking

Upon investigating the effect of BPIFB3 silencing on the infection of viruses other than CVB, we observed the striking effect that depletion of BPIFB3 in hBMECs led to a dramatic increase in

syncytia formation in VSV-infected cells (Figure 18A). However, the increase in syncytia formation was not merely a reflection of increased VSV titers, since plaque assays of VSV propagated in hBMECs transfected with siCON or siBPIFB3 actually showed a moderate (!1.5-fold) decrease in VSV titers in the absence of BPIFB3 (Figure 18B). It is important to note that the VSV glycoprotein (VSV-G) can act as a fusogenic protein, and that its fusogenic properties are highly dependent on pH (250). However, data generated by others in the lab showed that both extracellular and cytosolic pH remained unchanged in the absence of BPIFB3 (data not shown), suggesting that the mechanism of VSV-mediated-syncytia enhancement in the absence of BPIFB3 is independent of a global change in cellular pH. For further exploration into the mechanism of syncytia enhancement we performed EM on hBMECs transfected with siCON or siBPIFB3 and left untreated or treated with BafA to 'freeze' progression of the endosomal pathway (251), in order to look for alterations in vesicular trafficking. Examination of the resulting intracellular vesicular environment showed an enhancement of the size and number of vesicles (Figure 18C). Immunofluorescence microscopy performed by others in the lab revealed the identity of these vesicles as early endosomes and lysosomes (data not shown). Together, these data suggest that depletion of BPIFB3 results in significant alterations in intracellular vesicular trafficking, and that these alterations could lead to incorrect VSV trafficking and syncytia formation.

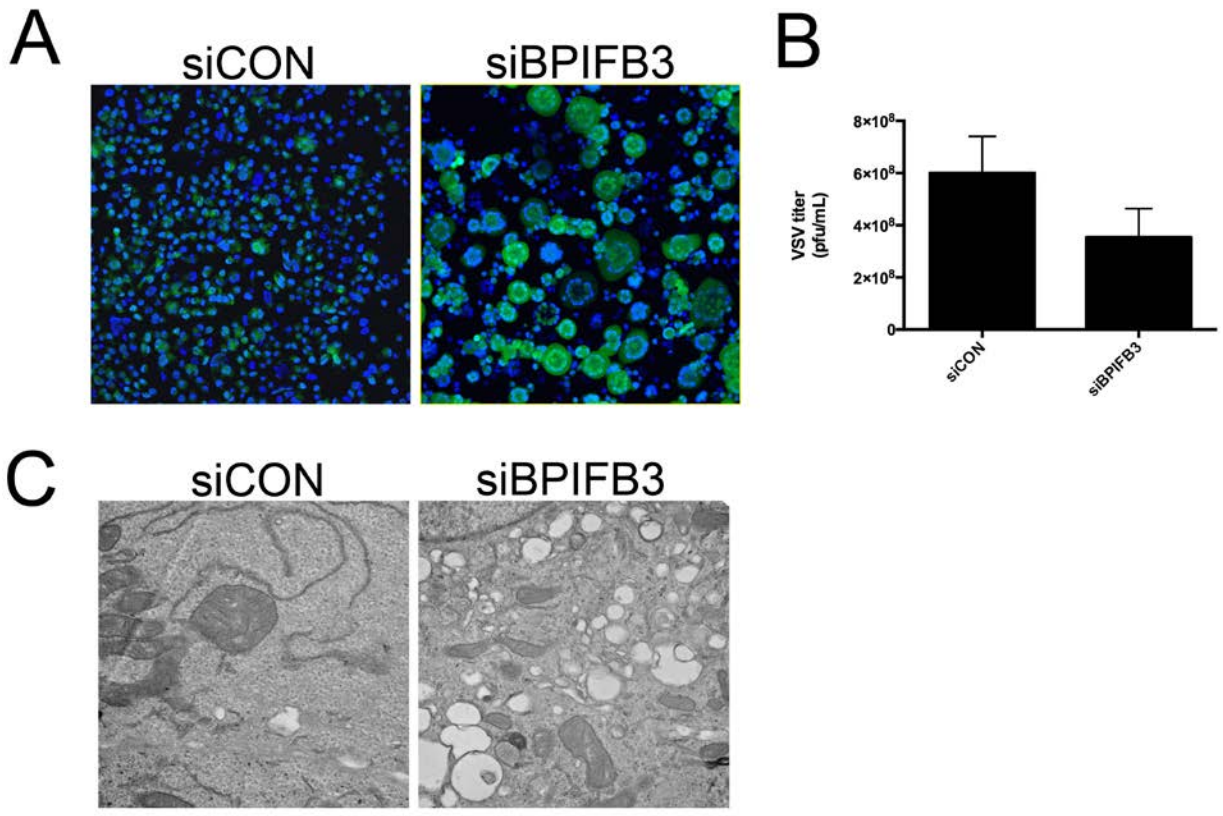

Figure 18. BPIFB3 regulates intracellular vesicular trafficking, affecting VSV syncytia formation. **(A),** VSV-GFP-induced syncytia in hBMECs transfected with siCON or siBPIFB3 and infected with VSV-GFP ~16 hrs. VSV-GFP is shown in green and DAPI-stained nuclei are shown in blue. **(B),** Titers (pfu/mL) of VSV-GFP propagated for ~16 hrs on hBMECs transfected with siBPIFB3 or siCON. **(C),** Electron microscopy was performed on hBMECs transfected with siCON or siBPIFB3 and treated with 2 nm BafA for 3 hours. Cells were treated by Dr. Carolyn Coyne, sections prepared by the University of Pittsburgh Center for Biological Imaging EM Core, and microscopy was performed by Dr. Elizabeth Delorme-Axford. Data in (A) are representative of at least 3 independent experiments, and data in (C) are representative of at least 2 different experiments. Data in (B) are from at least 3 independent experiments, and are presented as mean ± standard deviation.

5.2.6 BPIFB3 plays a role in infection of diverse viruses

As discussed above, the host cell ER is co-opted by a variety of different viruses for completion of their life cycles in a variety of different ways. In order to further delineate the role of BPIFB3 in CVB infection we tested the effect of BPIFB3 depletion on the infection of two other enteroviruses that also likely use ER-derived membranes for their replication. As expected, BPIFB3 depletion resulted in significant enhancement of both PV and enterovirus 71 (EV71) infection (~1.5-2-fold) (Figure 19A). To examine this point even further we tested the effect of BPIFB3 depletion on the infection of VSV (a negative-sense RNA virus) and VV (a DNA virus). Indeed, depletion of BPIFB3 affected infection of these viruses, but in contrast to its effect on enteroviruses, it actually decreased the infection of VSV and VV by more than 50% (Figure 19B). This outcome likely reflects the differential use of host-derived membranes in the life cycles of diverse viruses, but suggests that BPIFB3 is crucial for this process.

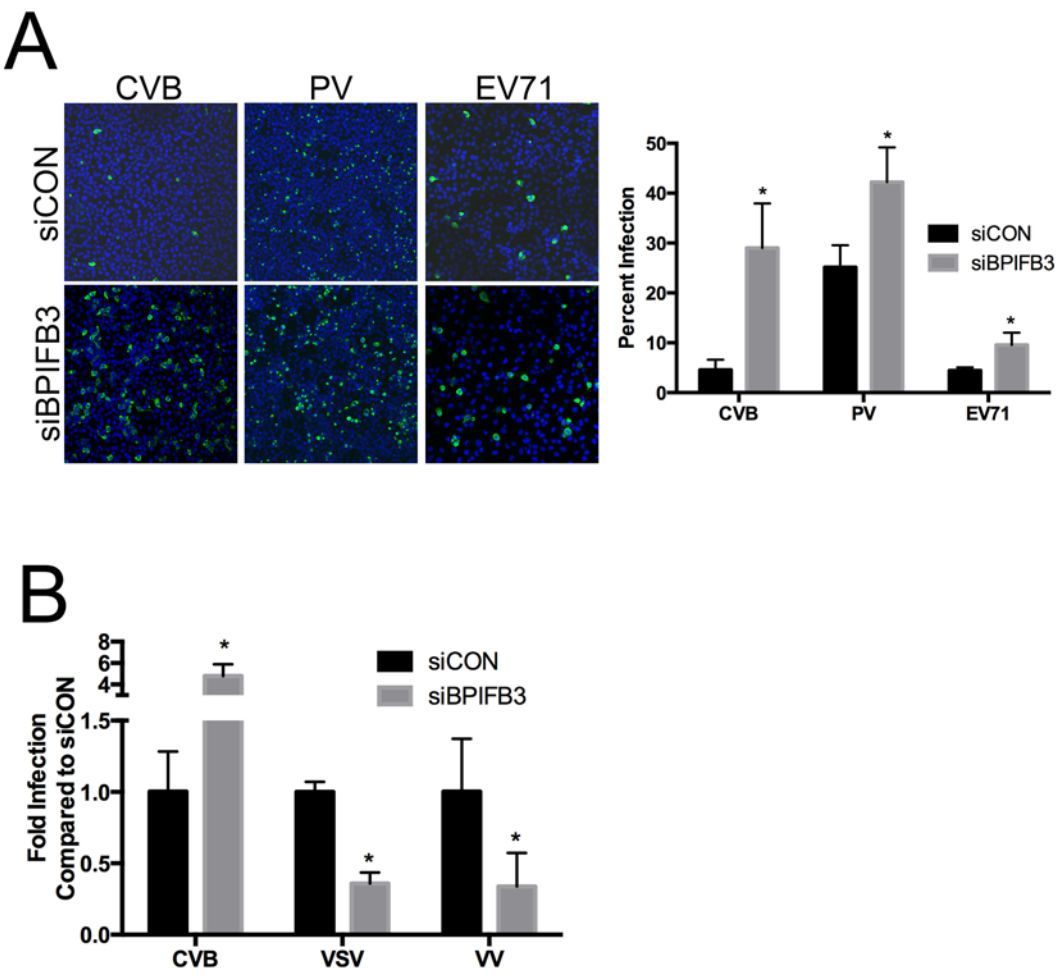

Figure 19. BPIFB3 plays a role in infection of diverse viruses.

(A), Enhanced CVB, PV, and EV71 infection in hBMECs transfected with siBPIFB3 compared to siCON, as assessed by immunofluorescence microscopy at 16 hrs post-infection. VP1 staining is shown in green and DAPI-stained nuclei are shown in blue. **(B),** Decreased VSV-GFP and VV-YFP infection in hBMECs transfected with siBPIFB3 compared to siCON, as assessed by qPCR 16 hrs post-infection. All data are from at least 3 independent experiments and are presented as mean ± standard deviation (*$p<0.05$).

5.3 DISCUSSION

Here we report on the characterization of BPIFB3 (LPLUNC3), a previously un-characterized protein identified as a regulator of enterovirus replication by unbiased high-throughput screening. The BPI/LBP family of proteins contains members with lipid-binding and antimicrobial properties (191). The PLUNC subfamily (including BPIFB3) consists of largely uncharacterized BPI homologs that seem to retain the BPI/LBP family's lipid-binding properties, but not the ability to neutralize or kill bacteria (202). Since BPIFB3 contains a lipid-binding region suggesting it could play a role in regulating lipids/membranes required for viral replication, and its function has not been clearly reported, we found it to be an interesting protein for follow up.

We showed that BPIFB3 is localized to the ER, and that depletion of BPIFB3 resulted in a disruption of ER morphology and calcium homeostasis. These results suggest that BPIFB3 is a novel component of the ER, and that it plays a role in maintenance of ER morphology and structure. The enhancement of this phenotype in the presence of ER stress induced by BafA treatment further confirms a role for BPIFB3 in maintenance of ER structure and morphology, as this would suggest an inability of the ER to counter stress-induced alterations in the absence of BPIFB3. Because of the presence of two lipid binding regions in its structure, it is possible that BPIFB3 is an integral membrane component of the ER, inserting directly into the membrane via its lipid binding regions. In this capacity BPIFB3 could play a role as an adaptor or regulator (either directly or indirectly) of important ER membrane-bound proteins known to play a role in ER morphology. Interestingly, EM pictures of the ER in the absence of BPIFB3 showed a disruption of flat, perinuclear, closely spaced and stacked ER sheets, resulting in a less spatially organized series of ER sheets that showed more curvature, and therefore seemed tubular in nature. This phenotype was exaggerated in the presence of BafA-induced ER stress, with evidence of

thickening of the ER sheets. ER morphology is largely maintained by a group of ER-membrane proteins, with membrane curvature induced by the reticulon and DP1/Yop1p proteins (163-165). In contrast, the flatness and intralumenal spacing of stacked perinuclear ER sheets is maintained by the Climp63, p180, and kinectin proteins (164, 166). The function of these ER morphology-generating proteins rely on their insertion into the ER membrane, and they could therefore interact with ER-membrane localized BPIFB3. Since depletion of BPIFB3 generated a more curved ER membrane phenotype, BPIFB3 could have a positive regulatory role on p180 or kinectin via direct protein-protein interaction, since these two proteins have been shown to maintain flatness of perinuclear ER sheets. Conversely, BPIFB3 could have a negative regulatory role via direct interaction with the reticulon and/or DP1/Yop1p proteins, since they have direct roles in generating and maintaining ER curvature. An increase in ER membrane curvature could, in turn, affect the function of many other ER membrane-bound proteins. For example, the conformation of ER membrane-bound calcium release receptors responsible for calcium homeostasis such as IP3 could be disrupted and therefore function aberrantly due to the unusual amount of curvature in the membrane, accounting for the loss of calcium homeostasis seen in BPIFB3-depleted cells.

Also among the candidates for interaction with BPIFB3 in the ER membrane are phosphatidylinositol kinases (PIK). They are responsible for phosphorylation of PIs, which are important components of cellular membranes. The distribution of PI and its various phosphorylation states (or PIPs), along with the group of membrane-bound proteins associated with a particular organelle's "lipid signature" essentially determines the identity and function of an organelle (252-254). Disruption of the function of PIKs and therefore distribution of PI and its various phosphorylation states can have many consequences for the cell. For example, PI composition of membranes can affect the size, shape and rigidity of the ER. In this scenario,

BPIFB3 interaction and regulation of an ER-bound PIK could impact the morphology of the ER simply by triggering over or under-production of a key PI required for flattened membrane morphology. Importantly, IP3, a metabolite of the phosphorylated membrane PI PI(4,5)P2, regulates calcium homeostasis of the ER by binding to IP3 receptors on the smooth ER, initiating calcium release into the cytosol (255, 256). This could provide an explanation for the disruption of calcium homeostasis seen with BPIFB3 depletion since overproduction of this phosphorylated form of PI due to increased PIK activity could provide abnormally high levels of IP3, therefore trapping the IP3 receptor in an "open" conformation and dis-regulating calcium homeostasis.

The interesting finding that depletion of BPIFB3 resulted in greatly enhanced VSV-mediated syncytia formation independent of a titer increase was unexpected. The process of VSV-mediated syncytia formation has been previously recognized but remains poorly characterized (257). VSV contains a highly fusogenic surface glycoprotein used for entry (VSV-G), and its fusogenic properties are reported to be pH-dependent and thus only activated once in the vesicular compartment containing the correct pH (250). Since others in the lab found that both extracellular and cytosolic pH were unchanged upon depletion of BPIFB3, we reasoned that the increased fusogenecity of VSV could be due to an increased availability of low pH-containing vesicles. Indeed, EM showed an increase in size and number of vesicular structures, and immunofluorescence microscopy done by others in the lab showed an increase in size and number of early endosomes and lysosomes in BPIFB3-depleted cells. This would provide the appropriate environment for enhanced fusion and could explain the increase in VSV-mediated syncytia. Recent work has shown that significant contact between the ER and the endosomal/lysosomal system occurs to facilitate interactions between membrane components of the ER and endosomes/lysosomes (159, 258, 259), which would provide an explanation for how BPIFB3, an

ER-localized protein, could affect the endosomal/lysosomal pathway. This interaction is known to occur along the smooth, peripheral ER, and since depletion of BPIFB3 results in a higher level of curvature mimicking the morphology of the smooth ER, a higher level of contact between ER and endosomes in the absence of BPIFB3 is possible. Maturation of endosomes requires "PI conversion" to progressively higher phosphorylated species of PI in the endosomal membrane, a process requiring PIK (168, 169, 171, 177, 178). Thus, a higher level of ER-endosome contact, or altered levels of PIK activity in the absence of BPIFB3 could provide a larger and/or more available pool of resources (i.e., PIK and/or highly phosphorylated PIs) for enhanced maturation of endosomes to the larger and lower pH-containing species of mature endosomes/lysosomes. This would, in turn, provide a larger reservoir of low-pH containing mature endosomes/lysosomes for increased fusogenic activity of VSV-G. Conversely, data have shown that inhibition of PI conversion leads to a highly vacuolated phenotype and enlarged endosomes (179-181), raising the notion that altered levels of PIK activity in the absence of BPIFB3 could also provide a smaller or less available pool of PIK or PIP, leading to the same outcome of enhanced size/number of endosomes/lysosomes and an enhanced reservoir of low-pH containing mature endosomes/lysosomes for increased fusogenic activity of VSV-G.

Enteroviruses utilize components derived from the ER and secretory system, such as the ER-Golgi intermediate compartment (ERGIC) and Golgi to form replication complexes (19, 260, 261). Disruption of ER morphology upon depletion of BPIFB3 would likely lead to dysfunction/disassembly of components of the secretory pathway, therefore providing a source of material for increased replication complex assembly. This could explain the increase in enterovirus infection observed upon BPIFB3 depletion. Alternatively, the increase in membrane curvature evident in the absence of BPIFB3 could provide increased surface area for formation of

secondary viral replication complexes. Secondary viral replication centers were shown to form at ER exit sites, which exist in areas of high membrane curvature (19, 162). This idea is bolstered by the finding that PV utilizes the host protein ARF1 to recruit other host proteins responsible for increasing the membrane curvature at areas of viral replication (20, 21), showing that enteroviruses favor highly curved membranes for their replication. The possible role for BPIFB3 in regulation of PI kinase activity discussed above could provide another possible explanation for enhancement of enteroviral infection in the absence of BPIFB3. Enteroviruses have been shown to recruit and require PI4KIIIβ for their replication, therefore a scenario in which BPIFB3 depletion enhances the availability or activity of this kinase would increase enteroviral replication.

Depletion of BPIFB3 resulted in a marked decrease in both VV and VSV infection. Different viruses have different requirements of intracellular membranes for their replication. In the case of VV, cytoplasmic replication is organized into foci that are surrounded by rough ER (247-249). The finding that BPIFB3 depletion led to disruption of closely stacked ER sheets and higher curvature in the ER membrane could account for this, since the absence of traditional rough ER morphology could cause problems with VV recruitment of membranes for viral replication. As for VSV, VSV-G trafficking through the Golgi is vital for completion of its lifecycle and release of new infectious virions (262, 263). The increase in endosomal/lysosomal vesicular compartments in the absence of BPIFB3 could make VSV-G trafficking and hence assembly of new viral particles difficult due to the availability of low pH-containing endosomes/lysosomes for fusion, which are known to cycle from the Golgi compartment as well as the endocytic compartment (168). This would shuttle the VSV-G away from the secretory system and to the endosomal/lysosomal system, sequestering it from the plasma membrane where VSV requires it for assembly and budding.

Overall, we have made significant progress towards the characterization of a novel regulator of ER morphology identified by high throughput RNAi screening. We have provided evidence that BPIFB3 plays a significant role in the replication of a diverse set of viruses, the differing effect of its depletion on infection highlighting the known differences between their replication cycles. Importantly, this work has also shown that BPIFB3 plays a role in regulation of the endosomal/lysosomal pathway, likely indirectly through its effects on the ER and the known interaction between the endosomal/lysosomal pathway and the ER. Important work is ongoing in the lab to determine the exact mechanism(s) by which BPIFB3 achieves these effects.

6.0 FINAL DISCUSSION

Understanding the interactions between a virus and its host cell is critical in order to improve upon existing treatments and vaccines. Towards the goal of better understanding this interaction, we previously conducted a high-throughput RNAi screen for host cell factors involved in enterovirus infection (205). Whereas similar screens have been reported this screen was particularly innovative since it was performed in a polarized cell type, more closely resembling the conditions of physiological infection. Of the ~5,000 genes screened for their effect on enterovirus infection, 117 'hits' were identified whose depletion affected enterovirus infection. Of the 117 hits, 46 genes were found whose depletion led to a decrease in both CVB and PV infection and were considered to be broadly pro-viral and 17 genes were found whose depletion led to an increase in both CVB and PV infection and were considered to be broadly anti-viral. Of these hits, we chose two different genes for follow up: Gp78 and BPIFB3.

The multitude of interesting targets yielded by the RNAi screen has opened up possibilities for many different future directions in identifying previously uncharacterized interactions between the host cell and virus. Indeed, some of these 'hits' are being pursued in the lab, and many more remain to be investigated. The knowledge regarding host-virus interactions to be gained from pursuit of these targets will provide critical information on previously unrecognized interactions that could be exploited for the purpose of novel treatments or vaccines.

Depletion of Gp78 resulted in a decrease of enterovirus infection, and we found it to be an interesting target due to its E3 ligase activity and its localization at the MAM in close proximity to the MAVS-containing innate immune signaling synapse. We went on to further characterize the mechanism of siGp78-mediated repression of enteroviral replication and found that its

depletion resulted in decreased infection of other RNA viruses as well. This effect was later found to be due to the ability of Gp78 to repress type I interferon signaling. Gp78 achieves this effect by two mechanisms, causing degradation of the MAM-localized RLR signaling adaptor protein MAVS, and binding directly to MAVS, preventing critical upstream and downstream interaction. Therefore, Gp78 is not pro-viral in the traditional sense (i.e., the virus does not use it directly for completion of its life cycle), but rather the host cell uses it as a mechanism to prevent excessive inflammation by downregulating expression and repressing activity of a key innate immune mediator. In conclusion, pursuit of the screen 'hit' Gp78 as a potential regulator of virus infection resulted in successful description of a novel function for Gp78 in regulation of type I interferon signaling.

Although the role of Gp78 in virus infection has been described in chapter 4 of this dissertation, there are many remaining questions for follow-up studies to address. For example, it would be interesting to expand upon the virus panel used, testing the effect of Gp78 depletion on infection of a few more viruses known to signal through MAVS, as well as a few that do not signal through MAVS. A further characterization of the interaction between MAVS and Gp78 would also be informative. Our data show that Gp78 expression is not induced upon SeV, purified IFN, or poly(I:C) treatment, and that the expression of ISG56 increased slightly upon depletion of Gp78 in the absence of stimulation. Both of these observations suggest that Gp78 plays a housekeeping role in MAVS downregulation, preventing excessive inflammation. This is crucial in preventing autoimmunity or cellular/tissue damage due to the onslaught of inflammation in the absence of an invading threat. However, it is possible that the strength or amount of interaction between MAVS and Gp78 could increase in the presence of type I interferon signaling, and this could be tested by performing coimmunoprecipitation studies in the presence and absence of SeV, purified IFN, or

poly(I:C). If the interaction is indeed increased in the presence of stimulation it would suggest that, whereas Gp78 expression itself is not inducible, the interaction between Gp78 and MAVS is at least partly inducible. Although this would not negate the possibility of a housekeeping role for Gp78 in MAVS regulation, it would further explain how Gp78 could prevent excessive inflammation with a negative feedback system.

Additionally, mapping of the regions of MAVS required for interaction with Gp78 would further clarify which MAVS interactions are disrupted by its interaction with Gp78. Our data show that Gp78 interacts with both the C- and N-terminal fragments of MAVS, but only the N-terminus is required for Gp78-mediated degradation. It is likely that an independent interaction is necessary to achieve each mechanism of downregulation (i.e., degradation and interaction causing disruption of critical signaling interactions), and further mapping MAVS interaction sites may lead to important information about the interaction. For example, if the CARD of MAVS contains the area of ubiquitination and therefore the first area of interaction mediating ubiquitination/degradation, then the C-terminal fragment must contain the residues responsible for the interaction causing signaling disruption. If this is the case, then Gp78-MAVS interaction must disrupt the ability of MAVS to bind to the downstream signaling partner TRAF3, since this is the only known binding region in the C-terminus corresponding to up/downstream MAVS signaling partners. Of course, it is possible that multiple interactions between Gp78 and MAVS occur and cause blocking of more than one critical up/downstream signaling interaction. Mapping of the MAVS sites of interaction would further clarify these questions.

From the data presented, it is not clear whether the interaction between Gp78 and MAVS is a direct interaction or an indirect interaction in a multi-protein complex. Direct interaction could be tested using recombinant MAVS and Gp78 in a cell-free system. If the interaction is not direct,

identification of any additional interacting partners could be achieved by performing mass spectrometry on the complex pulled down in a coimmunoprecipitation study.

Interestingly, our collaborator Dr. Ivan Nabi's group is currently searching for the motif within Gp78 responsible for tethering it to the MAM. Unpublished data from another group has shown that Gp78 leaves the MAM in the context of viral infection, which is consistent with our findings that it negatively regulates MAVS in a housekeeping manner. Results from both of these studies would provide valuable insight to the function of Gp78 in the context of viral infection.

Depletion of BPIFB3 resulted in an enhancement of enterovirus infection, and we chose to pursue this target due to its lack of characterization, and reports of lipid-binding properties given its sequence and structural similarities to BPI. As we went on to further characterize its role in enterovirus infection, we surprisingly found that its depletion led to a decrease of infection of VSV and VV, as well as significant enhancement of VSV-mediated syncytia. Examination of its subcellular localization revealed a largely ER-centered localization pattern, and EM of cells lacking BPIFB3 showed disrupted ER architecture, a phenomenon that was greatly enhanced under conditions of ER stress, and disruption of calcium homeostasis, along with enhanced numbers and size of endosomes/lysosomes. Taken together, these observations and data suggested that the previously uncharacterized BPIFB3 is a novel component of the ER with a role in maintenance of ER architecture and the endosomal/lysosomal pathway, perhaps by affecting ER morphology-inducing proteins or lipid organization/content. This in turn affects the replication of any virus that utilizes intracellular membranes in their replication. These findings are quite surprising, given that other members of the PLUNC subfamily of proteins, along with members of the BPI/LBP family, have been reported to function as secreted antimicrobial peptides (197-203). This highlights the need for further work in characterization of this family of proteins.

Work described in Chapter 5 of this dissertation represents a major stride toward characterization of BPIFB3. However, there are many remaining questions for future study and further characterization, some of which are being pursued in the lab currently. The most important question to address is regarding the mechanism for maintenance of ER morphology. How does BPIFB3 maintain, or help to maintain, correct ER architecture? We have speculated that BPIFB3 could insert into the ER membrane via its lipid binding domains and therefore interact with proteins that are required for maintenance of ER morphology, such as the reticulons, DP1 proteins, Climp63, kinectin, or p180. As discussed earlier, this would have implications for the replication of ER-requiring viruses, endosome/lysosome trafficking, as well as calcium homeostasis. The ability of BPIFB3 to insert into the membrane could be tested by mutational analysis of the lipid binding regions followed by confocal microscopy-based localization studies. The interaction between BPIFB3 and proteins involved in ER morphology maintenance could be tested using a protein interaction assay, such as yeast-two hybrid using BPIFB3 as bait. Identifying any interacting partners of BPIFB3 that are involved in ER morphology induction/maintenance would be helpful in moving toward finding the mechanism of BPIFB3-induced ER morphology maintenance.

We have also speculated that BPIFB3 could alter ER morphology by altering the membrane lipid content via interactions with PIK in the ER membrane. As discussed earlier, this would have implications in the replication of PIK-requiring viruses, endosome/lysosome trafficking, as well as calcium homeostasis. Interaction between BPIFB3 and various PIKs could be tested by yeast-two hybrid as well, again using the BPIFB3 as bait. Measurement of the level of PIPs, as well as overall lipid content of the cells in the absence of BPIFB3 could also be informative in investigating this hypothesis.

Based on the results of our studies, we have hypothesized that depletion of BPIFB3 could affect viral replication as a result of ER morphology disruption. This is presently being tested by performing EM on BPIFB3-depleted cells that have been infected with the various viruses used in the study. The imaging results will provide insight into the formation of ER or secretory system-derived viral replication centers in the absence of BPIFB3, as well as the architecture of the VSV-induced syncytia present in BPIFB3-depleted cells.

BPIFB3 is a member of the PLUNC subfamily of proteins, many members of which have yet to be fully characterized. Therefore, the testing of other family members represents an interesting area for follow-up that could give good insight into the function of BPIFB3. This work is also ongoing in the lab.

In conclusion, the results obtained from the studies in this dissertation have provided a significant amount of new information for the field of virus-host interaction. We have contributed new and important insight into regulation of the host innate immune response to viruses, identifying Gp78 as a novel regulator of the immune adaptor MAVS. We have also taken strides towards identifying the function of a novel component of the ER, which seems to play an important role in regulation of ER morphology and endo/lysosomal trafficking and therefore in the infection of diverse viruses. Interestingly, both of these regulators of viral infection function from the ER (Figure 20). Although some important questions remain unanswered, these studies have contributed to and underscored the need to continue work on virus-host interaction.

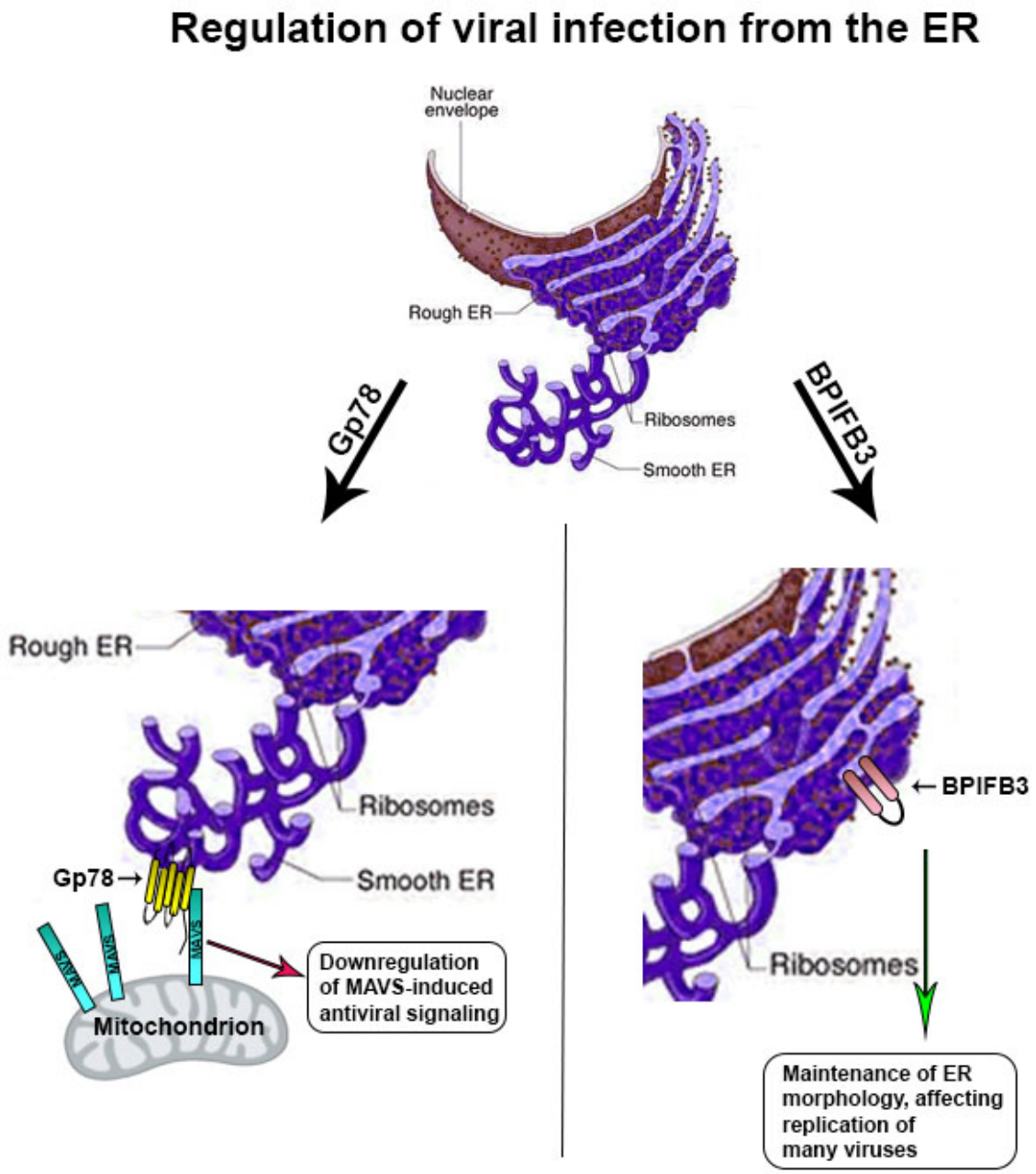

Figure 20. RNAi HTS identifies two regulators of viral infection that regulate from the ER.

This dissertation has described two regulators of viral infection, both of which regulate from the ER. Gp78 is localized to the peripheral ER in close association with mitochondria, and interacts with MAVS to downregulate MAVS-

induced antiviral signaling. BPIFB3 is localized to the ER and plays a role in maintenance of correct ER morphology, thereby affecting replication of any viruses that utilize the ER for replication.

7.0 PUBLIC HEALTH SIGNIFICANCE

To develop highly effective and targeted therapeutics for viral infections it is crucial to gain a more complete understanding of the complex interaction between the virus and its host cells. The host cell factors that are co-opted by the virus for its own use, as well as host strategies to contain viral infection and the resulting viral evasion techniques that evolve may all contain possible therapeutic targets buried within them. A highly efficient way of analyzing this interaction is using RNAi screens within relevant biological systems. This dissertation is an example of two novel and important virus-host interactions that were identified and characterized as a result of an RNAi screen. This work has public health significance because these findings will further our understanding of the virus-host interaction, which will, in turn, lead to the ability to better develop antiviral therapeutics.

In Chapter 4 of this dissertation we describe a novel modulator of antiviral immunity, providing further characterization of the innate antiviral immune response. The innate antiviral immune response is an important host-virus interaction to understand due to the role of host immunity in vaccine effectiveness. The more we know about the physiological events following a natural infection, the more we can try to modulate it for the purpose of vaccination or treatment.

Finally, in Chapter 5 of this dissertation we describe a novel component/regulator of ER morphology and function and show its importance in the replication of a diverse set of viruses. The process of viral co-opting of host cell membranes is just beginning to be appreciated as a highly important host-virus interaction. Any step in which a virus is at the mercy of the host cell for acquisition of components crucial to complete its life cycle is a step that could potentially be used for development of anti-viral therapeutics.

APPENDIX A: ABBREVIATIONS USED

5'-ppp: 5' triphosphate

AIP4: Atrophin-I-interacting protein 4

AMF: Autocrine motility factor

AMFR: Autocrine motility factor receptor

AMPK: Adenosine 5' monophosphate-activated protein kinase

ANOVA: Analysis of variance

ATG5: Autophagy protein 5

ATP: Adenosine triphosphate

BafA: Bafilomycin A

BPI: Bactericidal/permeability increasing

BPIFB3: BPI fold containing family B, member 3

Ca^{2+}: Calcium

CAR: Coxsackievirus and adenovirus receptor

CARD: Caspase activation and recruitment domain

CARDIF: CARD adapter inducing interferon-beta

CCCP: Carbonyl cyanide m-chlorophenylhydrazone

CD: Cluster of differentiation

cDNA: Complementary DNA

CETP: Cholesterylester transfer protein

Cig5: Cytomegalovirus-induced gene 5

COX5B: Cytochrome C oxidase 5B

CT: C terminus

CUE: Coupling of ubiquitin to ER degradation

CVB: Coxsackievirus B

DAF: Decay accelerating factor

DAPI: 4′,6-diamidino-2-phenylindole

DEAD: Asparagine-Glutamine-Alanine-Asparagine

DMEM-H: Dulbecco's modified eagle medium high glucose

DNA: Deoxyribonucleic acid

dsRNA: Double stranded RNA

ΔψM: Mitochondrial membrane potential

EDTA: Ethylenediaminetetraacetic acid

EGFP: Enhanced green fluorescent protein

EM: Electron microscopy

EMCV: Encephalomyocarditis virus

ER: Endoplasmic reticulum

ERAD: ER-associated degradation

EV71: Enterovirus 71

FAK: Focal adhesion kinase

FASN: Fatty acid synthase

FBS: Fetal bovine serum

G2BR: G2 binding region

GAPDH: Glyceraldehyde 3-phosphate dehydrogenase

gC1qR: Receptor for globular head domain of complement component C1q

GFP: Green fluorescent protein

Gp78: Glycoprotein 78

GTP: Guanosine triphosphate

HAU: Hemagglutination units

HBMEC: Human brain microvascular endothelial cells

HCl: Hydrochloric acid

HCV: Hepatitis C virus

HEK: Human embryonic kidney

hGp78: Human Gp78

HMW: High molecular weight

hrs: Hours

Hsp: Heat shock protein

IB: Immunoblot

IFIT3: Interferon-induced protein with tetratricopeptide repeats 3

IFN: Interferon

IgM: Immunoglobulin M

IKKe: Inhibitor-κB kinase ε

IP: Immunoprecipitation

IPS-1: Interferon-beta promoter stimulator 1

IRES: Internal ribosome entry site

IRF: Interferon regulatory factor

ISG: Interferon-stimulated gene

IκB: NF-κB inhibitor

K: Lysine

kDa: Kilodalton

LBP: LPS binding protein

LGP2: Laboratory of genetics and physiology gene 2

LPLUNC: Long PLUNC

LPS: Lipopolysaccharide

LRR: Leucine-rich-repeat

M: Molar

MAM: Mitochondria-associated ER membrane

MAVS: Mitochondrial antiviral signaling

MDA5: Melanoma differentiation-associated protein 5

MEF: Mouse embryonic fibroblast

MFN: Mitofusin

μg: Microgram

mg: Milligram

mGp78: Mouse Gp78

μL: Microliter

mL: Milliliter

μM: Micromolar

mM: Millimolar

mRNA: Messenger RNA

MyD88: Myeloid differentiation primary response gene 88

NaCl: Sodium chloride

NBD: Nucleotide-binding domain

Ndfip1: Nedd4 family interacting protein 1

Nedd4: Neural precursor cell expressed, developmentally down-regulated 4

NF-κB: Nuclear factor of kappa light polypeptide gene enhancer in B-cells

ng: Nanogram

NLRX1: Nucleotide-binding domain-and leucine-rich-repeat-containing family member 1

nM: Nanomolar

NP-40: Nonyl phenoxypolyethoxylethanol

NT: N terminus

PBS: Phophate-buffered saline

PCBP: Poly(rC) binding protein

PCR: Polymerase chain reaction

pDCs: Plasmacytoid dendritic cells

Pfu: Plaque forming units

PI4-kinase: Phosphatidylinositol 4-kinase

PLK1: Polo-like kinase 1

PLTP: Phospholipid transfer protein

PLUNC: Palate, lung and nasal epithelium clone

Poly-A: Poly-adenylate

Poly(I:C): Polyinosinic:polycytidylic acid

PSMA7: Proteasome subunit alpha type-7

PV: poliovirus

Rac: Ras-related C3 botulinum toxin substrate

RDRP: RNA-dependent RNA polymerase

Rf: RING finger

RFP: Red fluorescent protein

RIG-I: Retinoic acid-inducible gene I

RING: Really interesting new gene

RIPA: Radioimmunoprecipitation assay

RLR: RIG-I-like receptor

RNA: Ribonucleic acid

RNAi: RNA interference

ROI: Region of interest

ROS: Reactive oxygen species

RT-qPCR: Reverse transcriptase quantitative polymerase chain reaction

RT: Room temperature

SEM: Standard error of the mean

SeV: Sendai virus

Smurf1: SMAD specific E3 ubiquitin protein ligase 1

SPLUNC: Short PLUNC

ssRNA: Single stranded RNA

STING: Stimulator of interferon genes

TANK: TRAF family member-associated NF-κB activator

TBK1: TANK binding kinase 1

Thap: Thapsigargin

TLR: Toll like receptor

TNF: Tumor necrosis factor

Tom70: Translocase of outer membrane 70

TRADD: TNFR1-associated death domain protein

TRAF: TNF receptor associated factor

TRIF: TIR-domain-containing adapter-inducing interferon-β

TRIM25: Tripartite motif containing 25

TRIS: Trisaminomethane

TSPAN6: Tetraspanin protein 6

Tyr: Tyrosine

U: Units

VCP: Valosin-containing protein

VIM: VCP interacting motif

VISA: Virus-induced signaling adapter

VP1: Viral protein 1

VSV: Vesicular stomatitis virus

VV: Vaccinia virus

WT: Wild type

YFP: Yellow fluorescent protein

Δ: Deleted

APPENDIX B: CHOOSING THE TARGETS

As mentioned previously, the RNAi screen revealed a number of potential regulators of enterovirus infection. Therefore, it is important to describe our method for choosing the 'hits' Gp78 and BPIFB3 for follow-up study.

After assessing any reported functions for each screen hit we chose about 25 that we thought could be involved in innate immunity, including Gp78. We felt Gp78 may be involved in innate immunity due to its reported function as an E3 ubiquitin ligase (E3 ubiquitin ligases have been reported to regulate various aspects of innate immunity). We therefore screened the 25 hits we suspected of being involved in innate immunity in a luciferase reporter-based IFN-β promoter assay (data available upon request). Expression of Gp78 caused the most prominent reduction in IFN-β activity, so we chose to pursue the function of Gp78 in the innate antiviral immune response.

Our interest in BPIFB3 originated simply because its depletion resulted in the greatest increase in enterovirus infection, leading us to speculate that it could be a component of the innate antiviral response as well. Our interest was increased when we realized that BPIFB3 was not functionally characterized, but it was likely a lipid-binding protein (many lipid-binding proteins are known to be involved in innate antiviral immunity). We therefore chose to pursue characterization of the role of BPIFB3 in virus infection.

BIBLIOGRAPHY

1. **S.J. Flint LWE, V.R. Racaniello, A.M. Skalka.** 2009. Principles of Virology, Third ed, vol. 1: Molecular Biology. ASM Press, Washington DC.
2. **Stapleford KA, Miller DJ.** 2010. Role of cellular lipids in positive-sense RNA virus replication complex assembly and function. Viruses **2:**1055-1068.
3. **Vazquez-Calvo A, Saiz JC, McCullough KC, Sobrino F, Martin-Acebes MA.** 2012. Acid-dependent viral entry. Virus Res **167:**125-137.
4. **Yamashiro DJ, Maxfield FR.** 1984. Acidification of endocytic compartments and the intracellular pathways of ligands and receptors. J Cell Biochem **26:**231-246.
5. **Martinez-Salas E, Pacheco A, Serrano P, Fernandez N.** 2008. New insights into internal ribosome entry site elements relevant for viral gene expression. J Gen Virol **89:**611-626.
6. **Pisarev AV, Shirokikh NE, Hellen CU.** 2005. Translation initiation by factor-independent binding of eukaryotic ribosomes to internal ribosomal entry sites. Comptes rendus biologies **328:**589-605.
7. **Whitton JL, Cornell CT, Feuer R.** 2005. Host and virus determinants of picornavirus pathogenesis and tropism. Nature reviews. Microbiology **3:**765-776.
8. **Pelletier J, Sonenberg N.** 1988. Internal initiation of translation of eukaryotic mRNA directed by a sequence derived from poliovirus RNA. Nature **334:**320-325.
9. **Summers DF, Maizel JV, Jr.** 1968. Evidence for large precursor proteins in poliovirus synthesis. Proc Natl Acad Sci U S A **59:**966-971.
10. **Kitamura N, Semler BL, Rothberg PG, Larsen GR, Adler CJ, Dorner AJ, Emini EA, Hanecak R, Lee JJ, van der Werf S, Anderson CW, Wimmer E.** 1981. Primary structure, gene organization and polypeptide expression of poliovirus RNA. Nature **291:**547-553.
11. **Parsley TB, Towner JS, Blyn LB, Ehrenfeld E, Semler BL.** 1997. Poly (rC) binding protein 2 forms a ternary complex with the 5'-terminal sequences of poliovirus RNA and the viral 3CD proteinase. Rna **3:**1124-1134.
12. **Walter BL, Parsley TB, Ehrenfeld E, Semler BL.** 2002. Distinct poly(rC) binding protein KH domain determinants for poliovirus translation initiation and viral RNA replication. J Virol **76:**12008-12022.
13. **Nagy PD, Pogany J.** 2012. The dependence of viral RNA replication on co-opted host factors. Nature reviews. Microbiology **10:**137-149.
14. **Lee WM, Monroe SS, Rueckert RR.** 1993. Role of maturation cleavage in infectivity of picornaviruses: activation of an infectosome. J Virol **67:**2110-2122.
15. **Bienz K, Egger D, Troxler M, Pasamontes L.** 1990. Structural organization of poliovirus RNA replication is mediated by viral proteins of the P2 genomic region. J Virol **64:**1156-1163.
16. **Cho MW, Teterina N, Egger D, Bienz K, Ehrenfeld E.** 1994. Membrane rearrangement and vesicle induction by recombinant poliovirus 2C and 2BC in human cells. Virology **202:**129-145.

17. **Egger D, Teterina N, Ehrenfeld E, Bienz K.** 2000. Formation of the poliovirus replication complex requires coupled viral translation, vesicle production, and viral RNA synthesis. J Virol **74:**6570-6580.
18. **Schlegel A, Giddings TH, Jr., Ladinsky MS, Kirkegaard K.** 1996. Cellular origin and ultrastructure of membranes induced during poliovirus infection. J Virol **70:**6576-6588.
19. **Hsu NY, Ilnytska O, Belov G, Santiana M, Chen YH, Takvorian PM, Pau C, van der Schaar H, Kaushik-Basu N, Balla T, Cameron CE, Ehrenfeld E, van Kuppeveld FJ, Altan-Bonnet N.** 2010. Viral reorganization of the secretory pathway generates distinct organelles for RNA replication. Cell **141:**799-811.
20. **Belov GA, Ehrenfeld E.** 2007. Involvement of cellular membrane traffic proteins in poliovirus replication. Cell Cycle **6:**36-38.
21. **Belov GA, Habbersett C, Franco D, Ehrenfeld E.** 2007. Activation of cellular Arf GTPases by poliovirus protein 3CD correlates with virus replication. J Virol **81:**9259-9267.
22. **Berger KL, Cooper JD, Heaton NS, Yoon R, Oakland TE, Jordan TX, Mateu G, Grakoui A, Randall G.** 2009. Roles for endocytic trafficking and phosphatidylinositol 4-kinase III alpha in hepatitis C virus replication. Proc Natl Acad Sci U S A **106:**7577-7582.
23. **Vaillancourt FH, Pilote L, Cartier M, Lippens J, Liuzzi M, Bethell RC, Cordingley MG, Kukolj G.** 2009. Identification of a lipid kinase as a host factor involved in hepatitis C virus RNA replication. Virology **387:**5-10.
24. **Borawski J, Troke P, Puyang X, Gibaja V, Zhao S, Mickanin C, Leighton-Davies J, Wilson CJ, Myer V, Cornellataracido I, Baryza J, Tallarico J, Joberty G, Bantscheff M, Schirle M, Bouwmeester T, Mathy JE, Lin K, Compton T, Labow M, Wiedmann B, Gaither LA.** 2009. Class III phosphatidylinositol 4-kinase alpha and beta are novel host factor regulators of hepatitis C virus replication. J Virol **83:**10058-10074.
25. **Reiss S, Rebhan I, Backes P, Romero-Brey I, Erfle H, Matula P, Kaderali L, Poenisch M, Blankenburg H, Hiet MS, Longerich T, Diehl S, Ramirez F, Balla T, Rohr K, Kaul A, Buhler S, Pepperkok R, Lengauer T, Albrecht M, Eils R, Schirmacher P, Lohmann V, Bartenschlager R.** 2011. Recruitment and activation of a lipid kinase by hepatitis C virus NS5A is essential for integrity of the membranous replication compartment. Cell Host Microbe **9:**32-45.
26. **Denison MR.** 2008. Seeking membranes: positive-strand RNA virus replication complexes. PLoS Biol **6:**e270.
27. **Mackenzie J.** 2005. Wrapping things up about virus RNA replication. Traffic **6:**967-977.
28. **Salonen A, Ahola T, Kaariainen L.** 2005. Viral RNA replication in association with cellular membranes. Curr Top Microbiol Immunol **285:**139-173.
29. **den Boon JA, Diaz A, Ahlquist P.** 2010. Cytoplasmic viral replication complexes. Cell Host Microbe **8:**77-85.
30. **Nugent CI, Johnson KL, Sarnow P, Kirkegaard K.** 1999. Functional coupling between replication and packaging of poliovirus replicon RNA. J Virol **73:**427-435.
31. **Guinea R, Carrasco L.** 1990. Phospholipid biosynthesis and poliovirus genome replication, two coupled phenomena. Embo J **9:**2011-2016.
32. **Heaton NS, Perera R, Berger KL, Khadka S, Lacount DJ, Kuhn RJ, Randall G.** 2010. Dengue virus nonstructural protein 3 redistributes fatty acid synthase to sites of viral replication and increases cellular fatty acid synthesis. Proc Natl Acad Sci U S A **107:**17345-17350.

33. **Lee HK, Lund JM, Ramanathan B, Mizushima N, Iwasaki A.** 2007. Autophagy-dependent viral recognition by plasmacytoid dendritic cells. Science **315:**1398-1401.
34. **Manuse MJ, Briggs CM, Parks GD.** 2010. Replication-independent activation of human plasmacytoid dendritic cells by the paramyxovirus SV5 Requires TLR7 and autophagy pathways. Virology **405:**383-389.
35. **Botos I, Liu L, Wang Y, Segal DM, Davies DR.** 2009. The toll-like receptor 3:dsRNA signaling complex. Biochim Biophys Acta **1789:**667-674.
36. **Daffis S, Samuel MA, Suthar MS, Gale M, Jr., Diamond MS.** 2008. Toll-like receptor 3 has a protective role against West Nile virus infection. J Virol **82:**10349-10358.
37. **Diebold SS, Kaisho T, Hemmi H, Akira S, Reis e Sousa C.** 2004. Innate antiviral responses by means of TLR7-mediated recognition of single-stranded RNA. Science **303:**1529-1531.
38. **Heil F, Hemmi H, Hochrein H, Ampenberger F, Kirschning C, Akira S, Lipford G, Wagner H, Bauer S.** 2004. Species-specific recognition of single-stranded RNA via toll-like receptor 7 and 8. Science **303:**1526-1529.
39. **Lund JM, Alexopoulou L, Sato A, Karow M, Adams NC, Gale NW, Iwasaki A, Flavell RA.** 2004. Recognition of single-stranded RNA viruses by Toll-like receptor 7. Proc Natl Acad Sci U S A **101:**5598-5603.
40. **Tabeta K, Georgel P, Janssen E, Du X, Hoebe K, Crozat K, Mudd S, Shamel L, Sovath S, Goode J, Alexopoulou L, Flavell RA, Beutler B.** 2004. Toll-like receptors 9 and 3 as essential components of innate immune defense against mouse cytomegalovirus infection. Proc Natl Acad Sci U S A **101:**3516-3521.
41. **Hardarson HS, Baker JS, Yang Z, Purevjav E, Huang CH, Alexopoulou L, Li N, Flavell RA, Bowles NE, Vallejo JG.** 2007. Toll-like receptor 3 is an essential component of the innate stress response in virus-induced cardiac injury. Am J Physiol Heart Circ Physiol **292:**H251-258.
42. **Schulz O, Diebold SS, Chen M, Naslund TI, Nolte MA, Alexopoulou L, Azuma YT, Flavell RA, Liljestrom P, Reis e Sousa C.** 2005. Toll-like receptor 3 promotes cross-priming to virus-infected cells. Nature **433:**887-892.
43. **Fitzgerald KA, McWhirter SM, Faia KL, Rowe DC, Latz E, Golenbock DT, Coyle AJ, Liao SM, Maniatis T.** 2003. IKKepsilon and TBK1 are essential components of the IRF3 signaling pathway. Nat Immunol **4:**491-496.
44. **Hacker H, Redecke V, Blagoev B, Kratchmarova I, Hsu LC, Wang GG, Kamps MP, Raz E, Wagner H, Hacker G, Mann M, Karin M.** 2006. Specificity in Toll-like receptor signalling through distinct effector functions of TRAF3 and TRAF6. Nature **439:**204-207.
45. **Oganesyan G, Saha SK, Guo B, He JQ, Shahangian A, Zarnegar B, Perry A, Cheng G.** 2006. Critical role of TRAF3 in the Toll-like receptor-dependent and -independent antiviral response. Nature **439:**208-211.
46. **Sharma S, tenOever BR, Grandvaux N, Zhou GP, Lin R, Hiscott J.** 2003. Triggering the interferon antiviral response through an IKK-related pathway. Science **300:**1148-1151.
47. **Hoshino K, Sugiyama T, Matsumoto M, Tanaka T, Saito M, Hemmi H, Ohara O, Akira S, Kaisho T.** 2006. IkappaB kinase-alpha is critical for interferon-alpha production induced by Toll-like receptors 7 and 9. Nature **440:**949-953.
48. **Kawai T, Sato S, Ishii KJ, Coban C, Hemmi H, Yamamoto M, Terai K, Matsuda M, Inoue J, Uematsu S, Takeuchi O, Akira S.** 2004. Interferon-alpha induction through Toll-

like receptors involves a direct interaction of IRF7 with MyD88 and TRAF6. Nat Immunol **5:**1061-1068.

49. **Yoneyama M, Kikuchi M, Natsukawa T, Shinobu N, Imaizumi T, Miyagishi M, Taira K, Akira S, Fujita T.** 2004. The RNA helicase RIG-I has an essential function in double-stranded RNA-induced innate antiviral responses. Nat Immunol **5:**730-737.
50. **Yoneyama M, Fujita T.** 2008. Structural mechanism of RNA recognition by the RIG-I-like receptors. Immunity **29:**178-181.
51. **Gack MU, Shin YC, Joo CH, Urano T, Liang C, Sun L, Takeuchi O, Akira S, Chen Z, Inoue S, Jung JU.** 2007. TRIM25 RING-finger E3 ubiquitin ligase is essential for RIG-I-mediated antiviral activity. Nature **446:**916-920.
52. **Hornung V, Ellegast J, Kim S, Brzozka K, Jung A, Kato H, Poeck H, Akira S, Conzelmann KK, Schlee M, Endres S, Hartmann G.** 2006. 5'-Triphosphate RNA is the ligand for RIG-I. Science **314:**994-997.
53. **Pichlmair A, Schulz O, Tan CP, Naslund TI, Liljestrom P, Weber F, Reis e Sousa C.** 2006. RIG-I-mediated antiviral responses to single-stranded RNA bearing 5'-phosphates. Science **314:**997-1001.
54. **Saito T, Owen DM, Jiang F, Marcotrigiano J, Gale M, Jr.** 2008. Innate immunity induced by composition-dependent RIG-I recognition of hepatitis C virus RNA. Nature **454:**523-527.
55. **Schmidt A, Schwerd T, Hamm W, Hellmuth JC, Cui S, Wenzel M, Hoffmann FS, Michallet MC, Besch R, Hopfner KP, Endres S, Rothenfusser S.** 2009. 5'-triphosphate RNA requires base-paired structures to activate antiviral signaling via RIG-I. Proc Natl Acad Sci U S A **106:**12067-12072.
56. **Uzri D, Gehrke L.** 2009. Nucleotide sequences and modifications that determine RIG-I/RNA binding and signaling activities. J Virol **83:**4174-4184.
57. **Fredericksen BL, Keller BC, Fornek J, Katze MG, Gale M, Jr.** 2008. Establishment and maintenance of the innate antiviral response to West Nile Virus involves both RIG-I and MDA5 signaling through IPS-1. J Virol **82:**609-616.
58. **Kato H, Takeuchi O, Sato S, Yoneyama M, Yamamoto M, Matsui K, Uematsu S, Jung A, Kawai T, Ishii KJ, Yamaguchi O, Otsu K, Tsujimura T, Koh CS, Reis e Sousa C, Matsuura Y, Fujita T, Akira S.** 2006. Differential roles of MDA5 and RIG-I helicases in the recognition of RNA viruses. Nature **441:**101-105.
59. **Wilkins C, Gale M, Jr.** 2010. Recognition of viruses by cytoplasmic sensors. Curr Opin Immunol **22:**41-47.
60. **Yoneyama M, Kikuchi M, Matsumoto K, Imaizumi T, Miyagishi M, Taira K, Foy E, Loo YM, Gale M, Jr., Akira S, Yonehara S, Kato A, Fujita T.** 2005. Shared and unique functions of the DExD/H-box helicases RIG-I, MDA5, and LGP2 in antiviral innate immunity. J Immunol **175:**2851-2858.
61. **Kato H, Takeuchi O, Mikamo-Satoh E, Hirai R, Kawai T, Matsushita K, Hiiragi A, Dermody TS, Fujita T, Akira S.** 2008. Length-dependent recognition of double-stranded ribonucleic acids by retinoic acid-inducible gene-I and melanoma differentiation-associated gene 5. J Exp Med **205:**1601-1610.
62. **Gitlin L, Barchet W, Gilfillan S, Cella M, Beutler B, Flavell RA, Diamond MS, Colonna M.** 2006. Essential role of mda-5 in type I IFN responses to polyriboinosinic:polyribocytidylic acid and encephalomyocarditis picornavirus. Proc Natl Acad Sci U S A **103:**8459-8464.

63. **Kawai T, Takahashi K, Sato S, Coban C, Kumar H, Kato H, Ishii KJ, Takeuchi O, Akira S.** 2005. IPS-1, an adaptor triggering RIG-I- and Mda5-mediated type I interferon induction. Nat Immunol **6:**981-988.
64. **Meylan E, Curran J, Hofmann K, Moradpour D, Binder M, Bartenschlager R, Tschopp J.** 2005. Cardif is an adaptor protein in the RIG-I antiviral pathway and is targeted by hepatitis C virus. Nature **437:**1167-1172.
65. **Seth RB, Sun L, Ea CK, Chen ZJ.** 2005. Identification and characterization of MAVS, a mitochondrial antiviral signaling protein that activates NF-kappaB and IRF 3. Cell **122:**669-682.
66. **Xu LG, Wang YY, Han KJ, Li LY, Zhai Z, Shu HB.** 2005. VISA is an adapter protein required for virus-triggered IFN-beta signaling. Mol Cell **19:**727-740.
67. **Guo B, Cheng G.** 2007. Modulation of the interferon antiviral response by the TBK1/IKKi adaptor protein TANK. J Biol Chem **282:**11817-11826.
68. **Michallet MC, Meylan E, Ermolaeva MA, Vazquez J, Rebsamen M, Curran J, Poeck H, Bscheider M, Hartmann G, Konig M, Kalinke U, Pasparakis M, Tschopp J.** 2008. TRADD protein is an essential component of the RIG-like helicase antiviral pathway. Immunity **28:**651-661.
69. **Rothenfusser S, Goutagny N, DiPerna G, Gong M, Monks BG, Schoenemeyer A, Yamamoto M, Akira S, Fitzgerald KA.** 2005. The RNA helicase Lgp2 inhibits TLR-independent sensing of viral replication by retinoic acid-inducible gene-I. J Immunol **175:**5260-5268.
70. **Komuro A, Horvath CM.** 2006. RNA- and virus-independent inhibition of antiviral signaling by RNA helicase LGP2. J Virol **80:**12332-12342.
71. **Saito T, Hirai R, Loo YM, Owen D, Johnson CL, Sinha SC, Akira S, Fujita T, Gale M, Jr.** 2007. Regulation of innate antiviral defenses through a shared repressor domain in RIG-I and LGP2. Proc Natl Acad Sci U S A **104:**582-587.
72. **Satoh T, Kato H, Kumagai Y, Yoneyama M, Sato S, Matsushita K, Tsujimura T, Fujita T, Akira S, Takeuchi O.** 2010. LGP2 is a positive regulator of RIG-I- and MDA5-mediated antiviral responses. Proc Natl Acad Sci U S A **107:**1512-1517.
73. **Tang ED, Wang CY.** 2009. MAVS self-association mediates antiviral innate immune signaling. J Virol **83:**3420-3428.
74. **Venkataraman T, Valdes M, Elsby R, Kakuta S, Caceres G, Saijo S, Iwakura Y, Barber GN.** 2007. Loss of DExD/H box RNA helicase LGP2 manifests disparate antiviral responses. J Immunol **178:**6444-6455.
75. **Castanier C, Garcin D, Vazquez A, Arnoult D.** 2010. Mitochondrial dynamics regulate the RIG-I-like receptor antiviral pathway. EMBO Rep **11:**133-138.
76. **Koshiba T, Yasukawa K, Yanagi Y, Kawabata S.** 2011. Mitochondrial membrane potential is required for MAVS-mediated antiviral signaling. Sci Signal **4:**ra7.
77. **Jia Y, Song T, Wei C, Ni C, Zheng Z, Xu Q, Ma H, Li L, Zhang Y, He X, Xu Y, Shi W, Zhong H.** 2009. Negative regulation of MAVS-mediated innate immune response by PSMA7. J Immunol **183:**4241-4248.
78. **Allen IC, Moore CB, Schneider M, Lei Y, Davis BK, Scull MA, Gris D, Roney KE, Zimmermann AG, Bowzard JB, Ranjan P, Monroe KM, Pickles RJ, Sambhara S, Ting JP.** 2011. NLRX1 protein attenuates inflammatory responses to infection by interfering with the RIG-I-MAVS and TRAF6-NF-kappaB signaling pathways. Immunity **34:**854-865.

79. **Ling A, Soares F, Croitoru DO, Tattoli I, Carneiro LA, Boniotto M, Benko S, Philpott DJ, Girardin SE.** 2012. Post-transcriptional inhibition of luciferase reporter assays by the Nod-like receptor proteins NLRX1 and NLRC3. J Biol Chem **287:**28705-28716.
80. **Saha SK, Pietras EM, He JQ, Kang JR, Liu SY, Oganesyan G, Shahangian A, Zarnegar B, Shiba TL, Wang Y, Cheng G.** 2006. Regulation of antiviral responses by a direct and specific interaction between TRAF3 and Cardif. Embo J **25:**3257-3263.
81. **Rebsamen M, Vazquez J, Tardivel A, Guarda G, Curran J, Tschopp J.** 2011. NLRX1/NOD5 deficiency does not affect MAVS signalling. Cell Death Differ **18:**1387.
82. **Soares F, Tattoli I, Wortzman ME, Arnoult D, Philpott DJ, Girardin SE.** 2012. NLRX1 does not inhibit MAVS-dependent antiviral signalling. Innate Immun.
83. **Onoguchi K, Onomoto K, Takamatsu S, Jogi M, Takemura A, Morimoto S, Julkunen I, Namiki H, Yoneyama M, Fujita T.** 2010. Virus-infection or 5'ppp-RNA activates antiviral signal through redistribution of IPS-1 mediated by MFN1. PLoS Pathog **6:**e1001012.
84. **You F, Sun H, Zhou X, Sun W, Liang S, Zhai Z, Jiang Z.** 2009. PCBP2 mediates degradation of the adaptor MAVS via the HECT ubiquitin ligase AIP4. Nat Immunol **10:**1300-1308.
85. **Horner SM, Liu HM, Park HS, Briley J, Gale M, Jr.** 2011. Mitochondrial-associated endoplasmic reticulum membranes (MAM) form innate immune synapses and are targeted by hepatitis C virus. Proc Natl Acad Sci U S A **108:**14590-14595.
86. **Castanier C, Zemirli N, Portier A, Garcin D, Bidere N, Vazquez A, Arnoult D.** 2012. MAVS ubiquitination by the E3 ligase TRIM25 and degradation by the proteasome is involved in type I interferon production after activation of the antiviral RIG-I-like receptors. BMC Biol **10:**44.
87. **Yasukawa K, Oshiumi H, Takeda M, Ishihara N, Yanagi Y, Seya T, Kawabata S, Koshiba T.** 2009. Mitofusin 2 inhibits mitochondrial antiviral signaling. Sci Signal **2:**ra47.
88. **Wang Y, Tong X, Ye X.** 2012. Ndfip1 negatively regulates RIG-I-dependent immune signaling by enhancing E3 ligase Smurf1-mediated MAVS degradation. J Immunol **189:**5304-5313.
89. **Liu XY, Wei B, Shi HX, Shan YF, Wang C.** 2010. Tom70 mediates activation of interferon regulatory factor 3 on mitochondria. Cell Res **20:**994-1011.
90. **Wang Y, Tong X, Omoregie ES, Liu W, Meng S, Ye X.** 2012. Tetraspanin 6 (TSPAN6) negatively regulates retinoic acid-inducible gene I-like receptor-mediated immune signaling in a ubiquitination-dependent manner. J Biol Chem **287:**34626-34634.
91. **Liu XY, Chen W, Wei B, Shan YF, Wang C.** 2011. IFN-induced TPR protein IFIT3 potentiates antiviral signaling by bridging MAVS and TBK1. J Immunol **187:**2559-2568.
92. **Bozym RA, Delorme-Axford E, Harris K, Morosky S, Ikizler M, Dermody TS, Sarkar SN, Coyne CB.** 2012. Focal adhesion kinase is a component of antiviral RIG-I-like receptor signaling. Cell Host Microbe **11:**153-166.
93. **Vitour D, Dabo S, Ahmadi Pour M, Vilasco M, Vidalain PO, Jacob Y, Mezel-Lemoine M, Paz S, Arguello M, Lin R, Tangy F, Hiscott J, Meurs EF.** 2009. Polo-like kinase 1 (PLK1) regulates interferon (IFN) induction by MAVS. J Biol Chem **284:**21797-21809.
94. **Xu L, Xiao N, Liu F, Ren H, Gu J.** 2009. Inhibition of RIG-I and MDA5-dependent antiviral response by gC1qR at mitochondria. Proc Natl Acad Sci U S A **106:**1530-1535.

95. **Zhao Y, Sun X, Nie X, Sun L, Tang TS, Chen D, Sun Q.** 2012. COX5B regulates MAVS-mediated antiviral signaling through interaction with ATG5 and repressing ROS production. PLoS Pathog **8:**e1003086.
96. **Song T, Wei C, Zheng Z, Xu Y, Cheng X, Yuan Y, Guan K, Zhang Y, Ma Q, Shi W, Zhong H.** 2010. c-Abl tyrosine kinase interacts with MAVS and regulates innate immune response. FEBS Lett **584:**33-38.
97. **Wang P, Yang L, Cheng G, Yang G, Xu Z, You F, Sun Q, Lin R, Fikrig E, Sutton RE.** 2013. UBXN1 interferes with Rig-I-like receptor-mediated antiviral immune response by targeting MAVS. Cell reports **3:**1057-1070.
98. **Moore CB, Bergstralh DT, Duncan JA, Lei Y, Morrison TE, Zimmermann AG, Accavitti-Loper MA, Madden VJ, Sun L, Ye Z, Lich JD, Heise MT, Chen Z, Ting JP.** 2008. NLRX1 is a regulator of mitochondrial antiviral immunity. Nature **451:**573-577.
99. **Chan DC.** 2006. Mitochondrial fusion and fission in mammals. Annu Rev Cell Dev Biol **22:**79-99.
100. **de Brito OM, Scorrano L.** 2008. Mitofusin 2 tethers endoplasmic reticulum to mitochondria. Nature **456:**605-610.
101. **Hou F, Sun L, Zheng H, Skaug B, Jiang QX, Chen ZJ.** 2011. MAVS forms functional prion-like aggregates to activate and propagate antiviral innate immune response. Cell **146:**448-461.
102. **Soucy-Faulkner A, Mukawera E, Fink K, Martel A, Jouan L, Nzengue Y, Lamarre D, Vande Velde C, Grandvaux N.** 2010. Requirement of NOX2 and reactive oxygen species for efficient RIG-I-mediated antiviral response through regulation of MAVS expression. PLoS Pathog **6:**e1000930.
103. **Tal MC, Sasai M, Lee HK, Yordy B, Shadel GS, Iwasaki A.** 2009. Absence of autophagy results in reactive oxygen species-dependent amplification of RLR signaling. Proc Natl Acad Sci U S A **106:**2770-2775.
104. **Gonzalez-Dosal R, Horan KA, Rahbek SH, Ichijo H, Chen ZJ, Mieyal JJ, Hartmann R, Paludan SR.** 2011. HSV infection induces production of ROS, which potentiate signaling from pattern recognition receptors: role for S-glutathionylation of TRAF3 and 6. PLoS Pathog **7:**e1002250.
105. **Tal MC, Iwasaki A.** 2009. Autophagic control of RLR signaling. Autophagy **5:**749-750.
106. **Galati D, Srinivasan S, Raza H, Prabu SK, Hardy M, Chandran K, Lopez M, Kalyanaraman B, Avadhani NG.** 2009. Role of nuclear-encoded subunit Vb in the assembly and stability of cytochrome c oxidase complex: implications in mitochondrial dysfunction and ROS production. Biochem J **420:**439-449.
107. **Campian JL, Gao X, Qian M, Eaton JW.** 2007. Cytochrome C oxidase activity and oxygen tolerance. J Biol Chem **282:**12430-12438.
108. **Huang J, Lam GY, Brumell JH.** 2011. Autophagy signaling through reactive oxygen species. Antioxid Redox Signal **14:**2215-2231.
109. **Klionsky DJ, Emr SD.** 2000. Autophagy as a regulated pathway of cellular degradation. Science **290:**1717-1721.
110. **Boya P, Reggiori F, Codogno P.** 2013. Emerging regulation and functions of autophagy. Nat Cell Biol **15:**1017.
111. **Voges D, Zwickl P, Baumeister W.** 1999. The 26S proteasome: a molecular machine designed for controlled proteolysis. Annu Rev Biochem **68:**1015-1068.

112. **Coux O, Tanaka K, Goldberg AL.** 1996. Structure and functions of the 20S and 26S proteasomes. Annu Rev Biochem **65:**801-847.
113. **Makeyev AV, Liebhaber SA.** 2002. The poly(C)-binding proteins: a multiplicity of functions and a search for mechanisms. Rna **8:**265-278.
114. **Leffers H, Dejgaard K, Celis JE.** 1995. Characterisation of two major cellular poly(rC)-binding human proteins, each containing three K-homologous (KH) domains. Eur J Biochem **230:**447-453.
115. **Kiledjian M, Wang X, Liebhaber SA.** 1995. Identification of two KH domain proteins in the alpha-globin mRNP stability complex. Embo J **14:**4357-4364.
116. **Zhou X, You F, Chen H, Jiang Z.** 2012. Poly(C)-binding protein 1 (PCBP1) mediates housekeeping degradation of mitochondrial antiviral signaling (MAVS). Cell Res **22:**717-727.
117. **Mund T, Pelham HR.** 2009. Control of the activity of WW-HECT domain E3 ubiquitin ligases by NDFIP proteins. EMBO Rep **10:**501-507.
118. **Mund T, Pelham HR.** 2010. Regulation of PTEN/Akt and MAP kinase signaling pathways by the ubiquitin ligase activators Ndfip1 and Ndfip2. Proc Natl Acad Sci U S A **107:**11429-11434.
119. **Hemler ME.** 2005. Tetraspanin functions and associated microdomains. Nat Rev Mol Cell Biol **6:**801-811.
120. **Cheng KY, Lowe ED, Sinclair J, Nigg EA, Johnson LN.** 2003. The crystal structure of the human polo-like kinase-1 polo box domain and its phospho-peptide complex. Embo J **22:**5757-5768.
121. **Elia AE, Rellos P, Haire LF, Chao JW, Ivins FJ, Hoepker K, Mohammad D, Cantley LC, Smerdon SJ, Yaffe MB.** 2003. The molecular basis for phosphodependent substrate targeting and regulation of Plks by the Polo-box domain. Cell **115:**83-95.
122. **Garcia-Alvarez B, de Carcer G, Ibanez S, Bragado-Nilsson E, Montoya G.** 2007. Molecular and structural basis of polo-like kinase 1 substrate recognition: Implications in centrosomal localization. Proc Natl Acad Sci U S A **104:**3107-3112.
123. **Paz S, Vilasco M, Werden SJ, Arguello M, Joseph-Pillai D, Zhao T, Nguyen TL, Sun Q, Meurs EF, Lin R, Hiscott J.** 2011. A functional C-terminal TRAF3-binding site in MAVS participates in positive and negative regulation of the IFN antiviral response. Cell Res **21:**895-910.
124. **Pendergast AM.** 2002. The Abl family kinases: mechanisms of regulation and signaling. Adv Cancer Res **85:**51-100.
125. **Wen C, Yan Z, Yang X, Guan K, Xu C, Song T, Zheng Z, Wang W, Wang Y, Zhao M, Zhang Y, Xu T, Dou J, Liu J, Xu Q, He X, Wei C, Zhong H.** 2012. Identification of tyrosine-9 of MAVS as critical target for inducible phosphorylation that determines activation. PLoS One **7:**e41687.
126. **Liotta LA, Mandler R, Murano G, Katz DA, Gordon RK, Chiang PK, Schiffmann E.** 1986. Tumor cell autocrine motility factor. Proc Natl Acad Sci U S A **83:**3302-3306.
127. **Nabi IR, Raz A.** 1987. Cell shape modulation alters glycosylation of a metastatic melanoma cell-surface antigen. Int J Cancer **40:**396-402.
128. **Nabi IR, Raz A.** 1988. Loss of metastatic responsiveness to cell shape modulation in a newly characterized B16 melanoma adhesive cell variant. Cancer Res **48:**1258-1264.
129. **Nabi IR, Watanabe H, Raz A.** 1990. Identification of B16-F1 melanoma autocrine motility-like factor receptor. Cancer Res **50:**409-414.

130. **Silletti S, Watanabe H, Hogan V, Nabi IR, Raz A.** 1991. Purification of B16-F1 melanoma autocrine motility factor and its receptor. Cancer Res **51:**3507-3511.
131. **Watanabe H, Takehana K, Date M, Shinozaki T, Raz A.** 1996. Tumor cell autocrine motility factor is the neuroleukin/phosphohexose isomerase polypeptide. Cancer Res **56:**2960-2963.
132. **Shimizu K, Tani M, Watanabe H, Nagamachi Y, Niinaka Y, Shiroishi T, Ohwada S, Raz A, Yokota J.** 1999. The autocrine motility factor receptor gene encodes a novel type of seven transmembrane protein. FEBS Lett **456:**295-300.
133. **Meusser B, Hirsch C, Jarosch E, Sommer T.** 2005. ERAD: the long road to destruction. Nat Cell Biol **7:**766-772.
134. **Hershko A, Ciechanover A.** 1998. The ubiquitin system. Annu Rev Biochem **67:**425-479.
135. **Chen B, Mariano J, Tsai YC, Chan AH, Cohen M, Weissman AM.** 2006. The activity of a human endoplasmic reticulum-associated degradation E3, gp78, requires its Cue domain, RING finger, and an E2-binding site. Proc Natl Acad Sci U S A **103:**341-346.
136. **Fang S, Ferrone M, Yang C, Jensen JP, Tiwari S, Weissman AM.** 2001. The tumor autocrine motility factor receptor, gp78, is a ubiquitin protein ligase implicated in degradation from the endoplasmic reticulum. Proc Natl Acad Sci U S A **98:**14422-14427.
137. **Li W, Tu D, Brunger AT, Ye Y.** 2007. A ubiquitin ligase transfers preformed polyubiquitin chains from a conjugating enzyme to a substrate. Nature **446:**333-337.
138. **Ballar P, Shen Y, Yang H, Fang S.** 2006. The role of a novel p97/valosin-containing protein-interacting motif of gp78 in endoplasmic reticulum-associated degradation. J Biol Chem **281:**35359-35368.
139. **Lilley BN, Ploegh HL.** 2005. Multiprotein complexes that link dislocation, ubiquitination, and extraction of misfolded proteins from the endoplasmic reticulum membrane. Proc Natl Acad Sci U S A **102:**14296-14301.
140. **Ye Y, Meyer HH, Rapoport TA.** 2001. The AAA ATPase Cdc48/p97 and its partners transport proteins from the ER into the cytosol. Nature **414:**652-656.
141. **Zhong X, Shen Y, Ballar P, Apostolou A, Agami R, Fang S.** 2004. AAA ATPase p97/valosin-containing protein interacts with gp78, a ubiquitin ligase for endoplasmic reticulum-associated degradation. J Biol Chem **279:**45676-45684.
142. **Morito D, Hirao K, Oda Y, Hosokawa N, Tokunaga F, Cyr DM, Tanaka K, Iwai K, Nagata K.** 2008. Gp78 cooperates with RMA1 in endoplasmic reticulum-associated degradation of CFTRDeltaF508. Mol Biol Cell **19:**1328-1336.
143. **Song BL, Sever N, DeBose-Boyd RA.** 2005. Gp78, a membrane-anchored ubiquitin ligase, associates with Insig-1 and couples sterol-regulated ubiquitination to degradation of HMG CoA reductase. Mol Cell **19:**829-840.
144. **Liang JS, Kim T, Fang S, Yamaguchi J, Weissman AM, Fisher EA, Ginsberg HN.** 2003. Overexpression of the tumor autocrine motility factor receptor Gp78, a ubiquitin protein ligase, results in increased ubiquitinylation and decreased secretion of apolipoprotein B100 in HepG2 cells. J Biol Chem **278:**23984-23988.
145. **Tsai YC, Mendoza A, Mariano JM, Zhou M, Kostova Z, Chen B, Veenstra T, Hewitt SM, Helman LJ, Khanna C, Weissman AM.** 2007. The ubiquitin ligase gp78 promotes sarcoma metastasis by targeting KAI1 for degradation. Nature medicine **13:**1504-1509.
146. **Benlimame N, Le PU, Nabi IR.** 1998. Localization of autocrine motility factor receptor to caveolae and clathrin-independent internalization of its ligand to smooth endoplasmic reticulum. Mol Biol Cell **9:**1773-1786.

147. **Benlimame N, Simard D, Nabi IR.** 1995. Autocrine motility factor receptor is a marker for a distinct membranous tubular organelle. J Cell Biol **129:**459-471.
148. **Goetz JG, Genty H, St-Pierre P, Dang T, Joshi B, Sauve R, Vogl W, Nabi IR.** 2007. Reversible interactions between smooth domains of the endoplasmic reticulum and mitochondria are regulated by physiological cytosolic Ca2+ levels. J Cell Sci **120:**3553-3564.
149. **Wang HJ, Benlimame N, Nabi I.** 1997. The AMF-R tubule is a smooth ilimaquinone-sensitive subdomain of the endoplasmic reticulum. J Cell Sci **110 (Pt 24):**3043-3053.
150. **Wang HJ, Guay G, Pogan L, Sauve R, Nabi IR.** 2000. Calcium regulates the association between mitochondria and a smooth subdomain of the endoplasmic reticulum. J Cell Biol **150:**1489-1498.
151. **Fu M, St-Pierre P, Shankar J, Wang PT, Joshi B, Nabi IR.** 2013. Regulation of mitophagy by the Gp78 E3 ubiquitin ligase. Mol Biol Cell **24:**1153-1162.
152. **Baumann O, Walz B.** 2001. Endoplasmic reticulum of animal cells and its organization into structural and functional domains. International review of cytology **205:**149-214.
153. **Shibata Y, Hu J, Kozlov MM, Rapoport TA.** 2009. Mechanisms shaping the membranes of cellular organelles. Annu Rev Cell Dev Biol **25:**329-354.
154. **Shibata Y, Voeltz GK, Rapoport TA.** 2006. Rough sheets and smooth tubules. Cell **126:**435-439.
155. **Voeltz GK, Rolls MM, Rapoport TA.** 2002. Structural organization of the endoplasmic reticulum. EMBO Rep **3:**944-950.
156. **Park SH, Blackstone C.** 2010. Further assembly required: construction and dynamics of the endoplasmic reticulum network. EMBO Rep **11:**515-521.
157. **de Brito OM, Scorrano L.** 2010. An intimate liaison: spatial organization of the endoplasmic reticulum-mitochondria relationship. Embo J **29:**2715-2723.
158. **English AR, Voeltz GK.** 2013. Endoplasmic reticulum structure and interconnections with other organelles. Cold Spring Harbor perspectives in biology **5:**a013227.
159. **Friedman JR, Dibenedetto JR, West M, Rowland AA, Voeltz GK.** 2013. Endoplasmic reticulum-endosome contact increases as endosomes traffic and mature. Mol Biol Cell **24:**1030-1040.
160. **Rowland AA, Voeltz GK.** 2012. Endoplasmic reticulum-mitochondria contacts: function of the junction. Nat Rev Mol Cell Biol **13:**607-625.
161. **Voeltz GK, Prinz WA.** 2007. Sheets, ribbons and tubules - how organelles get their shape. Nat Rev Mol Cell Biol **8:**258-264.
162. **Okamoto M, Kurokawa K, Matsuura-Tokita K, Saito C, Hirata R, Nakano A.** 2012. High-curvature domains of the ER are important for the organization of ER exit sites in Saccharomyces cerevisiae. J Cell Sci **125:**3412-3420.
163. **Voeltz GK, Prinz WA, Shibata Y, Rist JM, Rapoport TA.** 2006. A class of membrane proteins shaping the tubular endoplasmic reticulum. Cell **124:**573-586.
164. **Shibata Y, Shemesh T, Prinz WA, Palazzo AF, Kozlov MM, Rapoport TA.** 2010. Mechanisms determining the morphology of the peripheral ER. Cell **143:**774-788.
165. **Shibata Y, Voss C, Rist JM, Hu J, Rapoport TA, Prinz WA, Voeltz GK.** 2008. The reticulon and DP1/Yop1p proteins form immobile oligomers in the tubular endoplasmic reticulum. J Biol Chem **283:**18892-18904.

166. **Klopfenstein DR, Klumperman J, Lustig A, Kammerer RA, Oorschot V, Hauri HP.** 2001. Subdomain-specific localization of CLIMP-63 (p63) in the endoplasmic reticulum is mediated by its luminal alpha-helical segment. J Cell Biol **153:**1287-1300.
167. **Puhka M, Vihinen H, Joensuu M, Jokitalo E.** 2007. Endoplasmic reticulum remains continuous and undergoes sheet-to-tubule transformation during cell division in mammalian cells. J Cell Biol **179:**895-909.
168. **Behnia R, Munro S.** 2005. Organelle identity and the signposts for membrane traffic. Nature **438:**597-604.
169. **Christoforidis S, Miaczynska M, Ashman K, Wilm M, Zhao L, Yip SC, Waterfield MD, Backer JM, Zerial M.** 1999. Phosphatidylinositol-3-OH kinases are Rab5 effectors. Nat Cell Biol **1:**249-252.
170. **Zerial M, McBride H.** 2001. Rab proteins as membrane organizers. Nat Rev Mol Cell Biol **2:**107-117.
171. **Zoncu R, Perera RM, Balkin DM, Pirruccello M, Toomre D, De Camilli P.** 2009. A phosphoinositide switch controls the maturation and signaling properties of APPL endosomes. Cell **136:**1110-1121.
172. **Hoepfner S, Severin F, Cabezas A, Habermann B, Runge A, Gillooly D, Stenmark H, Zerial M.** 2005. Modulation of receptor recycling and degradation by the endosomal kinesin KIF16B. Cell **121:**437-450.
173. **Nielsen E, Severin F, Backer JM, Hyman AA, Zerial M.** 1999. Rab5 regulates motility of early endosomes on microtubules. Nat Cell Biol **1:**376-382.
174. **Collinet C, Stoter M, Bradshaw CR, Samusik N, Rink JC, Kenski D, Habermann B, Buchholz F, Henschel R, Mueller MS, Nagel WE, Fava E, Kalaidzidis Y, Zerial M.** 2010. Systems survey of endocytosis by multiparametric image analysis. Nature **464:**243-249.
175. **Poteryaev D, Datta S, Ackema K, Zerial M, Spang A.** 2010. Identification of the switch in early-to-late endosome transition. Cell **141:**497-508.
176. **Rink J, Ghigo E, Kalaidzidis Y, Zerial M.** 2005. Rab conversion as a mechanism of progression from early to late endosomes. Cell **122:**735-749.
177. **Nicot AS, Fares H, Payrastre B, Chisholm AD, Labouesse M, Laporte J.** 2006. The phosphoinositide kinase PIKfyve/Fab1p regulates terminal lysosome maturation in Caenorhabditis elegans. Mol Biol Cell **17:**3062-3074.
178. **Rusten TE, Rodahl LM, Pattni K, Englund C, Samakovlis C, Dove S, Brech A, Stenmark H.** 2006. Fab1 phosphatidylinositol 3-phosphate 5-kinase controls trafficking but not silencing of endocytosed receptors. Mol Biol Cell **17:**3989-4001.
179. **Futter CE, Collinson LM, Backer JM, Hopkins CR.** 2001. Human VPS34 is required for internal vesicle formation within multivesicular endosomes. J Cell Biol **155:**1251-1264.
180. **Ikonomov OC, Sbrissa D, Shisheva A.** 2001. Mammalian cell morphology and endocytic membrane homeostasis require enzymatically active phosphoinositide 5-kinase PIKfyve. J Biol Chem **276:**26141-26147.
181. **Jefferies HB, Cooke FT, Jat P, Boucheron C, Koizumi T, Hayakawa M, Kaizawa H, Ohishi T, Workman P, Waterfield MD, Parker PJ.** 2008. A selective PIKfyve inhibitor blocks PtdIns(3,5)P(2) production and disrupts endomembrane transport and retroviral budding. EMBO Rep **9:**164-170.

182. **Calafat J, Janssen H, Tool A, Dentener MA, Knol EF, Rosenberg HF, Egesten A.** 1998. The bactericidal/permeability-increasing protein (BPI) is present in specific granules of human eosinophils. Blood **91:**4770-4775.
183. **Canny G, Levy O, Furuta GT, Narravula-Alipati S, Sisson RB, Serhan CN, Colgan SP.** 2002. Lipid mediator-induced expression of bactericidal/ permeability-increasing protein (BPI) in human mucosal epithelia. Proc Natl Acad Sci U S A **99:**3902-3907.
184. **Levy O, Sisson RB, Kenyon J, Eichenwald E, Macone AB, Goldmann D.** 2000. Enhancement of neonatal innate defense: effects of adding an N-terminal recombinant fragment of bactericidal/permeability-increasing protein on growth and tumor necrosis factor-inducing activity of gram-negative bacteria tested in neonatal cord blood ex vivo. Infect Immun **68:**5120-5125.
185. **Reichel PH, Seemann C, Csernok E, Schroder JM, Muller A, Gross WL, Schultz H.** 2003. Bactericidal/permeability-increasing protein is expressed by human dermal fibroblasts and upregulated by interleukin 4. Clin Diagn Lab Immunol **10:**473-475.
186. **Weiss J, Elsbach P, Olsson I, Odeberg H.** 1978. Purification and characterization of a potent bactericidal and membrane active protein from the granules of human polymorphonuclear leukocytes. J Biol Chem **253:**2664-2672.
187. **Mannion BA, Weiss J, Elsbach P.** 1990. Separation of sublethal and lethal effects of the bactericidal/permeability increasing protein on Escherichia coli. J Clin Invest **85:**853-860.
188. **Beamer LJ, Carroll SF, Eisenberg D.** 1997. Crystal structure of human BPI and two bound phospholipids at 2.4 angstrom resolution. Science **276:**1861-1864.
189. **Ooi CE, Weiss J, Doerfler ME, Elsbach P.** 1991. Endotoxin-neutralizing properties of the 25 kD N-terminal fragment and a newly isolated 30 kD C-terminal fragment of the 55-60 kD bactericidal/permeability-increasing protein of human neutrophils. J Exp Med **174:**649-655.
190. **Iovine NM, Elsbach P, Weiss J.** 1997. An opsonic function of the neutrophil bactericidal/permeability-increasing protein depends on both its N- and C-terminal domains. Proc Natl Acad Sci U S A **94:**10973-10978.
191. **Fenton MJ, Golenbock DT.** 1998. LPS-binding proteins and receptors. J Leukoc Biol **64:**25-32.
192. **Ulevitch RJ, Tobias PS.** 1999. Recognition of gram-negative bacteria and endotoxin by the innate immune system. Curr Opin Immunol **11:**19-22.
193. **Iovine N, Eastvold J, Elsbach P, Weiss JP, Gioannini TL.** 2002. The carboxyl-terminal domain of closely related endotoxin-binding proteins determines the target of protein-lipopolysaccharide complexes. J Biol Chem **277:**7970-7978.
194. **Gazzano-Santoro H, Meszaros K, Birr C, Carroll SF, Theofan G, Horwitz AH, Lim E, Aberle S, Kasler H, Parent JB.** 1994. Competition between rBPI23, a recombinant fragment of bactericidal/permeability-increasing protein, and lipopolysaccharide (LPS)-binding protein for binding to LPS and gram-negative bacteria. Infect Immun **62:**1185-1191.
195. **Opal SM, Palardy JE, Marra MN, Fisher CJ, Jr., McKelligon BM, Scott RW.** 1994. Relative concentrations of endotoxin-binding proteins in body fluids during infection. Lancet **344:**429-431.
196. **Tobias PS, Soldau K, Iovine NM, Elsbach P, Weiss J.** 1997. Lipopolysaccharide (LPS)-binding proteins BPI and LBP form different types of complexes with LPS. J Biol Chem **272:**18682-18685.

197. **Dear TN, Boehm T, Keverne EB, Rabbitts TH.** 1991. Novel genes for potential ligand-binding proteins in subregions of the olfactory mucosa. Embo J **10:**2813-2819.
198. **Andrault JB, Gaillard I, Giorgi D, Rouquier S.** 2003. Expansion of the BPI family by duplication on human chromosome 20: characterization of the RY gene cluster in 20q11.21 encoding olfactory transporters/antimicrobial-like peptides. Genomics **82:**172-184.
199. **Bingle CD, LeClair EE, Havard S, Bingle L, Gillingham P, Craven CJ.** 2004. Phylogenetic and evolutionary analysis of the PLUNC gene family. Protein Sci **13:**422-430.
200. **LeClair EE, Nomellini V, Bahena M, Singleton V, Bingle L, Craven CJ, Bingle CD.** 2004. Cloning and expression of a mouse member of the PLUNC protein family exclusively expressed in tongue epithelium. Genomics **83:**658-666.
201. **Weston WM, LeClair EE, Trzyna W, McHugh KM, Nugent P, Lafferty CM, Ma L, Tuan RS, Greene RM.** 1999. Differential display identification of plunc, a novel gene expressed in embryonic palate, nasal epithelium, and adult lung. J Biol Chem **274:**13698-13703.
202. **Canny G, Levy O.** 2008. Bactericidal/permeability-increasing protein (BPI) and BPI homologs at mucosal sites. Trends Immunol **29:**541-547.
203. **Bingle CD, Craven CJ.** 2002. PLUNC: a novel family of candidate host defence proteins expressed in the upper airways and nasopharynx. Hum Mol Genet **11:**937-943.
204. **Stins MF, Badger J, Sik Kim K.** 2001. Bacterial invasion and transcytosis in transfected human brain microvascular endothelial cells. Microb Pathog **30:**19-28.
205. **Coyne CB, Bozym R, Morosky SA, Hanna SL, Mukherjee A, Tudor M, Kim KS, Cherry S.** 2011. Comparative RNAi screening reveals host factors involved in enterovirus infection of polarized endothelial monolayers. Cell Host Microbe **9:**70-82.
206. **Coyne CB, Kim KS, Bergelson JM.** 2007. Poliovirus entry into human brain microvascular cells requires receptor-induced activation of SHP-2. Embo J **26:**4016-4028.
207. **Coyne CB, Bozym R, Morosky SA, Hanna SL, Mukherjee A, Tudor M, Kim KS, Cherry S.** 2011. Comparative RNAi screening reveals host factors involved in enterovirus infection of polarized endothelial monolayers. Cell host & microbe **9:**70-82.
208. **Delorme-Axford E, Donker RB, Mouillet JF, Chu T, Bayer A, Ouyang Y, Wang T, Stolz DB, Sarkar SN, Morelli AE, Sadovsky Y, Coyne CB.** 2013. Human placental trophoblasts confer viral resistance to recipient cells. Proc Natl Acad Sci U S A **110:**12048-12053.
209. **Mukherjee A, Morosky SA, Delorme-Axford E, Dybdahl-Sissoko N, Oberste MS, Wang T, Coyne CB.** 2011. The coxsackievirus B 3C protease cleaves MAVS and TRIF to attenuate host type I interferon and apoptotic signaling. PLoS Pathog **7:**e1001311.
210. **Livak KJ, Schmittgen TD.** 2001. Analysis of relative gene expression data using real-time quantitative PCR and the 2(-Delta Delta C(T)) Method. Methods **25:**402-408.
211. **Bozym RA, Morosky SA, Kim KS, Cherry S, Coyne CB.** 2010. Release of intracellular calcium stores facilitates coxsackievirus entry into polarized endothelial cells. PLoS Pathog **6:**e1001135.
212. **Kawai T, Akira S.** 2006. Innate immune recognition of viral infection. Nat Immunol **7:**131-137.
213. **Jacobs JL, Coyne CB.** 2013. Mechanisms of MAVS Regulation at the Mitochondrial Membrane. Journal of molecular biology.

214. **Csordas G, Renken C, Varnai P, Walter L, Weaver D, Buttle KF, Balla T, Mannella CA, Hajnoczky G.** 2006. Structural and functional features and significance of the physical linkage between ER and mitochondria. J Cell Biol **174:**915-921.
215. **Friedman JR, Lackner LL, West M, DiBenedetto JR, Nunnari J, Voeltz GK.** 2011. ER tubules mark sites of mitochondrial division. Science **334:**358-362.
216. **Rizzuto R, Pinton P, Carrington W, Fay FS, Fogarty KE, Lifshitz LM, Tuft RA, Pozzan T.** 1998. Close contacts with the endoplasmic reticulum as determinants of mitochondrial Ca2+ responses. Science **280:**1763-1766.
217. **Stone SJ, Vance JE.** 2000. Phosphatidylserine synthase-1 and -2 are localized to mitochondria-associated membranes. J Biol Chem **275:**34534-34540.
218. **Pottekat A, Menon AK.** 2004. Subcellular localization and targeting of N-acetylglucosaminyl phosphatidylinositol de-N-acetylase, the second enzyme in the glycosylphosphatidylinositol biosynthetic pathway. J Biol Chem **279:**15743-15751.
219. **Hayashi T, Su TP.** 2007. Sigma-1 receptor chaperones at the ER-mitochondrion interface regulate Ca(2+) signaling and cell survival. Cell **131:**596-610.
220. **Dennis EA, Kennedy EP.** 1972. Intracellular sites of lipid synthesis and the biogenesis of mitochondria. J Lipid Res **13:**263-267.
221. **Wieckowski MR, Giorgi C, Lebiedzinska M, Duszynski J, Pinton P.** 2009. Isolation of mitochondria-associated membranes and mitochondria from animal tissues and cells. Nat Protoc **4:**1582-1590.
222. **Zhou R, Yazdi AS, Menu P, Tschopp J.** 2011. A role for mitochondria in NLRP3 inflammasome activation. Nature **469:**221-225.
223. **St-Pierre P, Dang T, Joshi B, Nabi IR.** 2012. Peripheral endoplasmic reticulum localization of the Gp78 ubiquitin ligase activity. J Cell Sci **125:**1727-1737.
224. **Alexia C, Poalas K, Carvalho G, Zemirli N, Dwyer J, Dubois SM, Hatchi EM, Cordeiro N, Smith SS, Castanier C, Le Guelte A, Wan L, Kang Y, Vazquez A, Gavard J, Arnoult D, Bidere N.** 2013. The endoplasmic reticulum acts as a platform for ubiquitylated components of nuclear factor kappaB signaling. Sci Signal **6:**ra79.
225. **Castanier C, Zemirli N, Portier A, Garcin D, Bidere N, Vazquez A, Arnoult D.** 2012. MAVS ubiquitination by the E3 ligase TRIM25 and degradation by the proteasome is involved in type I interferon production after activation of the antiviral RIG-I-like receptors. BMC biology **10:**44.
226. **Castanier C, Arnoult D.** 2011. Mitochondrial localization of viral proteins as a means to subvert host defense. Biochim Biophys Acta **1813:**575-583.
227. **Lin R, Heylbroeck C, Pitha PM, Hiscott J.** 1998. Virus-dependent phosphorylation of the IRF-3 transcription factor regulates nuclear translocation, transactivation potential, and proteasome-mediated degradation. Mol Cell Biol **18:**2986-2996.
228. **Lawlor KE, Vince JE.** 2013. Ambiguities in NLRP3 inflammasome regulation: Is there a role for mitochondria? Biochim Biophys Acta.
229. **Misawa T, Takahama M, Kozaki T, Lee H, Zou J, Saitoh T, Akira S.** 2013. Microtubule-driven spatial arrangement of mitochondria promotes activation of the NLRP3 inflammasome. Nat Immunol **14:**454-460.
230. **Paz S, Vilasco M, Werden SJ, Arguello M, Joseph-Pillai D, Zhao T, Nguyen TL, Sun Q, Meurs EF, Lin R, Hiscott J.** 2011. A functional C-terminal TRAF3-binding site in MAVS participates in positive and negative regulation of the IFN antiviral response. Cell Res **21:**895-910.

231. **Arnoult D, Soares F, Tattoli I, Castanier C, Philpott DJ, Girardin SE.** 2009. An N-terminal addressing sequence targets NLRX1 to the mitochondrial matrix. J Cell Sci **122:**3161-3168.
232. **Jabaut J, Ather JL, Taracanova A, Poynter ME, Ckless K.** 2013. Mitochondria-targeted drugs enhance Nlrp3 inflammasome-dependent IL-1beta secretion in association with alterations in cellular redox and energy status. Free radical biology & medicine **60:**233-245.
233. **Goulet ML, Olagnier D, Xu Z, Paz S, Belgnaoui SM, Lafferty EI, Janelle V, Arguello M, Paquet M, Ghneim K, Richards S, Smith A, Wilkinson P, Cameron M, Kalinke U, Qureshi S, Lamarre A, Haddad EK, Sekaly RP, Peri S, Balachandran S, Lin R, Hiscott J.** 2013. Systems analysis of a RIG-I agonist inducing broad spectrum inhibition of virus infectivity. PLoS Pathog **9:**e1003298.
234. **Belgnaoui SM, Paz S, Samuel S, Goulet ML, Sun Q, Kikkert M, Iwai K, Dikic I, Hiscott J, Lin R.** 2012. Linear ubiquitination of NEMO negatively regulates the interferon antiviral response through disruption of the MAVS-TRAF3 complex. Cell Host Microbe **12:**211-222.
235. **Nakhaei P, Sun Q, Solis M, Mesplede T, Bonneil E, Paz S, Lin R, Hiscott J.** 2012. IkappaB kinase epsilon-dependent phosphorylation and degradation of X-linked inhibitor of apoptosis sensitizes cells to virus-induced apoptosis. J Virol **86:**726-737.
236. **Belgnaoui SM, Paz S, Hiscott J.** 2011. Orchestrating the interferon antiviral response through the mitochondrial antiviral signaling (MAVS) adapter. Curr Opin Immunol **23:**564-572.
237. **Tang ED, Wang CY.** 2009. MAVS self-association mediates antiviral innate immune signaling. Journal of virology **83:**3420-3428.
238. **Baril M, Racine ME, Penin F, Lamarre D.** 2009. MAVS dimer is a crucial signaling component of innate immunity and the target of hepatitis C virus NS3/4A protease. J Virol **83:**1299-1311.
239. **Bienz K, Egger D, Pasamontes L.** 1987. Association of polioviral proteins of the P2 genomic region with the viral replication complex and virus-induced membrane synthesis as visualized by electron microscopic immunocytochemistry and autoradiography. Virology **160:**220-226.
240. **Bienz K, Egger D, Rasser Y, Bossart W.** 1983. Intracellular distribution of poliovirus proteins and the induction of virus-specific cytoplasmic structures. Virology **131:**39-48.
241. **Dales S, Eggers HJ, Tamm I, Palade GE.** 1965. Electron Microscopic Study of the Formation of Poliovirus. Virology **26:**379-389.
242. **Bienz K, Egger D, Pfister T, Troxler M.** 1992. Structural and functional characterization of the poliovirus replication complex. J Virol **66:**2740-2747.
243. **Egger D, Bienz K.** 2005. Intracellular location and translocation of silent and active poliovirus replication complexes. J Gen Virol **86:**707-718.
244. **Lahaye X, Vidy A, Pomier C, Obiang L, Harper F, Gaudin Y, Blondel D.** 2009. Functional characterization of Negri bodies (NBs) in rabies virus-infected cells: Evidence that NBs are sites of viral transcription and replication. J Virol **83:**7948-7958.
245. **Negri A.** 1903. Contributions to the study of rabies zoology. Bull. Soc. Med. Surg. Pavia**:**88-114.

246. **Heinrich BS, Cureton DK, Rahmeh AA, Whelan SP.** 2010. Protein expression redirects vesicular stomatitis virus RNA synthesis to cytoplasmic inclusions. PLoS Pathog **6:**e1000958.
247. **Cairns J.** 1960. The initiation of vaccinia infection. Virology **11:**603-623.
248. **Kit S, Dubbs DR, Hsu TC.** 1963. Biochemistry of vaccinia-infected mouse fibroblasts (strain L-M). III. Radioautographic and biochemical studies of thymidine-H3 uptake into DNA of L-M cells and rabbit cells in primary culture. Virology **19:**13-22.
249. **Tolonen N, Doglio L, Schleich S, Krijnse Locker J.** 2001. Vaccinia virus DNA replication occurs in endoplasmic reticulum-enclosed cytoplasmic mini-nuclei. Mol Biol Cell **12:**2031-2046.
250. **Hernandez LD, Hoffman LR, Wolfsberg TG, White JM.** 1996. Virus-cell and cell-cell fusion. Annu Rev Cell Dev Biol **12:**627-661.
251. **Bayer N, Schober D, Prchla E, Murphy RF, Blaas D, Fuchs R.** 1998. Effect of bafilomycin A1 and nocodazole on endocytic transport in HeLa cells: implications for viral uncoating and infection. J Virol **72:**9645-9655.
252. **Nohturfft A, Zhang SC.** 2009. Coordination of lipid metabolism in membrane biogenesis. Annu Rev Cell Dev Biol **25:**539-566.
253. **De Matteis MA, Di Campli A, Godi A.** 2005. The role of the phosphoinositides at the Golgi complex. Biochim Biophys Acta **1744:**396-405.
254. **Sasaki T, Takasuga S, Sasaki J, Kofuji S, Eguchi S, Yamazaki M, Suzuki A.** 2009. Mammalian phosphoinositide kinases and phosphatases. Progress in lipid research **48:**307-343.
255. **Berridge MJ, Bootman MD, Roderick HL.** 2003. Calcium signalling: dynamics, homeostasis and remodelling. Nat Rev Mol Cell Biol **4:**517-529.
256. **Sammels E, Parys JB, Missiaen L, De Smedt H, Bultynck G.** 2010. Intracellular Ca2+ storage in health and disease: a dynamic equilibrium. Cell calcium **47:**297-314.
257. **Takehara M.** 1975. Polykaryocytosis induced by vesicular stomatitis virus infection in BHK-21 cells. Archives of virology **49:**297-306.
258. **Eden ER, White IJ, Tsapara A, Futter CE.** 2010. Membrane contacts between endosomes and ER provide sites for PTP1B-epidermal growth factor receptor interaction. Nat Cell Biol **12:**267-272.
259. **Rocha N, Kuijl C, van der Kant R, Janssen L, Houben D, Janssen H, Zwart W, Neefjes J.** 2009. Cholesterol sensor ORP1L contacts the ER protein VAP to control Rab7-RILP-p150 Glued and late endosome positioning. J Cell Biol **185:**1209-1225.
260. **Beske O, Reichelt M, Taylor MP, Kirkegaard K, Andino R.** 2007. Poliovirus infection blocks ERGIC-to-Golgi trafficking and induces microtubule-dependent disruption of the Golgi complex. J Cell Sci **120:**3207-3218.
261. **Doedens JR, Kirkegaard K.** 1995. Inhibition of cellular protein secretion by poliovirus proteins 2B and 3A. Embo J **14:**894-907.
262. **Gaudin Y, Tuffereau C, Durrer P, Flamand A, Ruigrok RW.** 1995. Biological function of the low-pH, fusion-inactive conformation of rabies virus glycoprotein (G): G is transported in a fusion-inactive state-like conformation. J Virol **69:**5528-5534.
263. **Roche S, Albertini AA, Lepault J, Bressanelli S, Gaudin Y.** 2008. Structures of vesicular stomatitis virus glycoprotein: membrane fusion revisited. Cellular and molecular life sciences : CMLS **65:**1716-1728.